WIND TUNNEL SITE ANALYSIS OF DOW CHEMICAL FACILITY AT ROCKY FLATS, COLORADO, PART II

by

R. N. Meroney
J. A. Peterka
T. G. Hoot

Prepared For

Research and Ecology
Rocky Flats Division
Dow Chemical Company
Golden, Colorado 80401

March, 1973

CER72-73RNM-JAP-TGH-16

ABSTRACT

This report deals with two separate problems occurring at the Dow Chemical Company Plutonium Recovery Facility, Rocky Flats Division, namely the dispersion of potential effluents and the protection of parking areas from the destructive action of high velocity west winds by the use of shelterbelts. The dispersion study is a continuation of a previous study and consisted of modeling the geography, wind and turbulence profiles and effluent releases in a wind tunnel study. Dispersion and trajectory behavior was determined by the use of Krypton-85 as a tracer gas. The results reinforce the conclusion advanced in the previous study that Pasquill-Gifford prediction methods apply well to the site. The shelterbelt study consisted of evaluating the effects of porosity, barrier height and length, geometric configuration of barriers, parking lot orientation and wind approach angle upon the protection of parking areas from high velocity wind action in assaulting vehicles with abrasive particles. Tests were accomplished by observing the effectiveness of the wind in transporting a zinc oxide-mineral oil suspension. This effectiveness was correlated to velocity reduction and wind profile modification effectiveness of shelterbelts. It was found that the most effective use of shelterbelts could be accomplished if the parking lot were reoriented with the long side running in a north-south direction.

TABLE OF CONTENTS

LIST OF TABLES

LIST OF FIGURES

LIST OF SYMBOLS

H	Shelterbelt height
L	Length scale
Q	Source strength
R	Count rate
t	Measurement time
u'	Turbulent intensity
U_∞	Free stream tunnel velocity
$\overline{u}$	Mean velocity at some reference height
V	Stack exit velocity
x,y,z	Coordinates
z_o	Roughness length
x	Concentration
σ	Standard deviation

Section I - Effluent Dispersion

1.0 INTRODUCTION

This report is issued as a supplemental study to the previously issued Report No. CER71-72RNM-FC45, "Wind Tunnel Site Analysis of Dow Chemical Facility at Rocky Flat, Colorado" (4). The initial report detailed the wind tunnel modeling of the transport and dispersion of potential windborne effluents released from five sources within the boundaries of the Dow Chemical Company Plutonium Recovery Facility, Rocky Flats Division. Four wind direction azimuths were examined. The degree of agreement with accepted prediction techniques was noted along with the effects of the local terrain. Several conclusions regarding effluent behavior were noted and recommendations as to the placement of monitoring devices were advanced.

The purpose of the supplemental study was to extend the previous investigation to include the following:

(1) The investigation of the dispersion of effluents from the five noted sources was performed for two additional wind directions.

(2) The proposed New Plutonium Recovery Facility, Bldg. No. 371 was added to the model. Effluents from two sources located at this facility were examined in combination with six wind directions.

(3) The effects of placing shelterbelts of varying heights and porosities in different configurations at the proposed parking lot adjacent to Bldg. No. 371 were examined. The purpose of the shelterbelts would be the protection of automobiles from windborne abrasive particles. Considerable

damage of this sort has been previously noted at the plant. Specifically, this portion of the study poses three questions:

(a) What height of shelterbelt is required to provide sufficient protection;

(b) Which type of belt in terms of effective porosity results in the greatest protection;

(c) Which geometric configuration of protection of the parking lot will be most beneficial?

2.0 APPARATUS AND TESTS

2.1 Wind Tunnel and Model

The effluent dispersion experimental work was performed in the environmental wind tunnel of the Fluid Dynamics and Diffusion Laboratory at Colorado State University. A 1:1000 scale model of the Rocky Flats Facility and the surrounding area was placed in the tunnel. Detailed descriptions of the wind tunnel and model construction are given by Meroney and Chaudhry (4). A 1:1000 scale model of the New Plutonium Recovery Facility, Bldg. No. 371 was added to the model. Two effluent sources (Nos. 6 and 7) were placed at the building. The source locations and a typical source detail are shown in Fig. No. 1.

2.2 Velocities, Turbulent Intensities and Concentrations

Meroney and Chaudhry (4) determined the field roughness height to be ~1 cm and showed that the proper flow modeling criteria was that the dynamic ratio $\frac{U^*}{\overline{U}_{(Z = 10\ m)}} \simeq 0.058$. This ratio was maintained in all tests. Velocities and turbulent intensities were measured as described by Meroney and Chaudhry (4).

Concentration measurements were obtained by releasing radioactive Krypton-85 gas from sources located in the model and using Geiger-Mueller tubes to determine the relative strength of the sampled mixture. A detailed description of the sampling and concentration determination procedure is given by Meroney and Chaudhry (4).

2.3 Data Collection Program

The data collected for this study included the following:

(1) Mean wind speed and temperature in the air stream approaching the model;

(2) Turbulence intensities in the approaching air stream;

(3) Concentrations downstream from the effluent sources.

Concentration distributions were determined for neutral flow conditions only.

The combinations of wind direction azimuths and sources used in the dispersion study were as follows:

Source No.	Location	Wind Direction Azimuth	Wind Direction Direction
1	Bldg. No. 881	135°	SE
		225°	SW
2	Bldg. No. 707	135°	SE
		225°	SW
3	Bldg. No. 776-777	135°	SE
		225°	SW
4	Cutting Oil Storage Area	135°	SE
		225°	SW
5	250 Foot Stack	135°	SE
		225°	SW
6*	New Facility Bldg. No. 371	45°	NE
		90°	E
		135°	SE
		225°	SW
		270°	W
		315°	NW
7	New Facility Bldg. No. 371	45°	NE
		90°	E
		135°	SE
		225°	SW
		270°	W
		315°	NW

*Sources 6 and 7 both located at Bldg. 371 (See Fig. No. 1)

3.0 TEST RESULTS

3.1 Velocities and Turbulence Intensities

Velocity and turbulence intensity measurements for both east and west winds were taken at the same locations as for the original study (4) in order to insure that flow conditions were similar for both studies. The data obtained was essentially identical to the original study.

3.2 Diffusion Data

Diffusion data was obtained from the five sources investigated by Meroney and Chaudhry for two additional wind directions, southwest and southeast. Data was also obtained from the two sources located at the New Facility, Bldg. No. 371, for six wind directions, northwest, west, southwest, southeast, east and northeast. Krypton-85 concentrations at ground level and in a vertical plane at plume center were obtained at scale downstream distances of 1000', 2500', 4500', 7000', and 10,000' for the two new sources with the west wind and at 1000', 2500', 4000', and 6000' for all sources with all other directions. These distances were determined by the length of the model in the various directions.

All concentration data used in preparing the ground level and vertical plane tables and isopleth plots are converted into non-dimensional form as $\frac{\chi \bar{u} L^2}{Q}$, where the variables indicated are the same as those used in the original study.

The non-dimensional diffusion data for various sources and wind directions is presented in tables I to VIII. The coordinates x, y, z, shown in the tables are as follows. The distance downstream

from the source is designated as x, lateral distances from centerline as y, with positive values of y denoting the righthand side of centerline when facing the flow direction, and z is vertical distance above the model.

3.3 Analysis of Diffusion Data

The data presented in tables I to VIII has been used to prepare concentration plots superimposed upon the Rocky Flats site plan. Figures 2 through 8 show traces of the positions of maximum, 50% of maximum and 10% of maximum concentration. Figures 2 through 6 were prepared by adding the traces for southwest and southeast winds to Figures 13 through 17 in Meroney and Chaudhry. The topographic effect is most pronounced for the wind from the southwest direction. The plumes originally travel parallel to the large plateau northwest of Walnut Creek and have a tendency to bend southward as they cross this creek due to the ridge formations lying just to the north. The most pronounced shifts occur in the plumes originating from sources Nos. 6 and 7 which are located in the new facility at the edge of Walnut Creek. A significant effect is even noticed on the ground level concentration distributions resulting from the plume originating from the 250 foot stack for this wind direction.

Isopleth plots of non-dimensional concentration were also prepared. The vertical plane profiles are shown in Figures 9 through 30. The most pronounced effects of topography occur when the wind direction is from the southwest. This is to be expected as this wind direction represents the greatest vertical variation of terrain with distance. The concentration isopleths to some extent follow the topographic undulations.

Distributions of concentration at ground level are shown for extreme cases of building complex and topographic entrainment (Fig. 31), topographic effect (Figs. 32 and 33), and maximum concentrations observed (Fig. 34). The maximum ground level concentrations noted at the inner and outer plant boundaries for all sources and wind directions are noted in Table IX.

3.4 Comparison with Pasquill-Gifford Estimation Technique

The Pasquill-Gifford estimation technique is described in detail by Meroney and Chaudhry (4). The experimentally determined concentration distributions were analyzed to obtain standard deviations in the vertical and lateral directions. Figure 35 shows plots of σ_z (the vertical standard deviation) versus downstream distance compared with the Pasquill Prediction curve. In almost all cases the observed points lie between Pasquill's "C" and "D" categories. The points appear to be approaching the "D" curve with increasing downstream distance, however, in all but the northwest and southwest winds. Apparently the increased spread is due to the rougher terrain in these wind directions.

The plots of σ_y (the lateral standard deviation) are shown in Figure 36. Fairly good agreement with the "D" curve is obtained for sources 6 and 7 with west and northwest winds and for all sources with a southwest wind. The "D" curve appears to somewhat over-predict the deviations at larger downstream distances in all other cases.

Variation of maximum ground level concentration with distance is shown in Figures 37 and 38 and compared with Pasquill's "D" category. The rate of decrease with distance and the prediction of

actual values matches well for all wind directions at the larger downstream distances. At the 1000' sampling position, the Pasquill curve tends to predict higher concentrations than observed for most wind directions. This is apparently an effect of increased diffusion in the wake of the building complex, as the standard deviations in both directions were considerably higher than predicted for Pasquill's "D" category in this region for almost all cases.

3.5 Conclusions and Recommendations

On the basis of the results from this study the recommendations advanced by Meroney and Chaudhry (4) are re-examined:

(1) Vertical concentration distributions and the resulting standard deviations noted exhibit the same pattern of behavior noted in the previous study, reinforcing the conclusion that effluents released in the immediate vicinity of a process building roof will be entrained in the wake of the building complex and detected by monitors at ground level.

(2) Although a greater terrain effect was noted for southwest winds in terms of plume centerline distortion and large downstream lateral spread of the region of low concentrations, the standard deviations of lateral and vertical concentrations and the downstream distribution of maximum concentrations closely follow Pasquill-Gifford theory.

(3) Although southwest winds seem to have a somewhat greater effect on the distortion of plume trajectory than other wind directions, the effect is not drastic. The plume dispersion

distortion caused by winds in this direction appears to be confined to an increased extent of regions of very low concentration and should not markedly affect the detection of higher concentrations.

(4) The recommendation as to the spacing of monitoring devices along the north-south road to the east of the plant apply to the data taken in the present study, as this data also correlates well to Pasquill-Gifford prediction technique.

(5) The maximum concentrations noted in table IX indicate a maximum dimensionless concentration of .064 at the inner security fence and .0055 at the outer security fence compared with .090 and .049 noted in the previous report.

Section II Shelterbelt Study

4.0 DELINEATION OF PERTINENT VARIABLES AFFECTING SHELTERBELT DESIGN

A comprehensive study (6) of windbreaks and shelterbelts has been prepared by the World Meteorological Organization. This study surveys large amounts of previous work done worldwide on the subject and presents several conclusions:

(1) The porosity of the belt, defined as the percentage ratio of the perforated area of the belt taken perpendicular to the wind direction to the total vertical area of the belt, is decisive. For dense and solid barriers the wind speed reduction immediately behind the obstacle is greater, the point of greatest wind reduction is closer to the obstacle, the zone of protection is relatively small and the recovery region immediately downstream from the protected region has high velocities and greater turbulence. Barriers of medium porosity result in larger zones of somewhat lesser protection and a recovery region with lower velocities and turbulence intensity. Very porous obstacles result in a very small degree of protection. Experiments have shown that the greatest area of velocity reduction for realistic protection occurs with a porosity of 40%, obtained with many uniform small openings in the barrier. The effectiveness does not decrease much as the porosity decreases to 20%, but it reduced much faster as the porosity increases above 40%. It is noted that the effect of porosity is the same whether obtained by use of wire mesh etc., or the planting of trees in a shelterbelt configuration. For "Artificial" shelterbelts, porosities

are classified roughly as "Dense" up to about 25%, "Medium" from 25% to 40%, "Loose" from 40% to 55% and "Very Loose" above 55%. Equivalent classifications for "Natural" belts are not available for most types of growth, however, W.M.O. (6) cites several types of hedges as "Dense", belts of Lombardy Poplar and Eucalyptus as "Medium", and high belts of thin Cottonwoods as "Very Loose".

(2) The downstream length of protected zones is roughly a linear function of shelterbelt height.

(3) Wind erosion of surface particles is observed to take place in three ways, "Surface Creep", that is rolling or slipping along the surface; "Saltation", in which the particles are lifted into the air stream and carried for varying distances by single gusts of wind; and "Suspension Transport", in which the particles travel as a suspension in the air. Estimates of the relative efficiency of the three mechanisms are available (6) and show that saltation is the major mechanism in wind-borne soil erosion and is the primary culprit in the present study. The effect of shelterbelts in its reduction is a prime consideration. A reduction in erosive capability of the wind is obtained when velocity gradients are attenuated. This is accomplished to an even greater degree than actual velocity reduction by the use of shelterbelts.

(4) A moderate dependence of shelterbelt effectiveness on belt length has been observed due to end effects. Experiments indicate that full effectiveness of the shelterbelt height H is not achieved for a distance of $6H$ from each end for a

flow perpendicular to the barrier, although 50% effectiveness is obtained at about 2H . Geometric variations in the shelterbelt greatly influence the area sheltered (5).

5.0 CRITERIA FOR SIMULATION AND DESCRIPTION OF EXPERIMENTS

Meroney and Plate (5) show that the wind tunnel modeling of wind breaks is valid if C_D (the wind break drag coefficient) and the ratio of wind break height to boundary layer thickness are the same for the model and the prototype. They also note that C_D is independent of Reynolds number for sharp edged wind breaks, and that the barrier height boundary layer thickness ratio is not critical, but can be adjusted by making the boundary layer as thick as possible. Jensen (2) suggests another criteria in terms of the surface roughness:

$$\left(\frac{H}{Z_o}\right)_{field} \sim \left(\frac{H}{Z_o}\right)_{model}$$

where H is the shelterbelt height and Z_o is the effective roughness. With those criteria as guides, wind tunnel measurements were performed in the low speed wind tunnel of the Fluid Dynamic and Diffusion Laboratory, Colorado State University. This tunnel has a 6ft x 6ft x 30ft test section. The model was located 19'-6" from the test section entrance. At this point the boundary layer thickness is approximately 12" for a free stream velocity of 45 ft per second. Velocity profiles are shown in Figure 40. The model scale was 1:250. A picture of the model is shown in Figure 39. The effective roughness determined from the upstream velocity profile was .0015 in. Field effective roughness at Rocky Flats was determined by Meroney and Chaudhry (4) to be $\simeq$1 cm $\simeq$ 0.4 in. Therefore, both sets of criteria are satisfied.

Variations in the following windbreak parameters were examined:

(1) Porosity

(a) Solid

(b) Medium (of approximately optimum value cited by W.M.O.)

(c) Very Loose

(2) Height

(a) 15 ft

(Prototype Heights)

(b) 30 ft

(3) Geometric Configuration

(a) "Straight Across", perpendicular to the wind direction

(b) 90° wedge

(c) 120° wedge

(d) Combinations of (a), (b) and (c) with breaks going "1/2 around" the parking lot

(e) Combinations of (a), (b) and (c) with breaks going "All Around" the parking lot

(f) "Straight Across" breaks dividing the parking lot into equal intervals

(4) Parking lot orientation

(a) Long side east and west

(b) Long side north and south

(5) Wind direction

(a) West

(b) Northwest

(6) Windbreak Length

The various porosities were obtained by using sheet metal and wire mesh strips. The solid barriers were modeled using No. 26 gauge sheet

metal, the medium porosity was obtained using J. C. Tyler Co. No. 865 ton cap type wire mesh, porosity ~39%, and wire diameter .025". The very loose porosity was duplicated using 18 x 14 mesh bronze screen, porosity ~68% and wire diameter 0.01".

The tests were conducted as follows. The parking lot was coated with a mixture of 97% common mineral oil and 3% zinc oxide, a flow visualization technique outlined by Maltby and Keating (3). The air flowing over the surface carries the entire mixture with it if the velocity and shear stress are high enough, leaving bare spots. For lesser velocities and shear rates the air is only able to move the mixture after a certain amount of the zinc oxide has settled from the suspension, thus reducing the effective viscosity. Thus the amount of zinc oxide remaining on the surface is an indication of the effectiveness of the windbreak in reducing surface shear and velocities. Photographs were taken of the parking lot with deposits of zinc oxide indicating relative zones of protection. Velocity profiles were taken at various locations to relate the various degrees of protection to quantitative information.

All tests were conducted at a free stream velocity of 45 ft per second, except that one test was conducted at 30 ft per second to ascertain whether the flow pattern was similar for different Reynolds numbers (thus, also different values of surface shear). Velocities were obtained using a pitot-static tube with a Transonic pressure transducer.

6.0 RESULTS OF EXPERIMENTS

The parking lot photographs indicated four degrees of relative protection based on the amount and character of the zinc oxide deposits remaining. These zones were converted to quantitative results by obtaining velocity profiles at points on the zone boundaries. The measure of protection chosen was to give the percentage ratio of the velocity measured at a prototype height of 3 feet at the zone boundary to that of the undisturbed velocity measured at that height. Three feet was chosen because it is far enough from the surface to give a measure of the velocity with which aggregates will be driven into the automobiles and close enough to the surface to give a measure of the surface velocity gradient. Descriptions of the relative velocity in the zones at a 3 ft height is shown in table X.

The results in general verify the conclusions advanced by the W.M.O. (6), with area of protection being approximately a linear function of barrier height, and barriers of medium porosity giving far superior protection to that offered by solid or loose belts. The least amount of protection is provided by a loose barrier as shown in Figure 41. Solid barriers provide protection only in the area immediately down-stream from the barrier. The pattern of protection down-stream from a barrier of medium porosity is shown in Figures 42 and 43.

Wedge shaped barriers of 90^{o} and 120^{o} included angle were tested and found to provide increased protection downstream and at the edges of the parking lot. However, a "Wedge Effect" resulting in an erosion zone in the central portion of the area is shown in Figure 44. The wedge effect was found to be more severe for a 90^{o} wedge. In general,

it was found that a "Straight Across" barrier provided better protection for distances less than 9H downstream, where H is the barrier height, while a 120^{o} wedge was better for distances greater than 9H. Figures 45 and 46 show the effect of placing barriers in an "All Around" configuration in conjunction with a 120^{o} wedge. A 30 ft barrier height in this configuration provides zone 1 protection to almost the entire area. "1/2 Around" configurations, with the front half of the area protected, proved to be only a slight improvement over a single barrier at the west edge.

Tests were also conducted with the parking lot oriented with the long side running north and south. As shown in Figure 47, a 30 ft barrier provides zone 1 protection to almost the entire area. Two equally spaced barriers 15 ft high provide good protection as shown in Figure 48. However, this height reduction to 15 ft causes the appearance of zones 2 and 4 at the downstream edge of the lot as shown in the figure. Three equally spaced barriers 15 ft high were tested with an east-west lot orientation and results were very similar to those obtained for two 15 ft barriers and a north-south orientation.

The previously described tests were all conducted with a west wind. To demonstrate the influence of wind direction, tests were also conducted for a northwest wind for "All Around" configurations with an east-west parking lot orientation, and for a single barrier with north-south parking lot orientation and having extensions of various lengths and orientations. The results for the "All Around" configuration were comparable to those obtained with a west wind, while the best protection provided with a single barrier was obtained with the arrangement depicted in Figure 49.

7.0 CONCLUSIONS AND RECOMMENDATIONS

1. Shelterbelts of medium porosity (approximately 40%) are recommended. If wire mesh is used this should be obtained through the use of many small uniform openings. If "Natural" Shelterbelts are used, the previously cited information from W.M.O. (6) should be considered.
2. If protection from westerly winds only is desired, the most effective solution is a reorientation of the parking lot to long side running north-south and the use of a single 30 ft barrier at the west edge or equally spaced smaller barriers whose heights add to 30 ft (two 15 ft, three 10 ft barriers etc.). If protection from northwest (or southwest) winds is also desired, extensions such as shown in Figure 49 are recommended.
3. If reorientation of the parking lot is not feasible, an "All Around" configuration with a 120^{o} wedge 30 ft high provides the best protection, with the added benefit of affording protection from winds of all directions. Following this arrangement in order of effectiveness are equally spaced smaller barriers within the parking lot whose heights add to 45 ft, a single 120^{o} wedge 30 ft high, and a 120^{o} wedge with "All Around" configuration 15 ft high.
4. Although only a limited number of cases were examined, sufficient data is available to show that a single barrier of height H at the west edge of the parking lot can be replaced with equally spaced smaller barriers in the interior

of the lot whose heights add to H. The only protection loss with this arrangement is the appearance of zones 2 and 4 at the downstream edge as shown in Figure 48.

REFERENCES

(1) Chepil, W. S., "The Use of Evenly Spaced Hemispheres to Evaluate Aerodynamic Forces on a Soil Surface," Transactions American Geophysical Union, 39, No. 3, June 1958.

(2) Jensen, M., "The Model Law for Phenomena in Natural Wind," Ingenieren-Internat. Edit., 2, No. 4.

(3) Maltby, R. L. and Keating, R. F. A., "Flow Visualization in Low Speed Wind Tunnels: Current British Practice," Technical Note Aeror 2715, Royal Aircraft Establishment, Farmborough, England, August 1960.

(4) Meroney, R. N. and Chaudhry, F. H., "Wind Tunnel Site Analysis of Dow Chemical Facility at Rocky Flats, Colorado," Colorado State University, Report Number CER71-72RNM-FC45, May 1972.

(5) Meroney, R. N. and Plate, E. J., "Wind Tunnel Investigation of Shapes for Balloon Shelters," Colorado State University, Report Number CEP71-72RNM-EJP37, January 1972.

(6) World Meteorological Association, "Windbreaks and Shelterbelts," Technical Note No. 59, 1964.

TABLE I WEST AND NORTHWEST WIND VERTICAL VARIATION OF CONCENTRATION AT PLUME AXIS

Source	x=1167'		x=2667'		x=4167'		x=6167'	
#6 N.W. Wind	Z	Conc	Z	Conc	Z	Conc	Z	Conc
	0	14467	0	5750	0	2710	0	1568
	42	9592	42	6438	42	3312	42	1690
	83	4078	83	4418	83	3122	83	1522
	125	1300	125	3063	167	2420	167	1074
	167	140	167	1935	250	1935	250	920
	250	52	250	435	333	1222	333	795
	333	36	333	181	417	612	417	295
	417	-	417	14	542	140	542	72
					667	-	667	-

Source	x=1000'		x=2500'		x=4000'		x=6000'	
#7 N.W.Wind	Z	Conc	Z	Conc	Z	Conc	Z	Conc
	0	16216	0	5836	0	2383	0	1482
	42	12845	42	6090	42	2569	42	1676
	83	6538	83	4780	83	2057	83	1414
	125	2053	125	3543	169	1908	167	1359
	167	390	167	2628	250	1508	250	965
	250	102	250	856	333	923	333	575
	333	23	333	231	417	440	417	353
	417	-	417	72	542	118	542	109
			542	-	667	17	667	-

Source #6	x=1200'		x=2700'		x=4700'		x=7200'		x=10200'	
#7	x=1000'		x=2500'		x=4500'		x=7000'		x=10000'	
W. Wind	Z	Conc	Z	Conc	Z	Conc	Z	Conc	Z	Conc
	0	18305	0	6049	0	3194	0	1169	0	884
	42	20104	42	6928	42	3679	42	1572	42	938
	83	15156	83	5467	83	3181	83	1513	83	748
	167	2148	167	2864	167	2492	167	1214	167	630
	250	-	250	838	250	1604	250	766	250	458
			333	185	333	435	333	367	417	213
			417	63	417	367	417	281	542	136
			542	-	542	-	542	59	667	-

TABLE II EAST AND NORTHEAST WIND VERTICAL VARIATION OF CONCENTRATION AT PLUME AXIS

Source	x=1000'		x=2500'		x=4000'		x=6000'	
	Z	Conc	Z	Conc	Z	Conc	Z	Conc
#6 East Wind	0	21001	0	9520	0	5206	0	2516
	42	17521	42	8990	42	4259	42	2845
	83	8659	83	6901	83	3412	83	2333
	125	1989	125	4794	167	2170	167	1858
	167	485	167	3303	250	920	250	1228
	250	53	250	983	333	213	333	843
	333	36	333	208	417	50	417	426
	417	-	417	45	542	-	542	82

Source	x=1000'		x=2500'		x=4000'		x=6000	
	Z	Conc	Z	Conc	Z	Conc	Z	Conc
#6 N.E. Wind	0	19710	0	6108	0	3838	0	1912
	42	22166	42	6701	42	4191	42	2451
	83	12678	83	6090	83	3145	83	2166
	125	4363	125	4223	167	2084	167	1622
	167	543	167	2501	250	1038	250	1038
	250	102	250	788	333	421	333	648
	333	63	333	172	417	72	417	231
	417	14	417	23	542	23	542	59

Source	x=1200'		x=2700'		x=4200'		x=6200'	
	Z	Conc	Z	Conc	Z	Conc	Z	Conc
#7 East Wind	0	22007	0	8246	0	5206	0	2516
	42	17345	42	7888	42	4259	42	2845
	83	10938	83	6452	83	3412	83	2333
	125	3208	125	4640	167	2170	167	1858
	167	874	167	2922	250	920	250	1228
	250	91	250	956	333	213	333	843
	333	59	333	267	417	50	417	426
	417	-	417	45	542	-	542	82

Source	x=1125'		x=2625'		x=4125'		x=6125'	
	Z	Conc	Z	Conc	Z	Conc	Z	Conc
#7 N.E. Wind	0	16416	0	5437	0	3154	0	2053
	42	13321	42	5904	42	3090	42	2084
	83	7009	83	4078	83	2723	83	1667
	125	2406	125	2791	167	1609	167	1097
	167	340	167	1554	250	766	250	684
	250	92	250	449	333	240	333	449
	333	14	333	50	417	50	417	159
	417	-	417	36	542	14	542	95

TABLE III SOUTHEAST WIND VERTICAL VARIATION OF CONCENTRATION AT PLUME AXIS

Source	x=1000'		x=2500'		x=4000'		x=6000'		Source	x=1000'		x=2500'		x=4000'		x=6000'	
	Z	Conc	Z	Conc	Z	Conc	Z	Conc		Z	Conc	Z	Conc	Z	Conc	Z	Conc
# 1	0	26543	0	7118	0	2397	0	1613	# 2	0	20598	0	5437	0	3235	0	1980
	42	20580	42	6855	42	2293	42	1436		42	22306	42	4708	42	2719	42	1948
	83	6778	83	6140	83	2252	83	1572		83	16284	83	4381	83	2528	83	1935
	125	761	125	3838	125	1681	125	1110		125	4853	125	2456	125	1763	125	1500
	167	199	167	2524	167	1332	167	874		167	1001	167	1663	167	1260	167	1119
	250	36	250	589	250	421	250	548		250	210	250	421	250	575	250	761
	375	-	375	-	375	59	375	195		333	50	333	59	333	23	333	195
					500	-	500	95		417	-	417	36	458	14	458	118
																583	58

Source	x=1000'		x=2500'		x=4000'		x=5500'		Source	x=1000'		x=2500'		x=4000'		x=6000'	
	Z	Conc	Z	Conc	Z	Conc	Z	Conc		Z	Conc	Z	Conc	Z	Conc	Z	Conc
# 3	0	20457	0	6692	0	3937	0	2066	# 4	0	31799	0	8777	0	4178	0	2166
	42	13937	42	6173	42	3158	42	1989		42	16728	42	7322	42	3507	42	2152
	83	13018	83	5129	83	2904	83	2179		83	8912	83	6914	83	3629	83	2311
	125	6584	125	3018	125	2324	125	1776		125	1871	125	3706	125	2515	125	1980
	167	1722	167	1885	167	1545	167	1346		167	399	167	1994	167	2089	167	1436
	250	72	250	449	250	729	250	689		250	27	250	335	250	788	250	775
	333	-	333	36	333	195	375	267		333	-	333	36	333	50	333	472
			417	14	417	82	500	23				458	-	458	36	458	213
																573	93

Source	x=1000'		x=2500'		x=4000'		x=6000'		Source	x=1000'		x=2500'		x=4000'		x=6000'	
	Z	Conc	Z	Conc	Z	Conc	Z	Conc		Z	Conc	Z	Conc	Z	Conc	Z	Conc
# 5	0	59	0	1382	0	1726	0	1382	# 6	0	20915	0	7164	0	3480	0	1853
	83	870	83	1690	83	1609	83	1369		42	14635	42	6266	42	3865	42	1944
	167	6828	167	3376	167	1717	167	1341		83	10526	83	4730	83	3208	83	1753
	333	8523	333	2836	333	1323	333	1110		125	2895	125	2895	125	2478	125	1396
	417	779	417	1169	417	920	417	612		167	707	167	2003	167	2039	167	884
	500	180	500	113	500	353	500	462		250	41	250	381	250	716	250	521
	583	3 36	583	14	583	72	583	208		333	-	333	100	333	340	333	159
	667	23	667	-	667	59	667	72				458	14	458	82	458	72

Source	x=1167'		x=2667'		x=4167'		x=6167'	
	Z	Conc	Z	Conc	Z	Conc	Z	Conc
# 7	0	13267	0	6049	0	3036	0	1880
	42	9071	42	5755	42	3194	42	2012
	83	6429	83	4803	83	2710	83	1667
	125	1631	125	2945	125	2111	125	1337
	167	458	167	1849	167	1898	167	1169
	250	27	250	575	250	507	250	775
	333	14	333	145	333	340	375	440
	458	14	458	45	458	109	500	72

TABLE IV SOUTHWEST WIND VERTICAL VARIATION OF CONCENTRATION AT PLUME AXIS

Source	x=1000'		x=2500'		x=4000'		x=6000'	
	Z	Conc	Z	Conc	Z	Conc	Z	Conc
# 1	0	34535	0	8405	0	4477	0	2510
	42	32700	42	9619	42	4699	42	2397
	83	12397	83	7544	83	3983	83	2252
	125	2157	125	5079	125	3267	125	1858
	167	308	167	3634	167	1708	167	1368
	250	54	250	956	250	788	250	648
	333	23	333	72	375	222	375	512
	458	-	458	-	500	-	500	131
							625	45

Source	x=1000'		x=2500'		x=4000'		x=6000'	
	Z	Conc	Z	Conc	Z	Conc	Z	Conc
# 2	0	19139	0	6892	0	2868	0	1898
	42	22401	42	7019	42	2746	42	2188
	83	15496	83	5691	83	2654	83	1812
	125	8065	125	4150	125	1513	125	1405
	167	2546	167	3009	208	847	208	743
	250	54	250	1029	333	140	333	381
	333	23	333	304	458	14	458	222
	458	-	458	-	583	-	583	23

Source	x=1000'		x=2500'		x=4000'		x=6000'	
	Z	Conc	Z	Conc	Z	Conc	Z	Conc
# 3	0	24590	0	6135	0	3135	0	1753
	42	20163	42	5850	42	3484	42	1831
	83	9982	83	4150	83	2963	83	1658
	125	2456	125	2565	125	2383	125	1486
	167	788	167	1722	167	2111	208	1060
	250	27	250	367	250	1377	333	435
	333	-	333	36	375	331	458	181
			458	-	500	82	583	23

Source	x= 1000'		x=2500'		x=4000'		x=6000'	
	Z	Conc	Z	Conc	Z	Conc	Z	Conc
# 4	0	59333	0	10394	0	4649	0	2066
	42	30924	42	9479	42	4690	42	2972
	83	9823	83	5433	83	3072	83	2261
	125	2053	125	3063	125	2361	125	2324
	167	222	167	1731	208	1015	208	1849
	250	72	250	603	291	181	291	1137
	333	50	333	100	417	72	417	671
	458	14	458	-	542	-	542	236
							667	54

Source	x=1000'		x=2500'		x=4000'		x=6000'	
	Z	Conc	Z	Conc	Z	Conc	Z	Conc
# 5 Stack	0	326	0	1681	0	1495	0	1067
	83	1332	83	3000	83	1069	83	1377
	167	7458	167	3498	167	1441	167	1137
	250	11436	250	2111	250	1382	292	988
	333	5297	333	1169	333	1074	417	720
	417	507	417	308	417	634	542	295
	500	36	542	-	542	245	667	136
	583	36			667	109	792	14

Source	X=1125'		x=2625'		x=4125'		X=6125'	
	Z	Conc	Z	Conc	Z	Conc	Z	Conc
# 6	0	19470	0	5863	0	3095	0	2238
	42	22157	42	6244	42	4087	42	2256
	83	10793	83	4404	83	3389	83	2021
	125	3266	125	2148	125	2836	125	1681
	167	648	208	802	208	2098	208	1251
	250	110	291	54	291	915	291	648
	333	36	417	36	417	281	417	340
	458	-	667	-	667	36	667	95

Source	x=1000'		x=2500'		x=4000'		x=6000'	
	Z	Conc	Z	Conc	Z	Conc	Z	Conc
# 7	0	17920	0	5292	0	1341	0	1667
	42	17879	42	5093	42	3543	42	1772
	83	13099	83	3788	83	2959	83	1658
	125	6656	125	2814	125	2605	125	1405
	167	2524	167	1640	208	1998	167	1155
	250	140	250	562	291	1051	250	870
	333	36	333	136	417	272	375	258
	458	14	458	-	542	53	500	72

TABLE V WEST AND NORTHWEST WIND GROUND LEVEL CONCENTRATIONS

Source	x=1200'		x=2700'		x=4700'		x=7200'		x=10200'	
	Y	Conc	Y	Conc	Y	Conc	Y	Conc	Y	Conc
# 6 West Wind	354	27	354	127	833	-	833	23	917	27
	229	2397	187	1862	666	59	666	426	583	140
	146	5360	62	4114	500	498	416	947	250	603
	62	11092	-21	5795	292	1377	166	1377	0	893
	-21	18038	-146	7105	125	2383	0	1527	-167	1060
	-104	19660	-271	5446	0	3171	-83	1731	-417	983
	-187	14014	-438	2284	-83	4010	-250	1436	-750	295
	-312	7327	-645	852	-208	2660	-500	1110	-1084	72
	-396	2664	-812	544	-375	893	-750	507		
	-521	2121	-937	222	-583	308	-917	159		
	-646	621	-1062	82	-750	249	-1084	23		
	-771	50			-917	86				

Source	x=1167'		x=2667'		x=4167'		x=6167'	
	Y	Conc	Y	Conc	Y	Conc	Y	Conc
# 6 North-west Wind	375	154	542	-	437	72	792	-
	208	1853	354	557	229	127	542	59
	83	9678	187	3842	62	2043	417	299
	0	19284	62	4952	-62	2478	167	1228
	-83	21078	-62	6407	-187	3185	0	1717
	-208	14119	-145	6384	-354	3362	-125	1885
	-333	2918	-270	3040	-562	462	-208	1649
	-500	711	-437	526	-770	72	-375	1042
	-667	-	-604	140			-583	526
							-833	272
							-1000	159
							-1250	118

Source	x=1000'		x=2500'		x=4500'		x=7000'		x=10000'	
	Y	Conc	Y	Conc	Y	Conc	Y	Conc	Y	Conc
# 7 West Wind	375	20	333	113	833	-	833	23	917	27
	333	272	167	2139	666	59	666	426	583	140
	208	6730	42	4137	500	498	416	947	250	603
	83	16651	-42	6298	292	1377	166	1377	0	893
	-42	19837	-167	6869	125	2383	0	1527	-167	1060
	-125	16212	-292	5727	0	3171	-83	1731	-417	983
	-208	9307	-458	2284	-83	4010	-250	1436	-750	295
	-375	3276	-625	911	-208	2660	-500	1110	-1084	72
	-542	1944	-750	544	-375	893	-750	507		
	-583	1826	-875	222	-583	308	-917	159		
	-708	575	-1000	82	-750	249	-1084	23		
	-833	86			-917	86				

Source	x=1000'		x=2500'		x=4000'		x=6000'	
	Y	Conc	Y	Conc	Y	Conc	Y	Conc
# 7 North-West Wind	500	-	479	199	562	-	1042	41
	333	68	312	2025	354	126	792	45
	208	2166	187	3579	187	1232	542	299
	125	9443	62	5378	62	1799	292	893
	42	18192	-21	6239	-62	2737	125	1477
	-83	18967	-146	4490	-239	3067	0	1658
	-208	5351	-313	671	-447	621	-83	1862
	-375	1445	-480	45	-655	72	-250	1296
	-542	-					-458	793
							-708	136
							-1125	31

TABLE VI EAST AND NORTHEAST WIND GROUND LEVEL CONCENTRATIONS

Source	x=1000'		x=2500'		x=4000'		x=6000'	
	Y	Conc	Y	Conc	Y	Conc	Y	Conc
# 6 East Wind	292	-	458	72	625	-	667	41
	167	4005	292	766	417	231	417	127
	62	19007	125	4744	208	2238	208	544
	-42	41658	0	8532	42	3770	0	1513
	-125	20879	-125	10471	-83	5224	-208	2759
	-250	979	-250	5632	-250	4812	-458	2673
	-375	-	-417	390	-458	1232	-708	865
			-583	36	-667	118	-958	23

Source	x=1000'		x=2500'		x=4000'		x=6000'	
	Y	Conc	Y	Conc	Y	Conc	Y	Conc
# 6 North-East Wind	375	299	583	92	625	102	917	71
	208	13937	458	657	583	258	792	308
	83	25541	292	4735	375	1862	583	671
	-42	9633	125	7893	167	4323	417	2166
	-125	2383	0	6620	0	4055	250	2696
	-250	86	-125	4613	-125	3548	125	2288
	-375	-	-250	1971	-292	902	0	2003
			-487	353	-500	14	-167	1309
			-583	23			-333	353
							-542	45

Source	x=1200'		x=2700'		x=4200'		x=6000'	
	Y	Conc	Y	Conc	Y	Conc	Y	Conc
# 7 East Wind	313	-	479	-	645	14	687	-
	187	1717	313	557	437	208	437	267
	83	9107	146	3376	229	1065	229	877
	-21	26470	21	6611	62	2814	21	1835
	-104	22800	-104	9289	-62	4350	-187	2700
	-313	6452	-229	6914	-229	5587	-396	2238
	-480	131	-396	1051	-437	2759	-646	1015
			-563	95	-646	285	-896	36
					-750	-		

Source	x=1125'		x=2625'		x=4125'		x-6125'	
	Y	Conc	Y	Conc	Y	Conc	Y	Conc
# 7 North East Wind	542	140	625	71	750	140	917	-
	375	5650	583	385	542	1445	833	213
	250	17793	417	3009	333	3620	625	1794
	125	21023	250	6235	167	3770	458	2333
	42	17598	125	5927	42	1790	292	2121
	-83	10253	0	6466	-125	2306	167	2030
	-208	2273	-125	5011	-333	512	0	1844
	-375	59	-292	1686	-542	154	-167	1305
			-458	367	-667	101	-375	630
			-500	52	-917	62	-583	172
							-917	75

TABLE VII SOUTHEAST WIND GROUND LEVEL CONCENTRATIONS

Source	x=1000'		x=2500'		x=4000'		x=6000'	
	Y	Conc	Y	Conc	Y	Conc	Y	Conc
# 1	333	41	709	59	833	-	750	72
	208	5881	292	4005	667	285	500	766
	125	34322	167	9411	417	1237	250	1840
	42	41155	42	8052	250	2732	83	1835
	-42	19497	-42	6606	125	3385	0	2003
	-125	2759	-167	2886	0	3054	-167	1658
	-208	267	-292	1137	-125	2646	-417	634
	-417	-	-458	-	-292	1296	-667	109
					-542	190	-750	31
					-625	22		

Source	x=1000'		x=2500'		x=4000'		x=6000'	
	Y	Conc	Y	Conc	Y	Conc	Y	Conc
# 2	500	14	667	-	667	27	854	118
	333	3838	500	399	458	440	688	258
	208	18486	333	2293	292	2107	438	1065
	125	36461	208	6347	125	4522	230	2007
	42	27666	83	8749	0	4789	62	2478
	-42	14554	0	8165	-167	3167	-62	2796
	-125	5251	-125	6420	-375	720	230	1704
	-208	1246	-292	2959	-583	72	438	548
			-458	344			688	72
			-625	13				

Source	x=1000'		x=2500'		x=4000'		x=6000'	
	Y	Conc	Y	Conc	Y	Conc	Y	Conc
# 3	333	-	500	113	625	27	730	100
	208	671	292	924	375	335	480	140
	125	6742	125	3969	167	2623	229	630
	42	22451	0	7290	0	4327	62	1373
	-42	26266	-83	9551	-125	4554	-62	1980
	-125	15732	-208	8070	-292	3122	-229	2333
	-208	5415	-417	1953	-500	707	-480	1210
	-333	285	-625	403	-750	177	-730	249
	-417	-	-750	113	-917	23	-959	45

Source	x=1000'		x=2500'		x=4000'		x=6000'	
	Y	Conc	Y	Conc	Y	Conc	Y	Conc
# 4	333	27	583	-	583	-	667	24
	208	2003	459	412	562	72	625	100
	125	18011	250	3693	354	1110	375	1087
	42	59284	125	6828	187	3072	167	2456
	-42	54381	42	7802	62	4114	0	2895
	-125	15392	-42	8971	-62	5070	-125	2972
	-208	4703	-125	10226	-187	5392	-292	1831
	-333	-	-250	2651	-354	2261	-458	684
			-417	770	-562	476	-709	118
			-583	23	-625	53	-750	64

Source	x=1000'		x=2500'		x=4000'		x=6000'		x=7500'	
	Y	Conc	Y	Conc	Y	Conc	Y	Conc	Y	Conc
# 5	83	-	417	-	542	27	688	-	688	41
	0	36	250	150	333	313	438	476	458	394
	-62	82	125	761	167	979	229	1029	229	942
	-125	95	0	1205	0	1609	62	1337	62	1178
	-208	-	-125	1473	-125	1604	-62	1296	-62	1237
			-250	856	-292	915	-229	1237	-229	1047
			-375	353	-458	295	-438	648	-458	720
			-500	59	-625	82	-688	131	-688	263
							-833	-	-917	15

Source	x=1000'		x=2500'		x=4000'		x=6000'	
	Y	Conc	Y	Conc	Y	Conc	Y	Conc
# 6	458	27	542	-	645	72	833	27
	292	127	333	394	395	172	583	82
	167	4209	167	3738	187	2782	333	861
	62	14372	83	6466	83	2873	125	1763
	-42	22773	-21	8414	-42	4033	0	2053
	-167	21613	-146	7689	-208	3548	-208	2193
	-292	8464	-313	3299	-458	1454	-458	1355
	-500	449	-521	476	-709	426	-709	557
	-709	-	-709	-	-917	14	-959	145
							-1209	45

Source	x=1167'		x=2667'		x=4167'		x=6167'	
	Y	Conc	Y	Conc	Y	Conc	Y	Conc
# 7	500	-	625	-	771	59	709	14
	333	843	417	444	521	285	458	313
	167	13901	208	4771	271	2198	208	1051
	42	19751	42	6633	62	3425	0	1894
	-62	18002	-42	6371	-42	3244	-125	1898
	-167	13783	-146	5165	-167	2796	-333	1477
	-292	8604	-354	2714	-333	1704	-583	662
	-417	3054	-521	1223	-542	829	-833	285
	-625	177	-729	118	-792	199	-1083	36
	-667	22	-750	-	-917	23		

TABLE VIII SOUTHWEST WIND GROUND LEVEL CONCENTRATIONS

Source	x=1000'		x=2500'		x=4000'		x=6000'	
	Y	Conc	Y	Conc	Y	Conc	Y	Conc
# 1	333	59	458	14	583	59	667	14
	125	2216	250	1101	333	335	417	372
	42	21178	83	4576	125	1658	167	2333
	-42	32220	0	8450	0	2981	0	2039
	-125	21939	-83	8142	-83	4164	-125	1817
	-208	4984	-292	4558	-250	4490	-333	1155
	-333	381	-458	1024	-417	2247	-583	503
	-417	-	-625	36	-625	72	-833	95
							-917	-

Source	x=1000'		x=2500'		x=4000'		x=6000'	
	Y	Conc	Y	Conc	Y	Conc	Y	Conc
# 2	375	27	521	-	875	-	1000	100
	250	1355	313	104	625	739	667	797
	125	5170	146	2832	375	1631	417	1550
	42	13067	21	5714	167	2478	167	1894
	-42	14912	-62	7648	0	3113	0	2062
	-125	20553	-187	6642	-167	3589	-250	1309
	-250	24436	-354	2392	-375	3752	-500	392
	-375	7354	-604	557	-625	639	-833	82
	-500	82	-792	-	-833	36	-917	18
	-709	36						

Source	x=1000'		x=2500'		x=4000'		x=6000'	
	Y	Conc	Y	Conc	Y	Conc	Y	Conc
# 3	375	-	688	41	875	86	1837	48
	250	150	438	3031	583	485	1125	285
	125	3353	271	6090	333	2855	875	498
	42	18890	146	7372	125	3901	625	1192
	-42	30589	62	7648	0	3598	375	1609
	-125	18672	-21	7349	-125	1772	167	1989
	-250	4767	-187	4264	-333	381	0	2121
	-375	227	-396	1210	-583	36	-167	1844
	-500	36	-625	-			-417	195
							-667	36

Source	x=1000'		x=2500'		x=4000'		x=6000'	
	Y	Conc	Y	Conc	Y	Conc	Y	Conc
# 4 Oil Site	333	-	458	41	833	14	833	41
	208	45	250	6937	625	335	583	349
	125	3231	83	13928	500	1137	333	1622
	42	32279	0	13185	375	2179	83	2515
	-42	71581	-83	11821	208	4164	-83	2039
	-125	37680	-208	7676	42	5813	333	888
	-208	4377	-375	929	0	5800	583	208
	-333	59	-583	-	-83	4794	833	72
					-250	3018		
					-417	449		
					-625	100		
					-833	59		

Source	x=1000'		x=2500'		x=4000'		x=6000'	
	Y	Conc	Y	Conc	Y	Conc	Y	Conc
# 5 Stack	187	-	625	86	833	86	875	41
	104	50	458	245	583	240	625	290
	42	72	292	920	375	1296	458	689
	0	104	167	1527	208	1849	333	1001
	-62	54	83	1921	83	1300	208	1391
	-146	36	0	2193	0	1169	42	1364
	-271	14	-125	1686	-125	603	-167	453
			-292	440	-292	222	-417	154
			-542	-	-500	23	-833	52

Source	x=1125'		x=2625'		x=4125'		x=6125'	
	Y	Conc	Y	Conc	Y	Conc	Y	Conc
# 6	625	27	1000	118	1042	45	1542	14
	417	2972	833	684	875	199	1375	159
	250	9071	583	4758	625	1803	1084	580
	125	16969	375	6343	375	3956	833	1622
	42	9325	208	6516	208	3208	625	2574
	-83	1531	83	6149	83	1613	500	2546
	-250	36	-42	4150	-83	716	333	2166
	-458	-	-250	865	-333	159	83	965
			-500	45	-583	72	-208	412
							-458	122
							-709	23

Source	x=1000'		x=2500'		x=4000'		x=6000'	
	Y	Conc	Y	Conc	Y	Conc	Y	Conc
# 7	542	72	917	-	959	72	1712	59
	333	91	667	1880	709	580	1209	313
	167	3099	417	5917	500	3376	959	893
	42	18119	208	6561	333	4830	709	1876
	-42	18002	42	4005	250	4232	542	1953
	-167	4785	-83	1935	83	1717	458	2111
	-333	159	-208	689	-125	598	292	1491
	-542	59	-417	50	-375	36	42	331
			-667	-			-208	199
							-667	98

TABLE IX NONDIMENSIONAL CONCENTRATIONS AT INNER AND OUTER PLANT BOUNDARIES

	Source Number	# 1		# 2		# 3		(Oil Site) # 4		(Stack) # 5		# 6		# 7	
Wind Direction		Inner	Outer	Inner	Outer	Inner	Outer	Inner	Outer	Inner	Outer	Inner	Outer	Inner	Outer
Southwest		5400	2080	10800	1440	21600	1520	64000	5500	104	1280	10800	1880	10400	1520
Southeast		5000	1380	11600	2000	15200	1920	6450	1680	880	1210	38000	2160	30400	1900
East		FOR VALUES IN THIS REGION SEE PREVIOUS REPORT										52000	4900	27000	4600
Northeast												12000	2720	7400	2320
Northwest												4100	1680	3920	1520
West												4400	2280	4480	2320

TABLE X CORRELATION OF PROTECTION ZONES TO VELOCITIES AS PERCENT OF AMBIENT

Zone No.	Velocity Range As Percent of Ambient
1	0 - 25%
2	25 - 45%
3	45 - 70%
4	70 - 100%

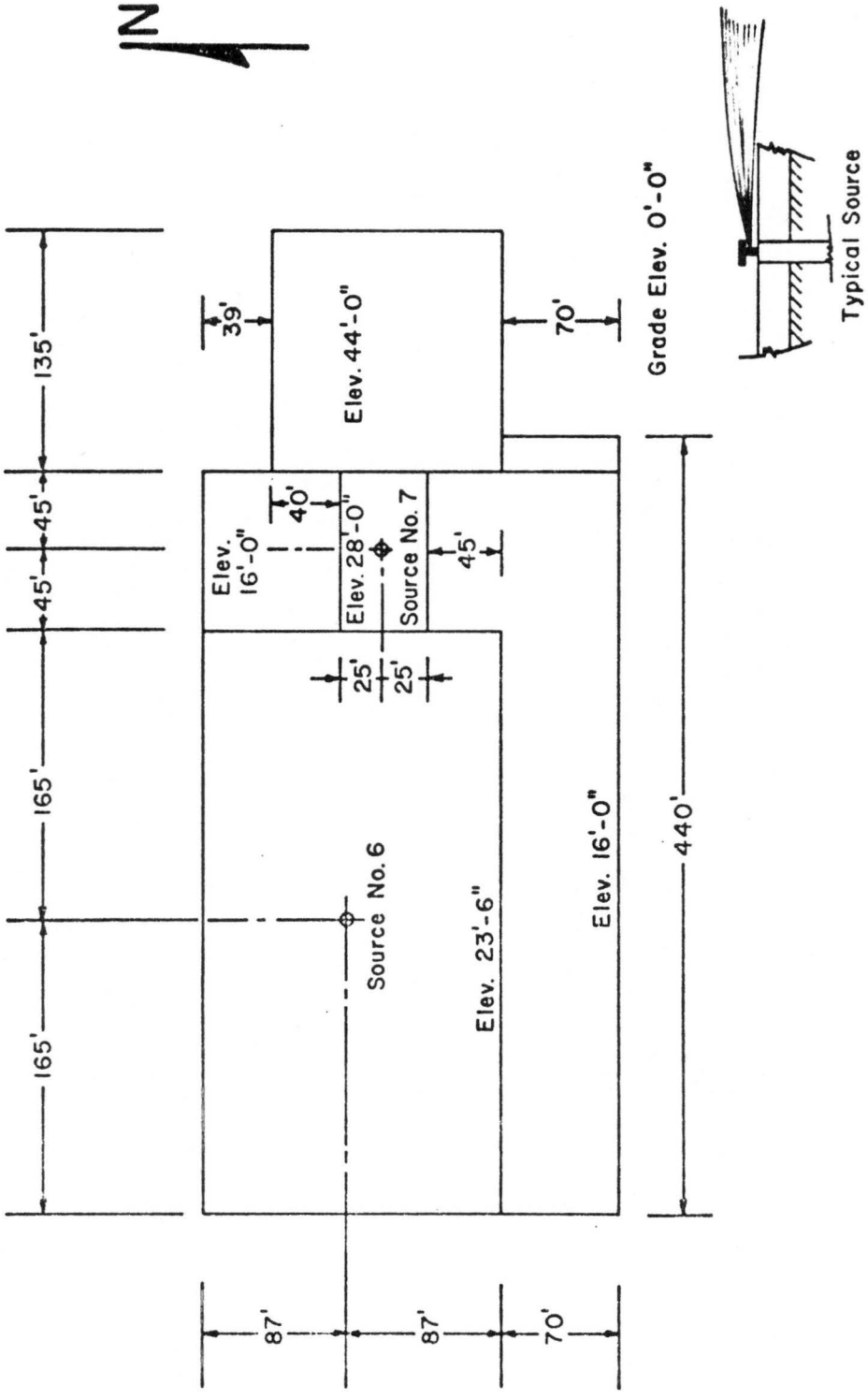

Fig. 1. Bldg. No. 371 - Source Nos. 6 and 7

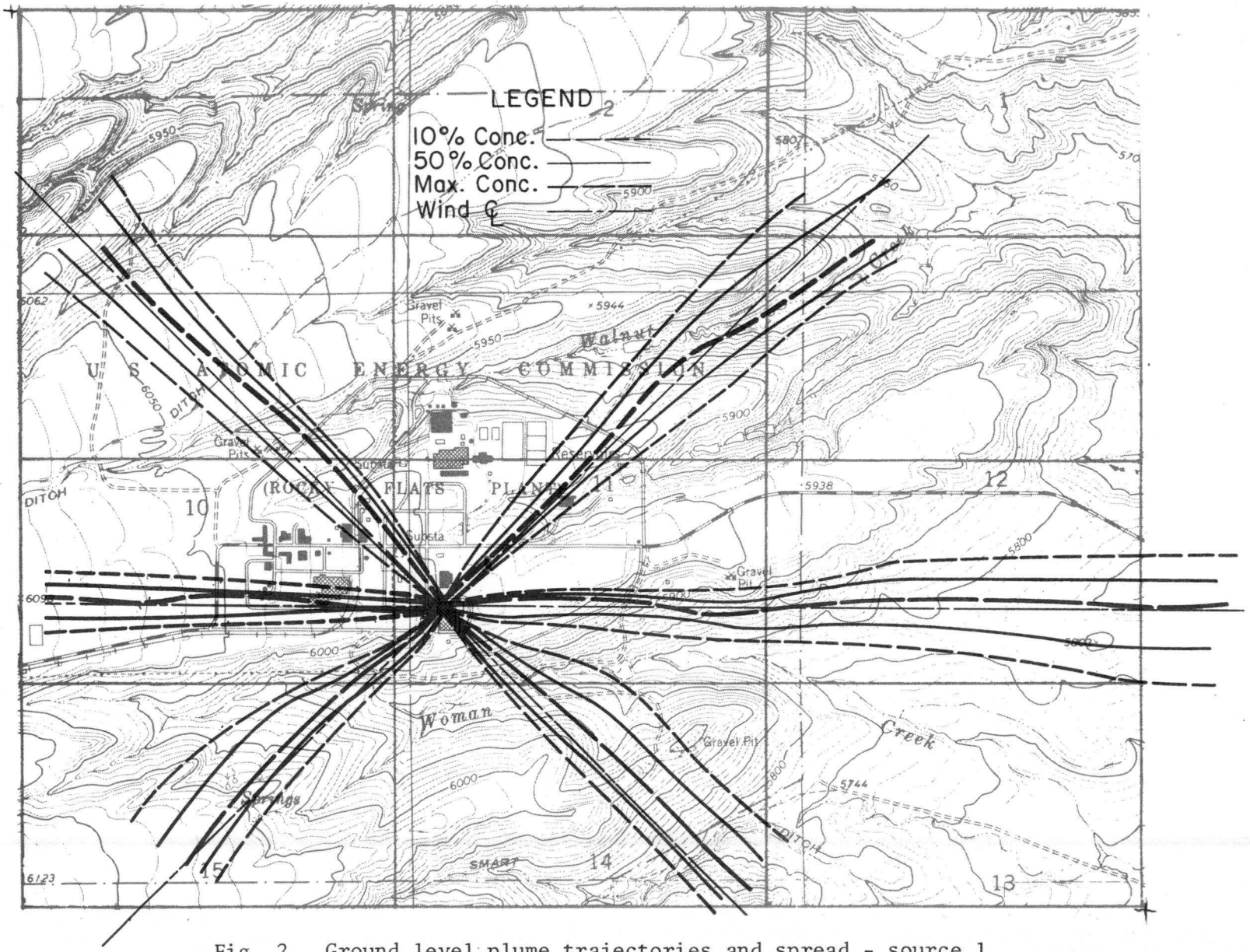

Fig. 2. Ground level plume trajectories and spread - source 1

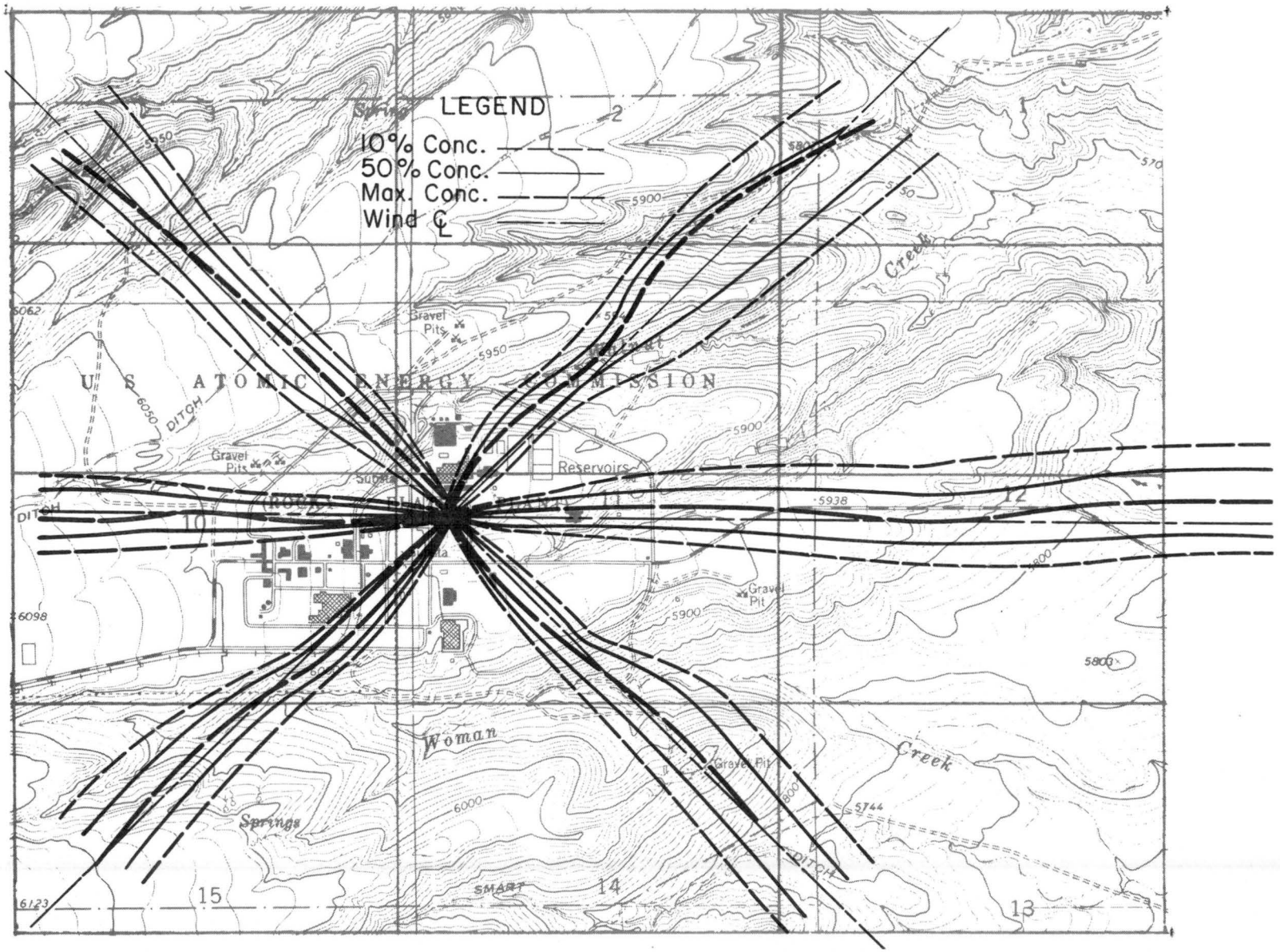

Fig. 3. Ground level plume trajectories and spread - source 2

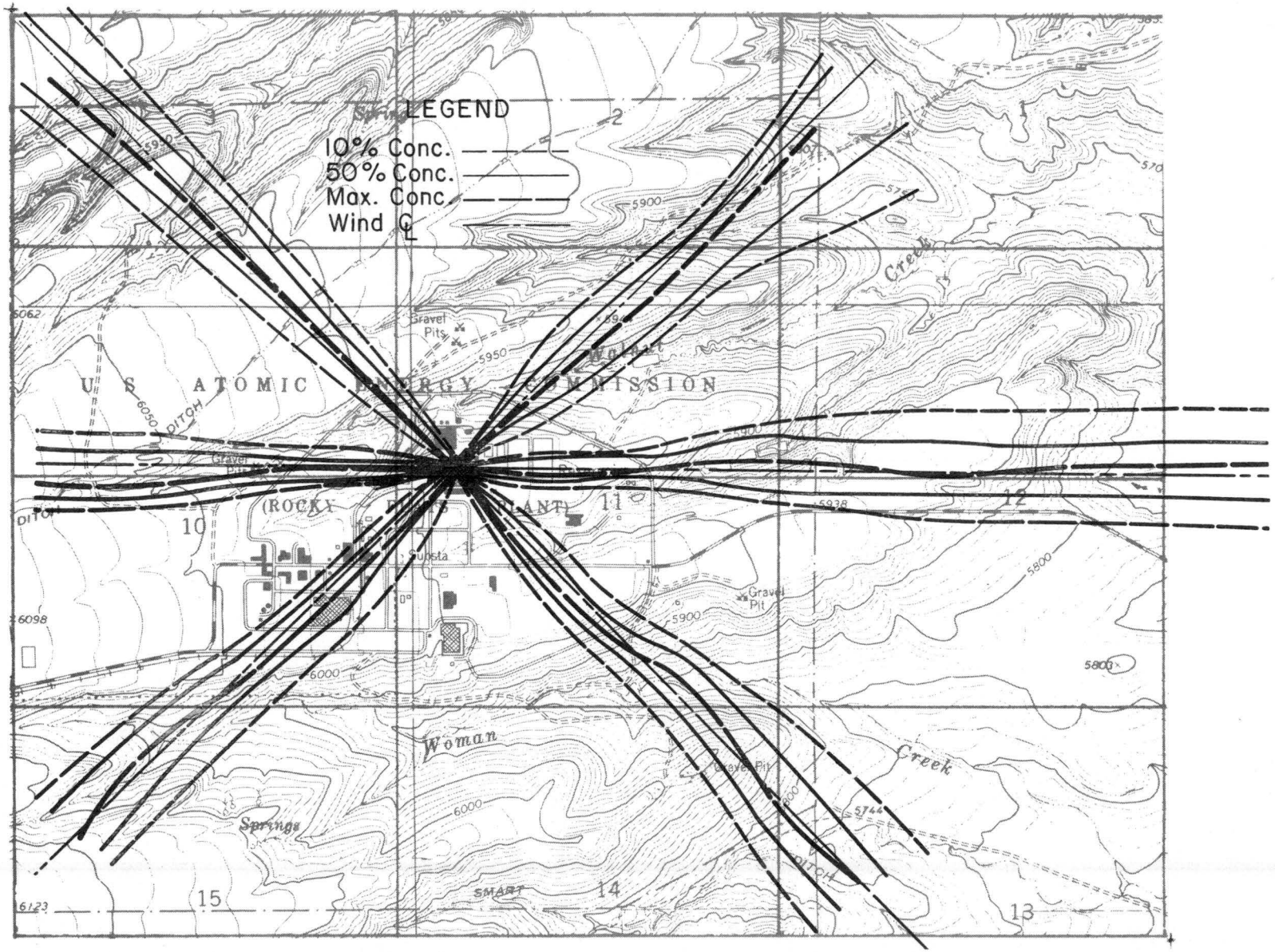

Fig. 4. Ground level plume trajectories and spread - source 3

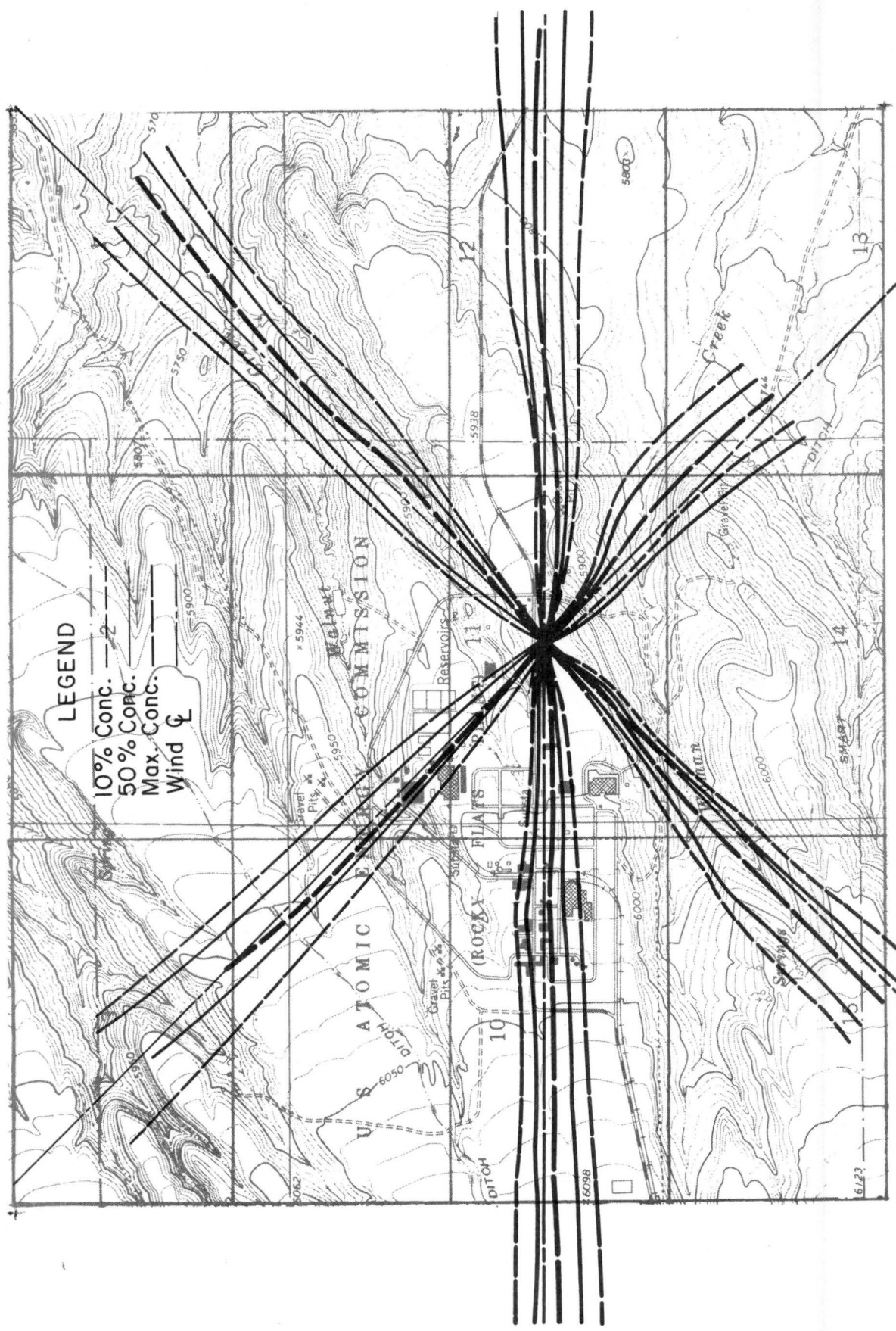

Fig. 5. Ground level plume trajectories and spread - source 4

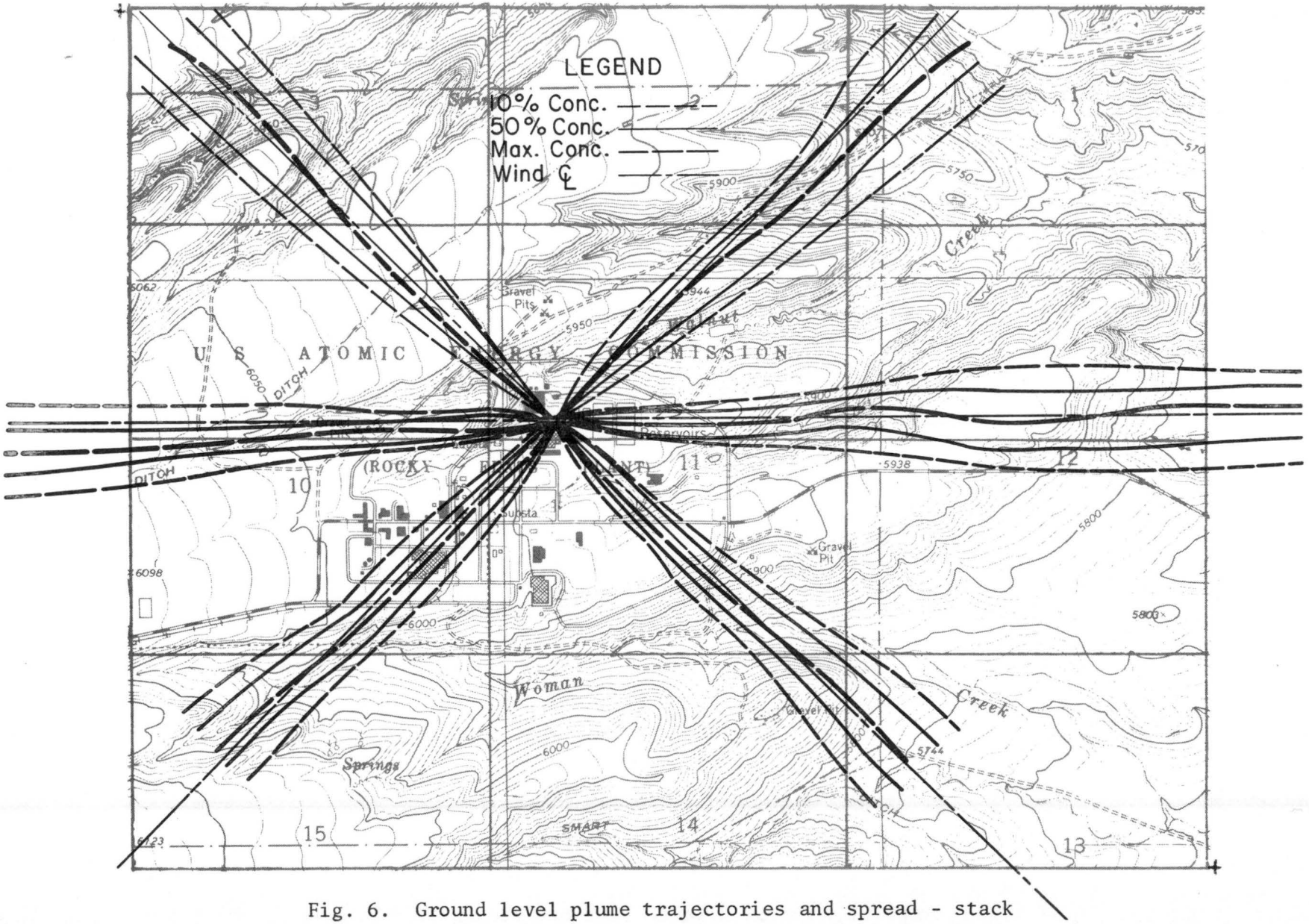

Fig. 6. Ground level plume trajectories and spread - stack

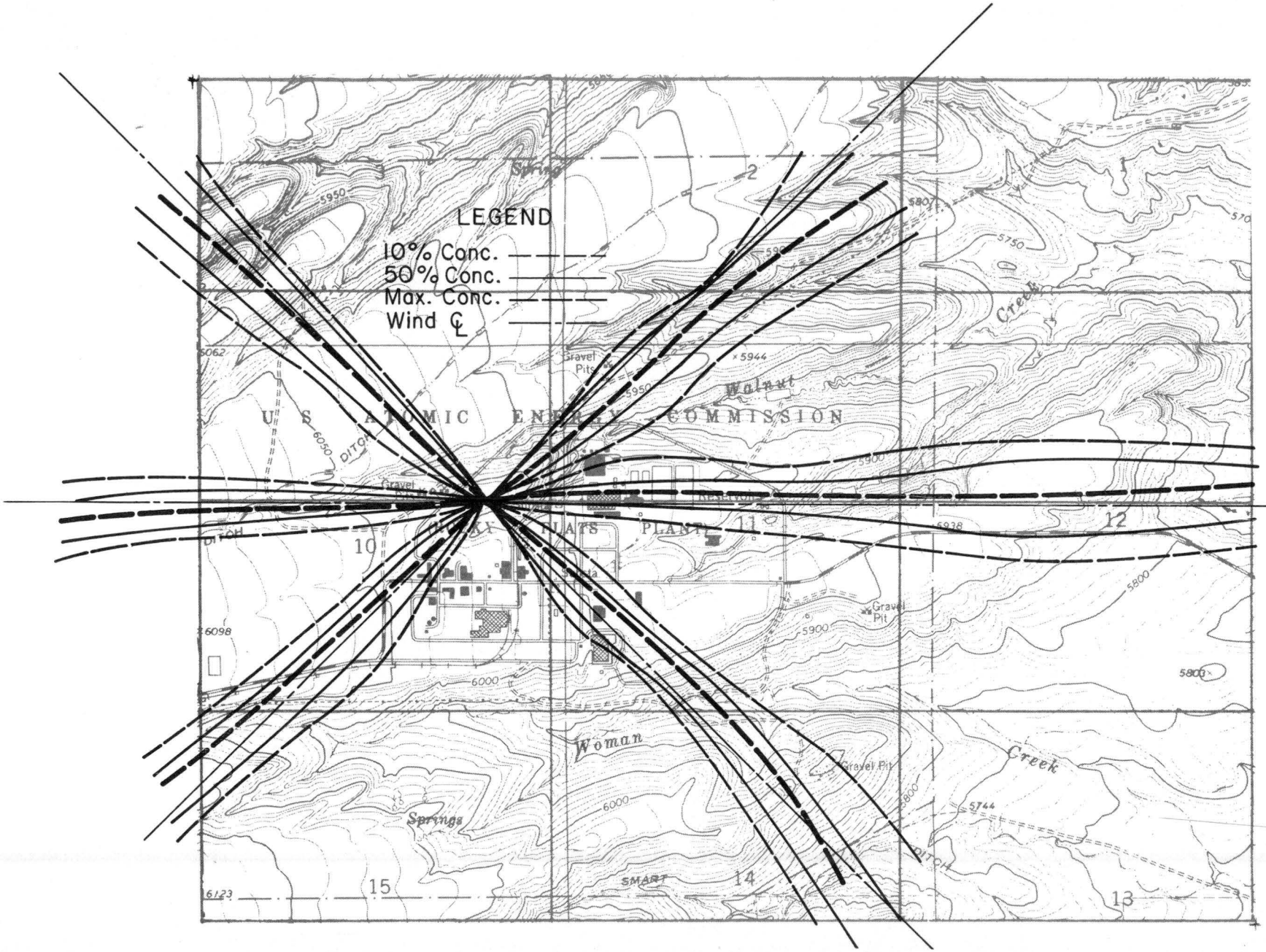

Fig. 7. Ground level plume trajectories and spread - source 6

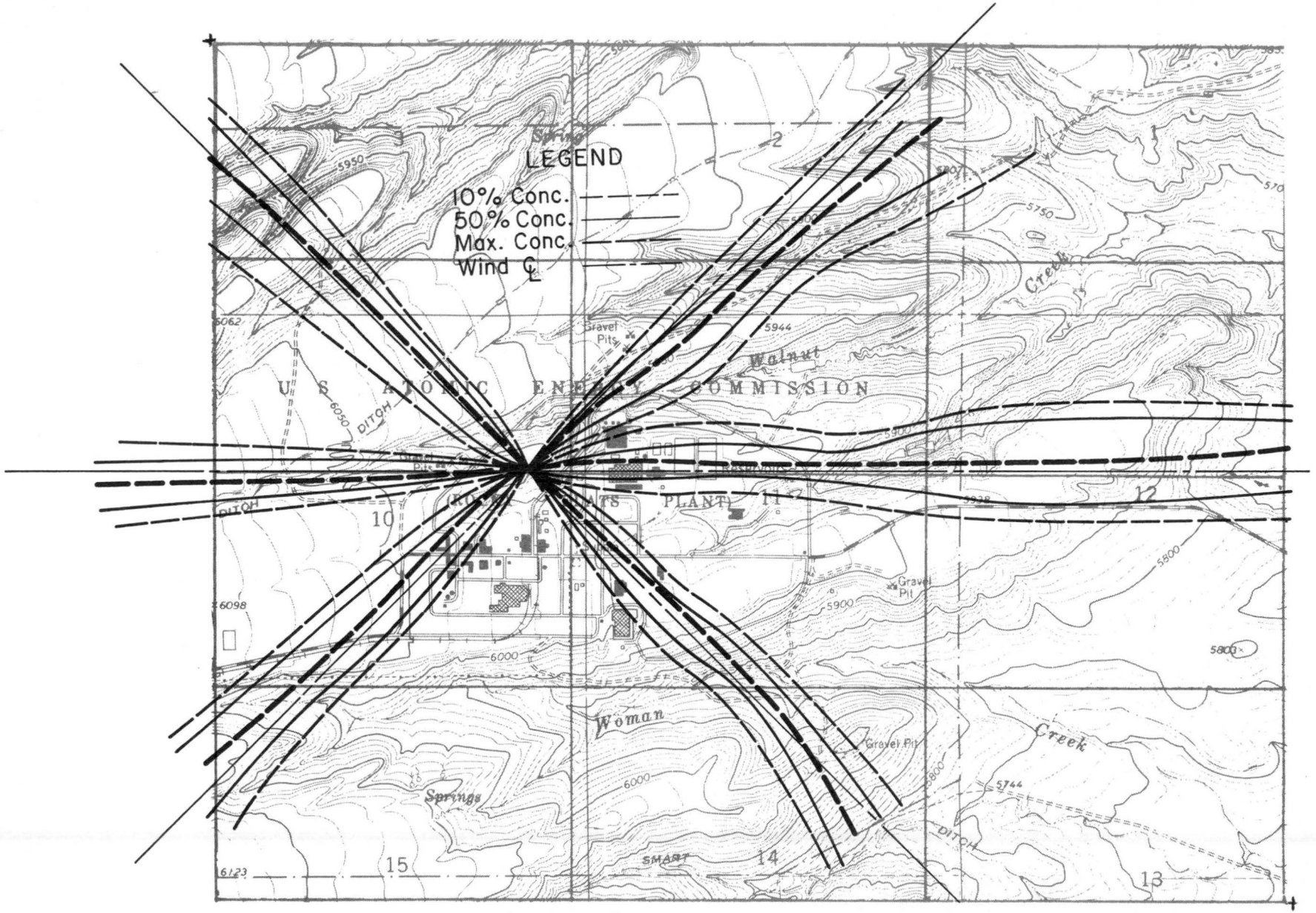

Fig. 8. Ground level plume trajectories and spread - source 7

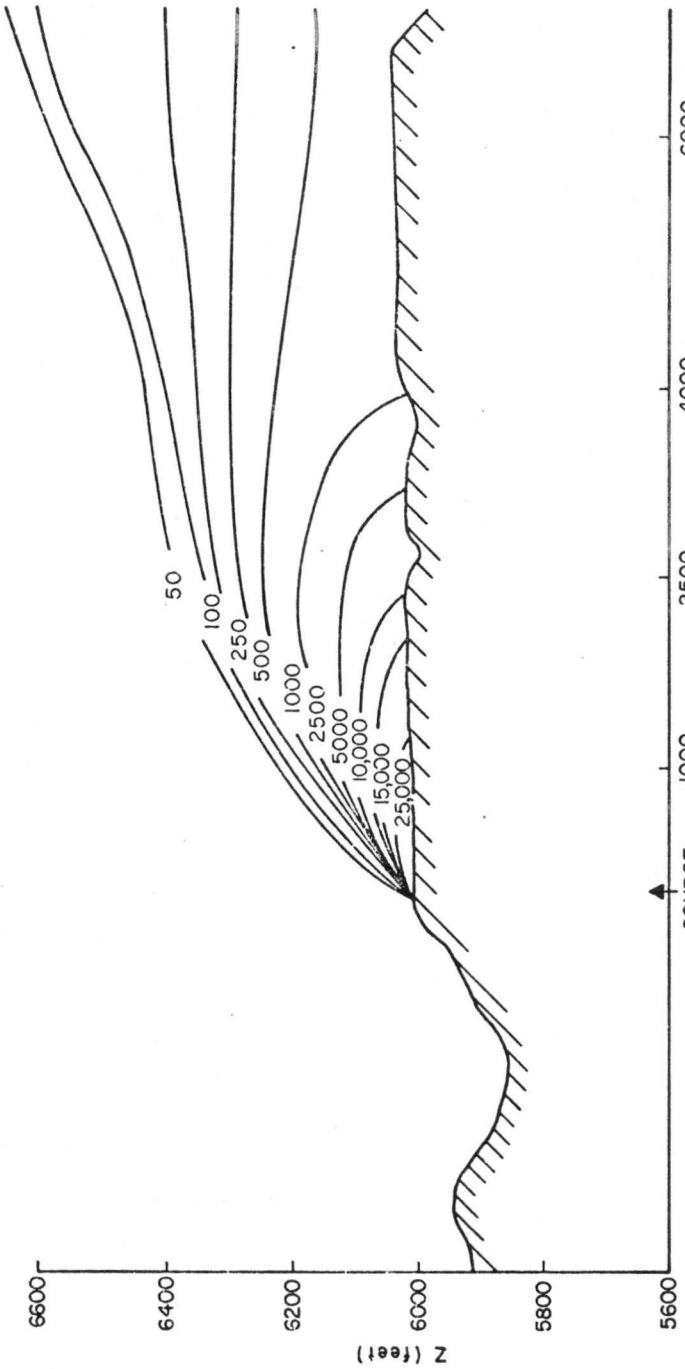

Fig. 9. Vertical concentration isopleth - source 1, wind orientation SE

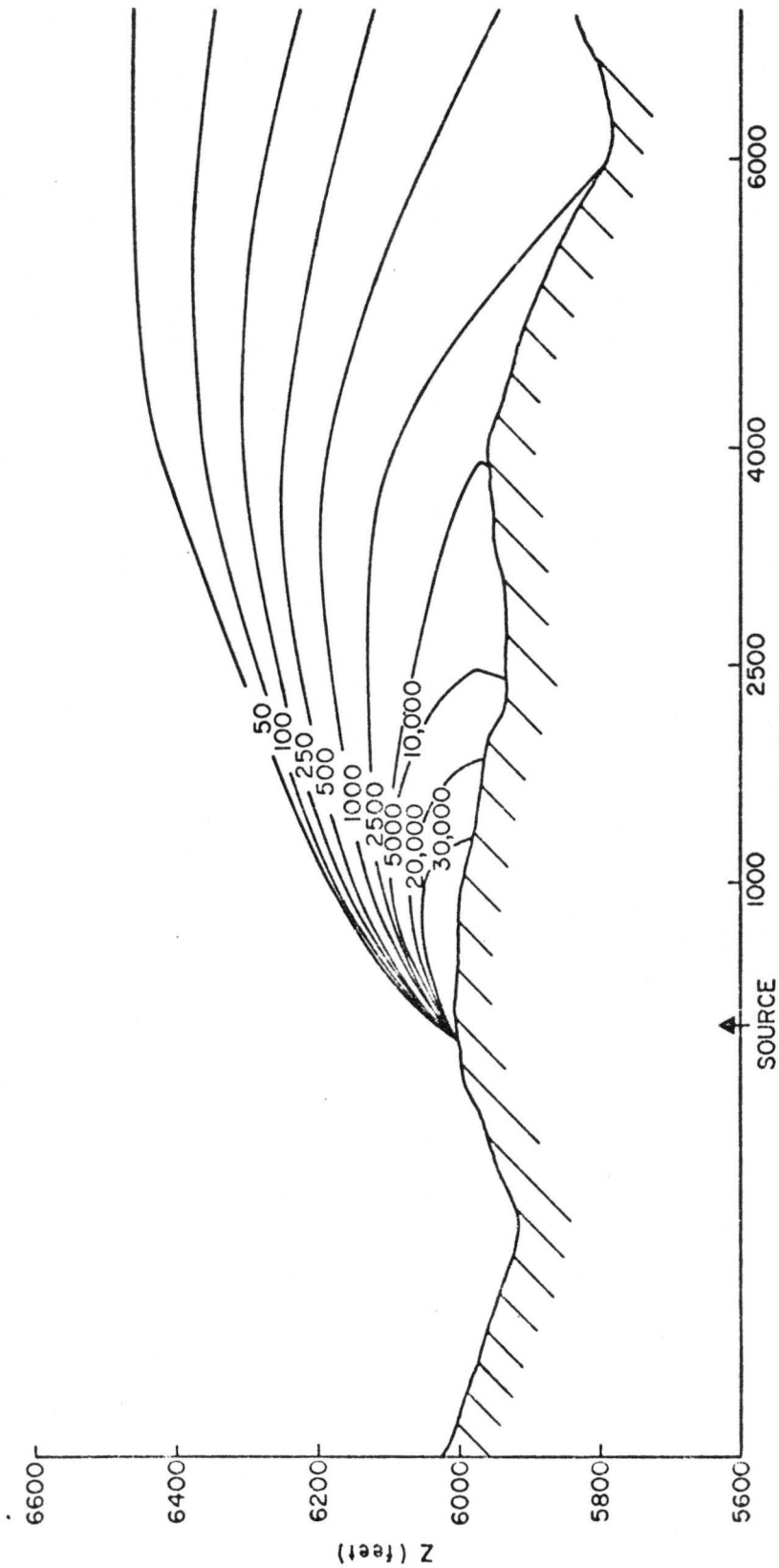

Fig. 10. Vertical concentration isopleth - source 1, wind orientation SW

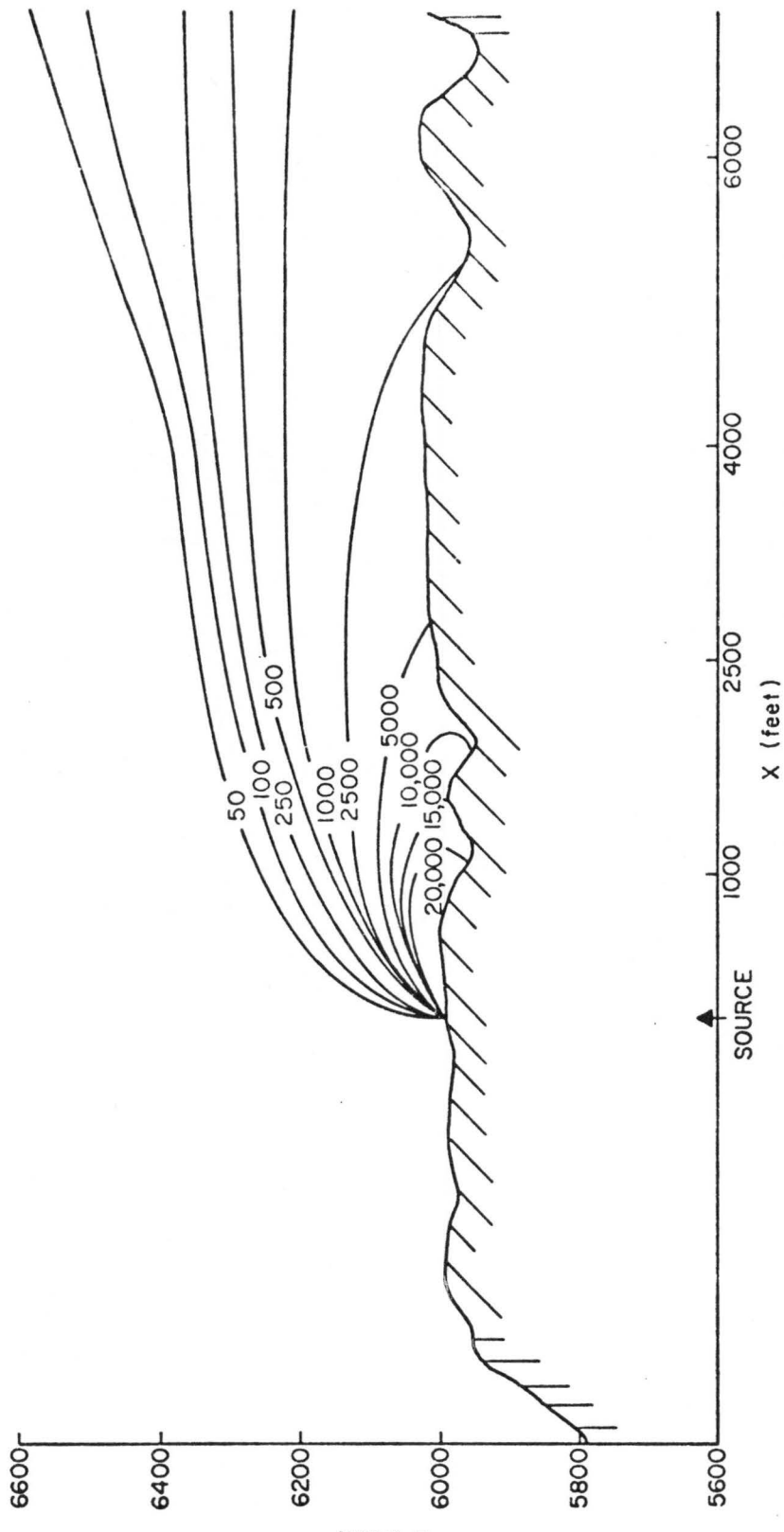

Fig. 11. Vertical concentration isopleth - source 2, wind orientation SE

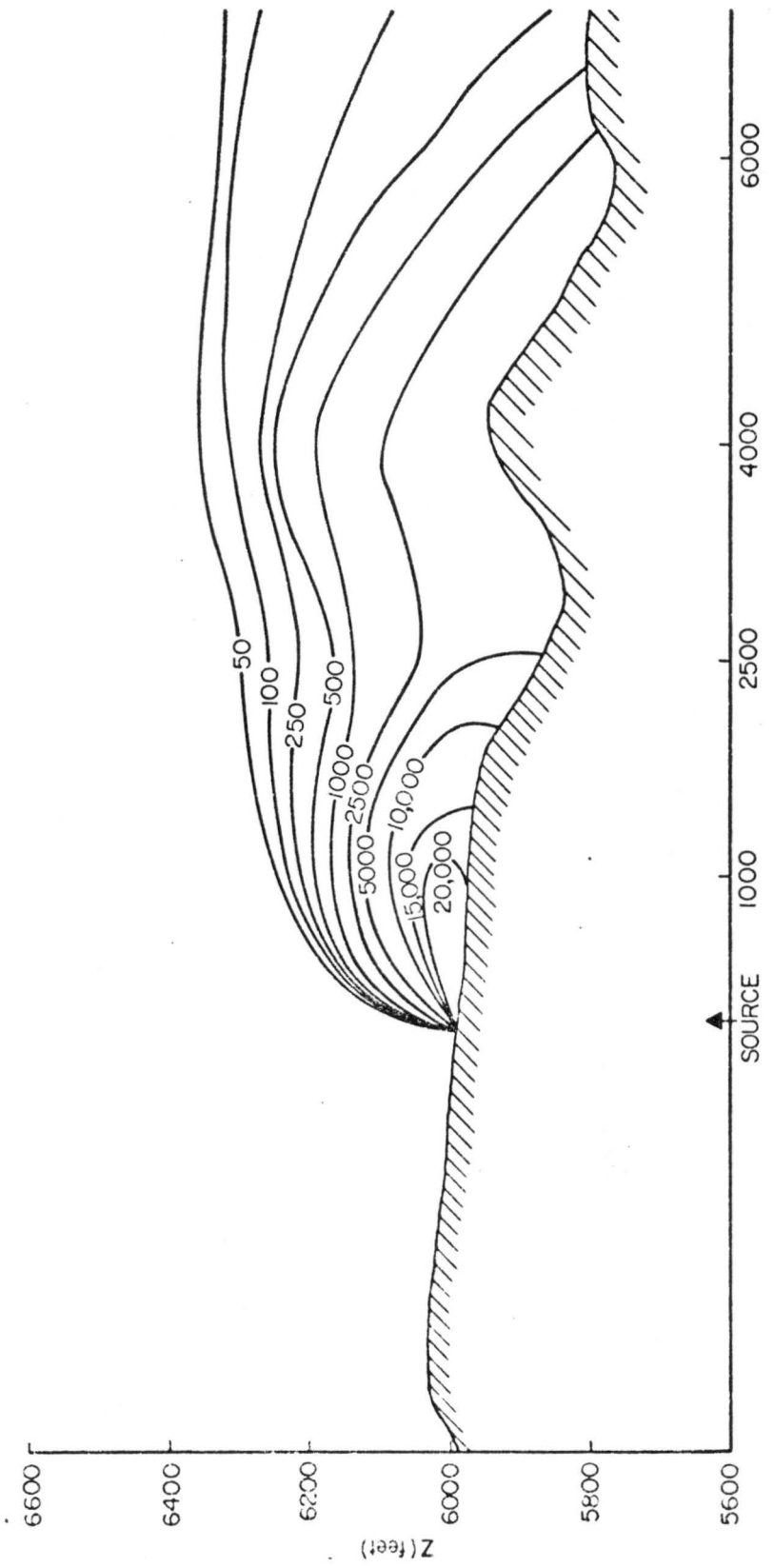

Fig. 12. Vertical concentration isopleth - source 2, wind oreintation SW

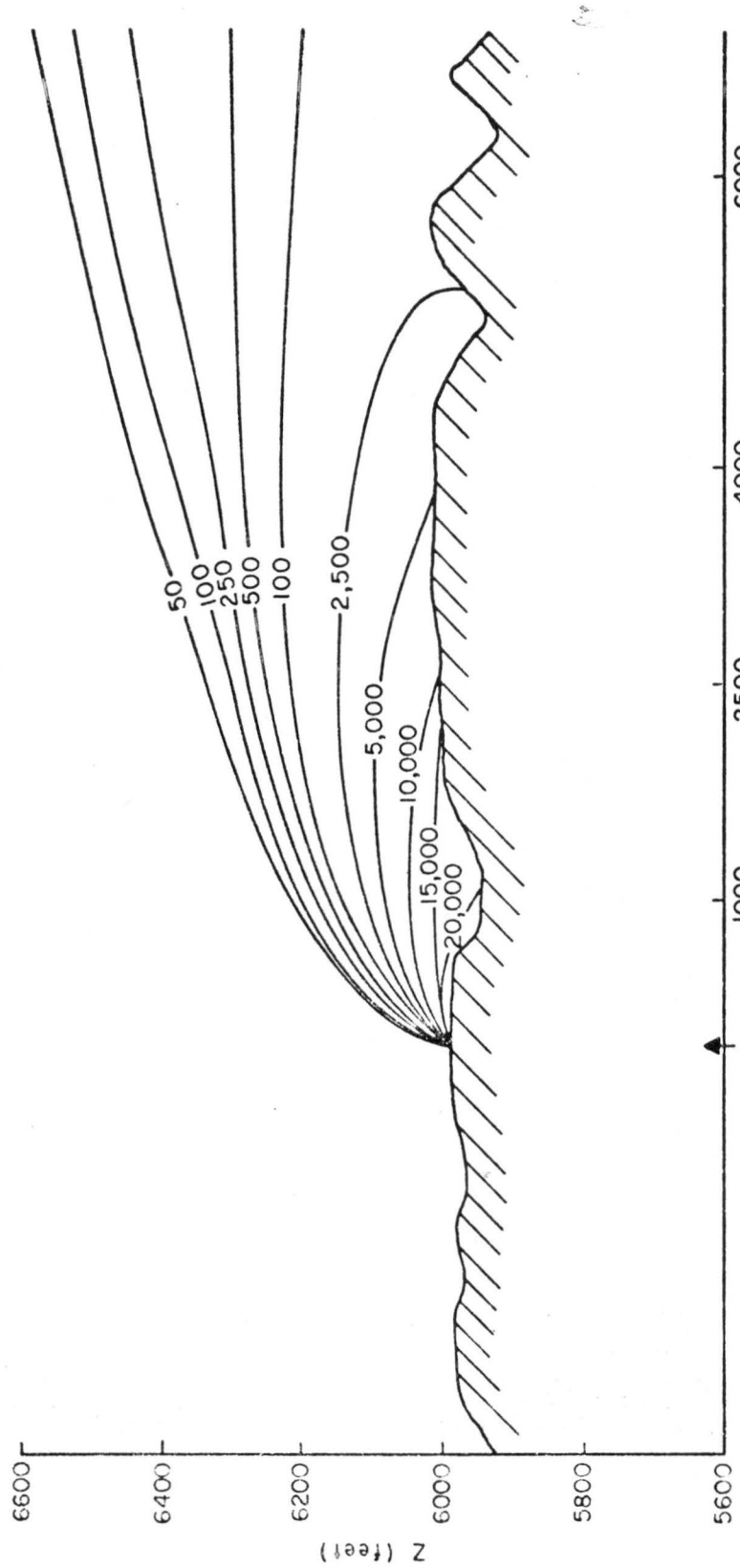

Fig. 13. Vertical concentration isopleth - source 3, wind orientation SE

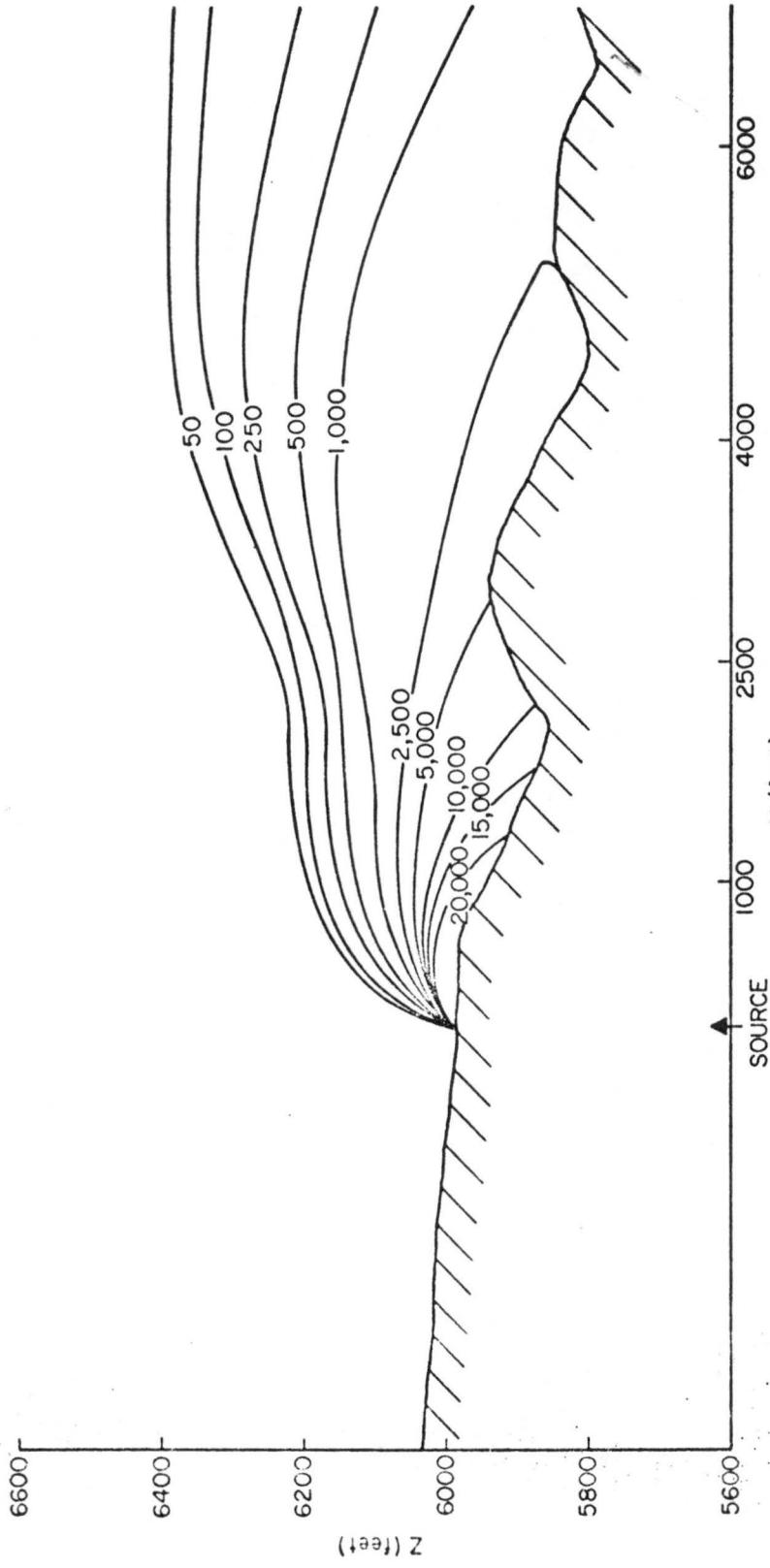

Fig. 14. Vertical concentration ispoleth - source 3, wind orientation SW

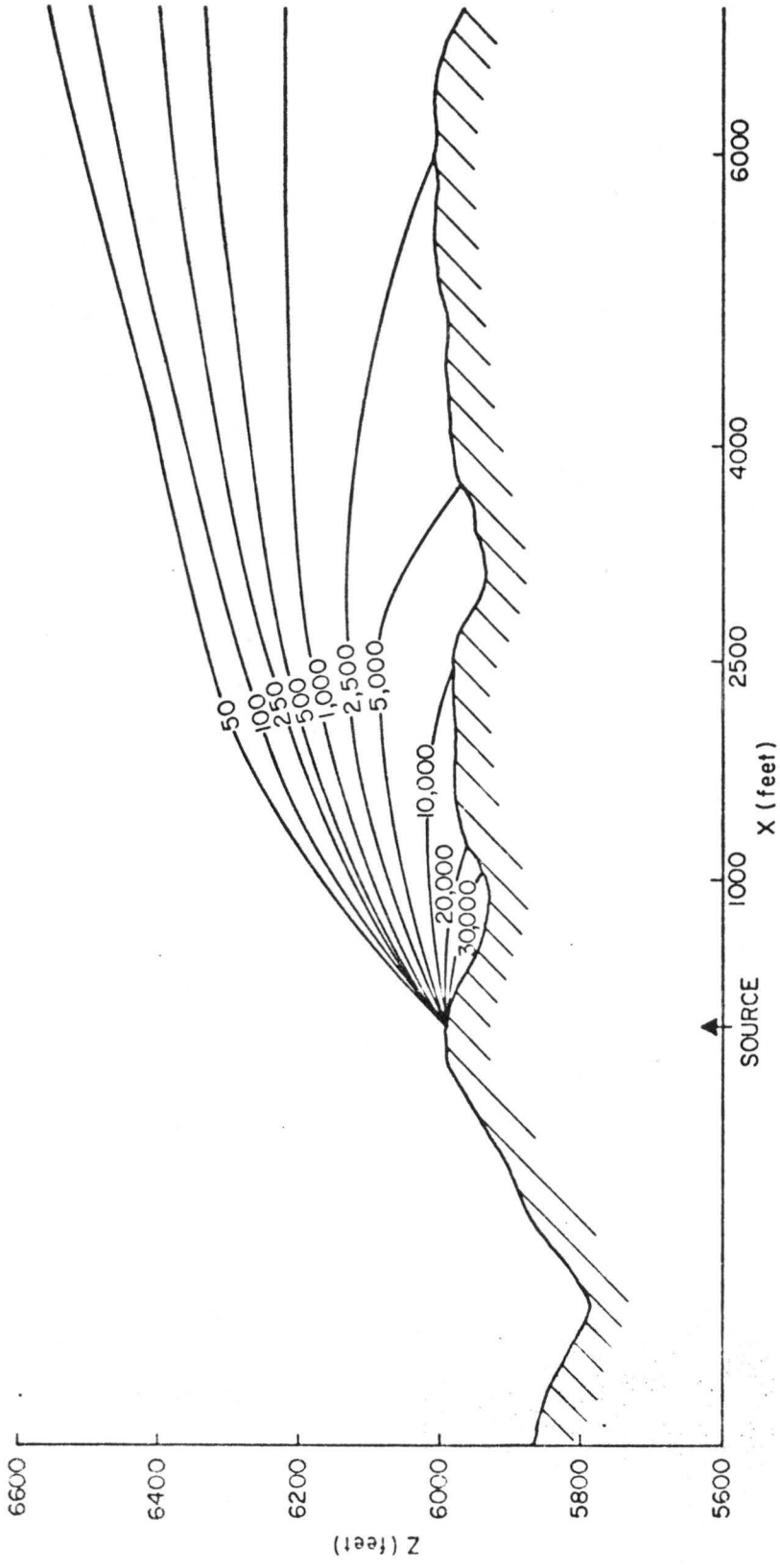

Fig. 15. Vertical concentration isopleth - source 4, wind orientation SE

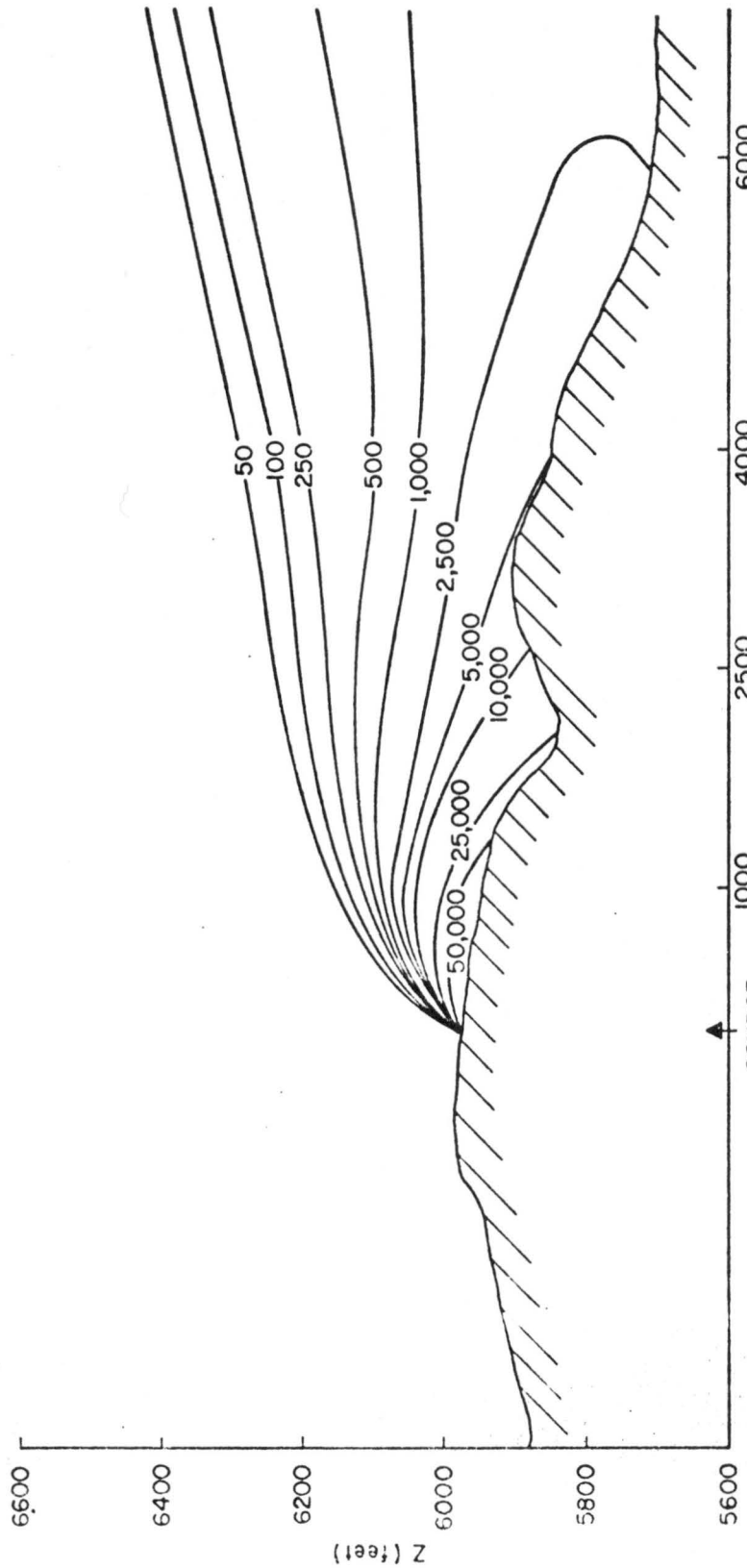

Fig. 16. Vertical concentration isopleth - source 4, wind orientation SW

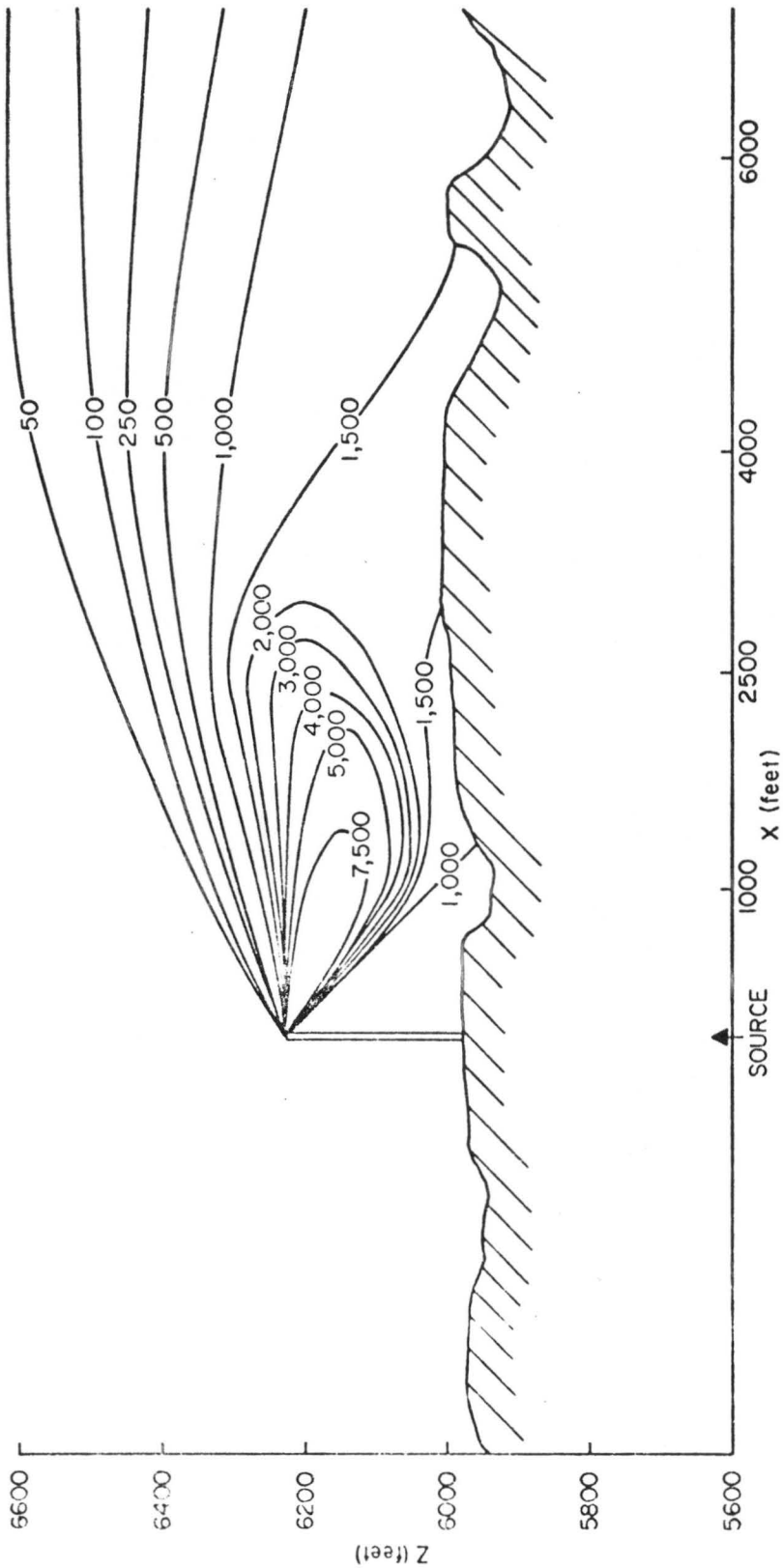

Fig. 17. Vertical concentration isopleth - source stack, wind orientation SE

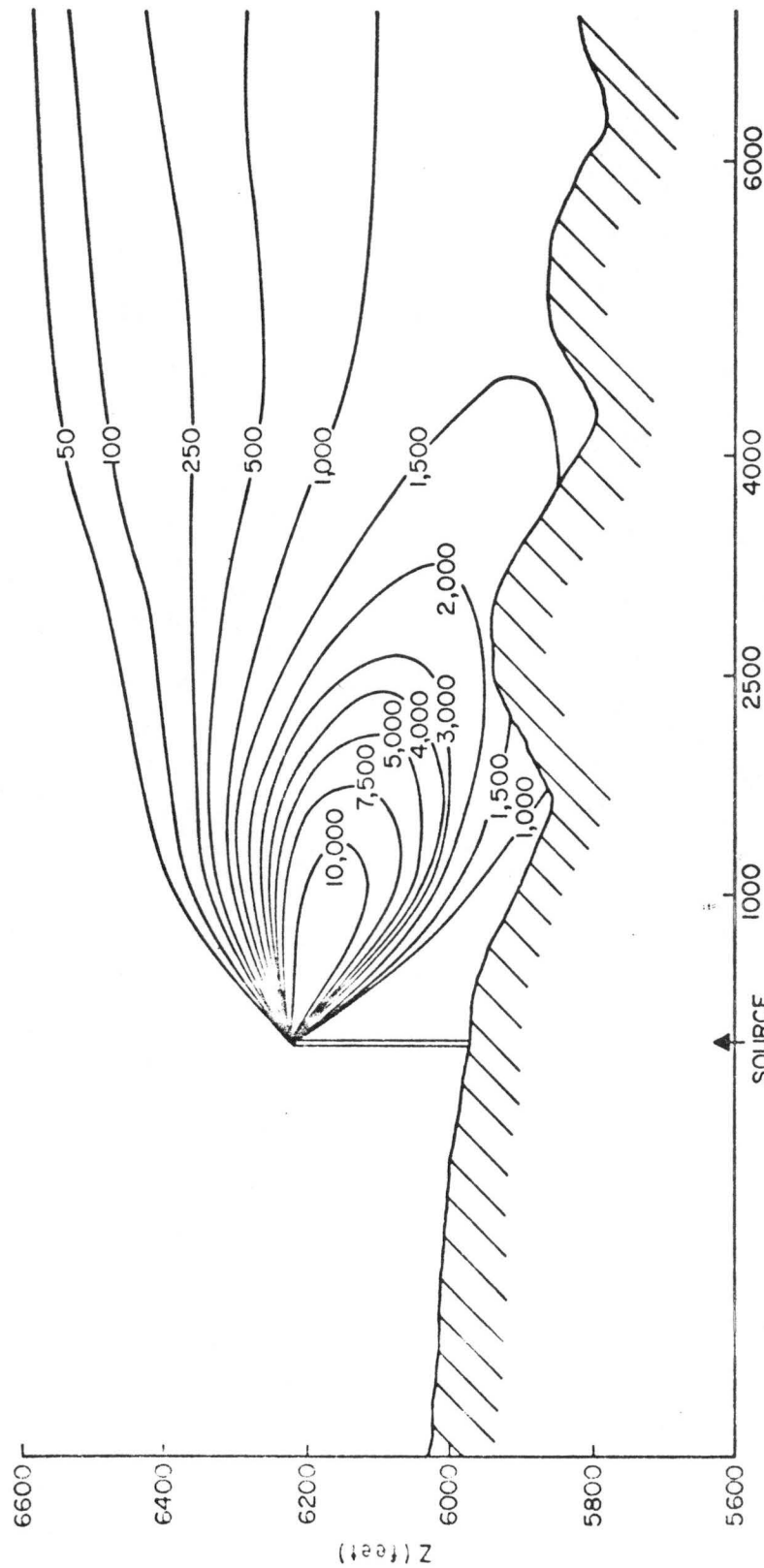

Fig. 18. Vertical concentration isopleth - source stack, wind orientation SW

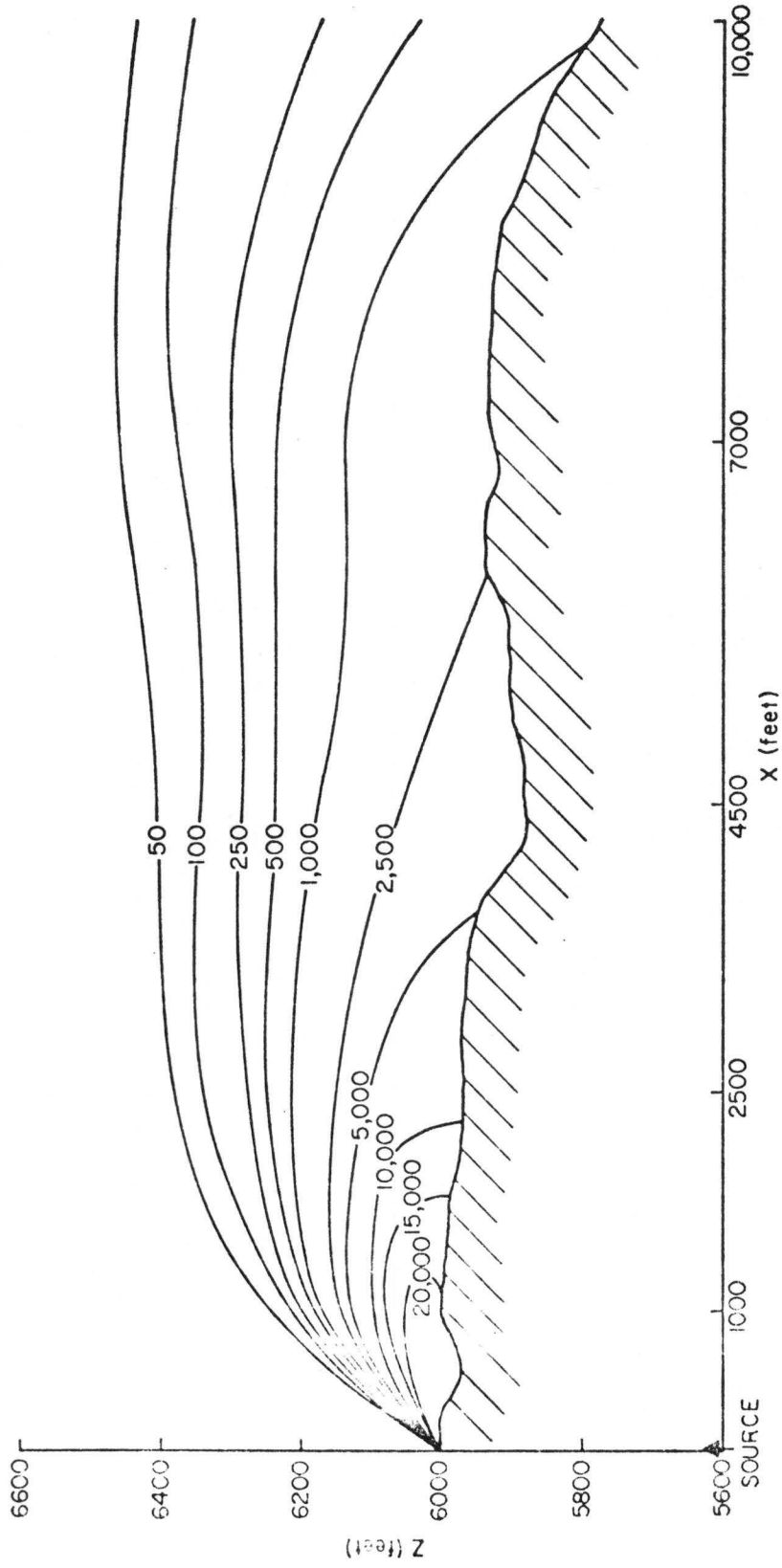

Fig. 19. Vertical concentration isopleth - source 6, wind orientation W

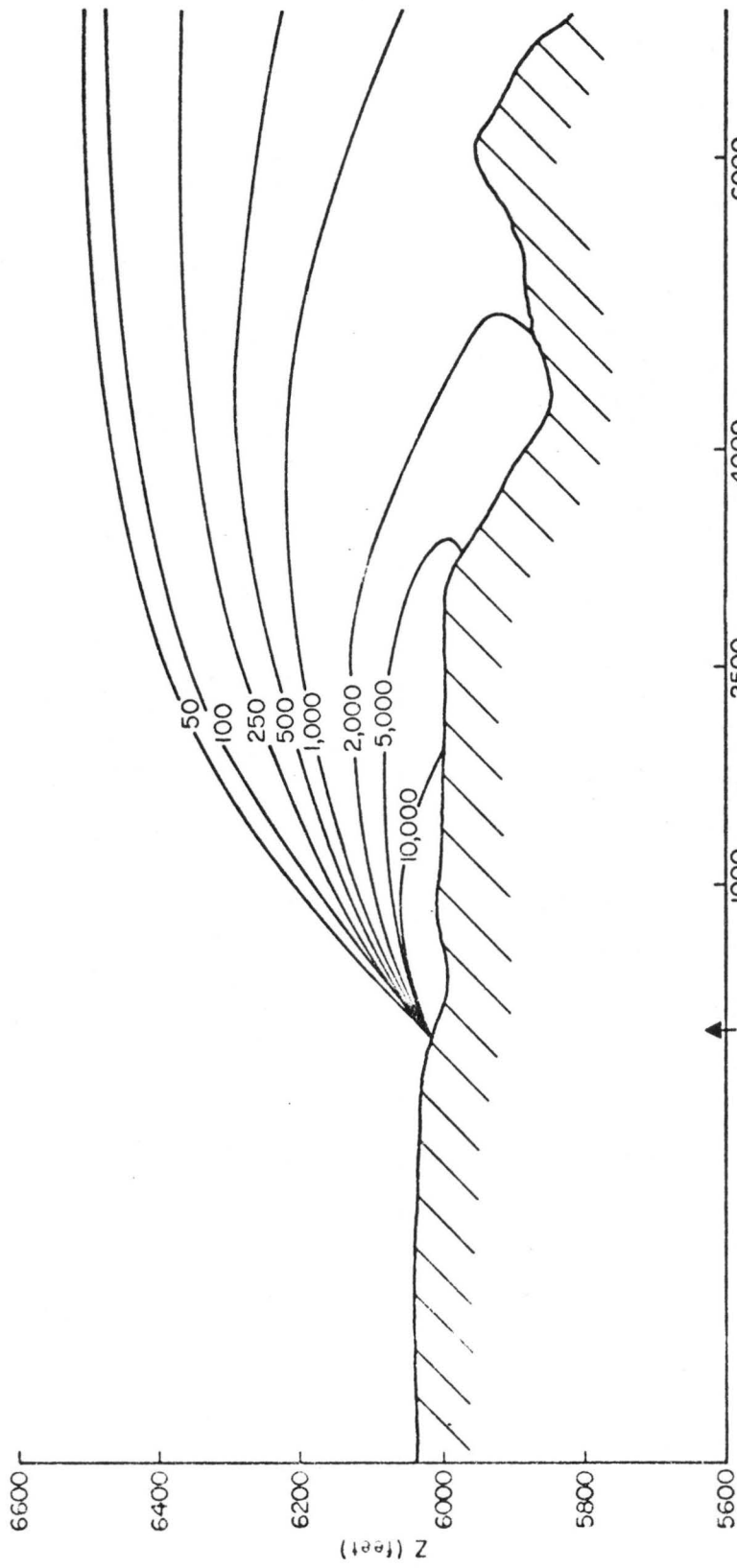

Fig. 20. Vertical concentration isopleth - source 6, wind orientation NW

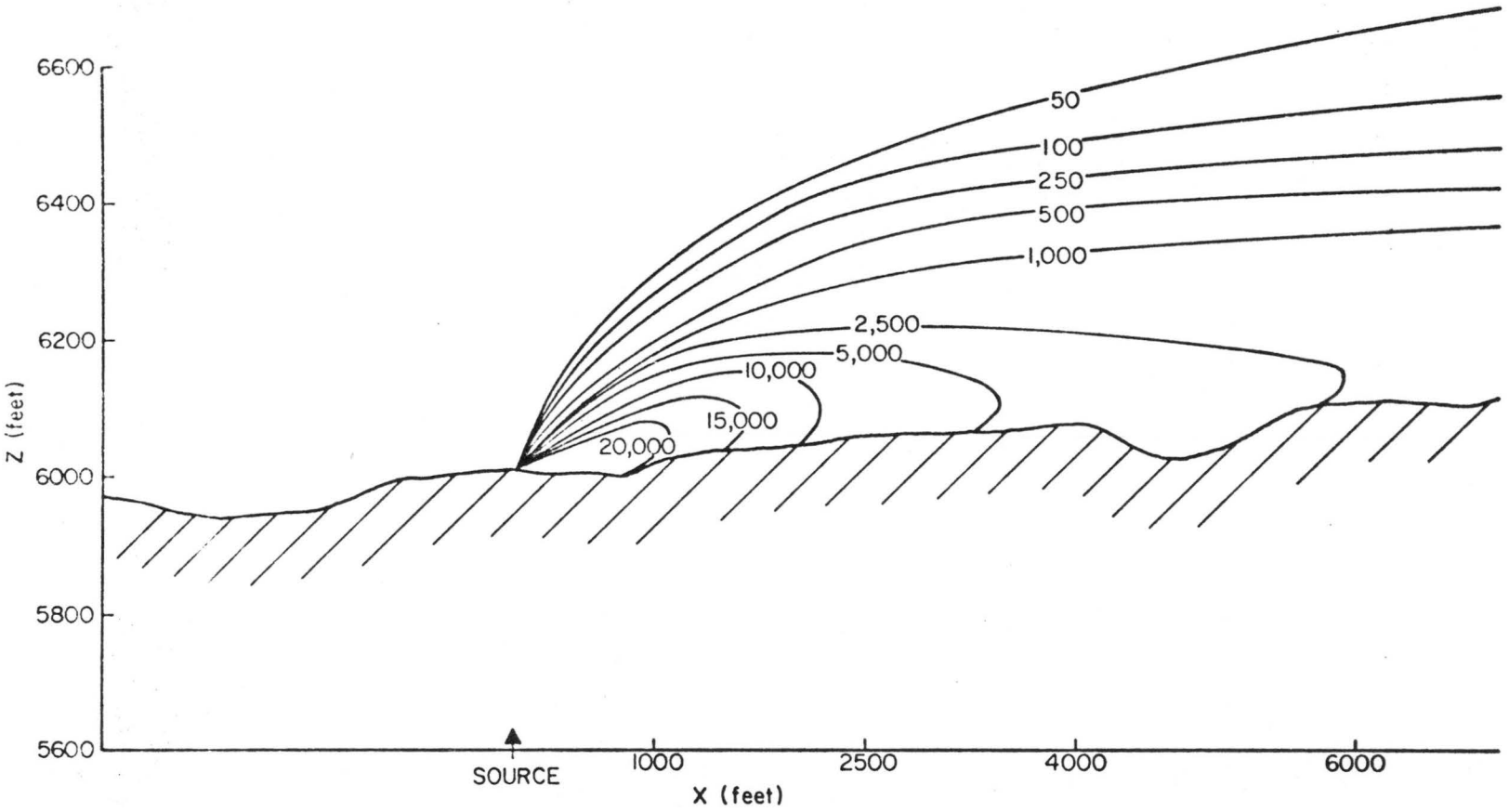

Fig. 21. Vertical concentration isopleth - source 6, wind orientation NE

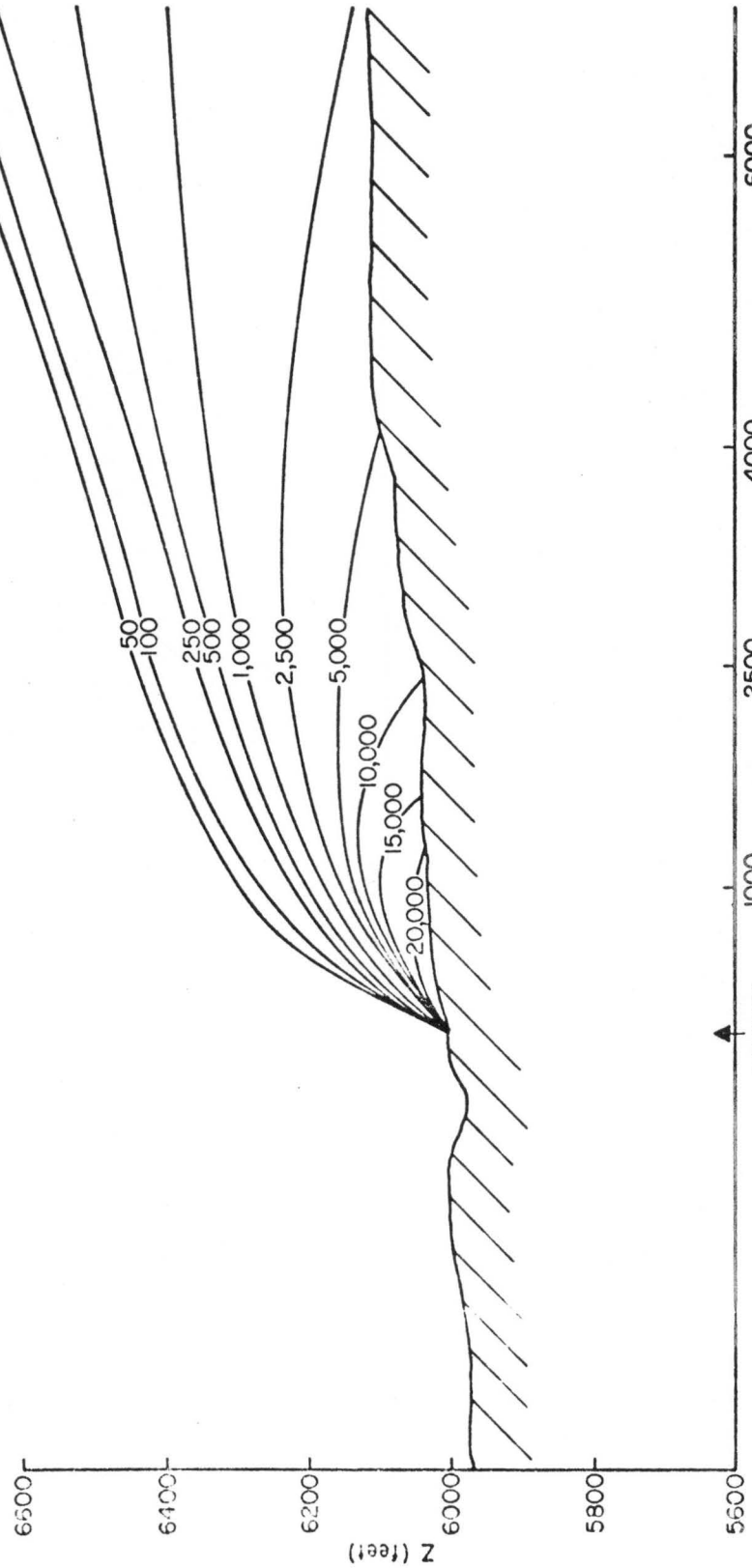

Fig. 22. Vertical concentration isopleth - source 6, wind orientation E

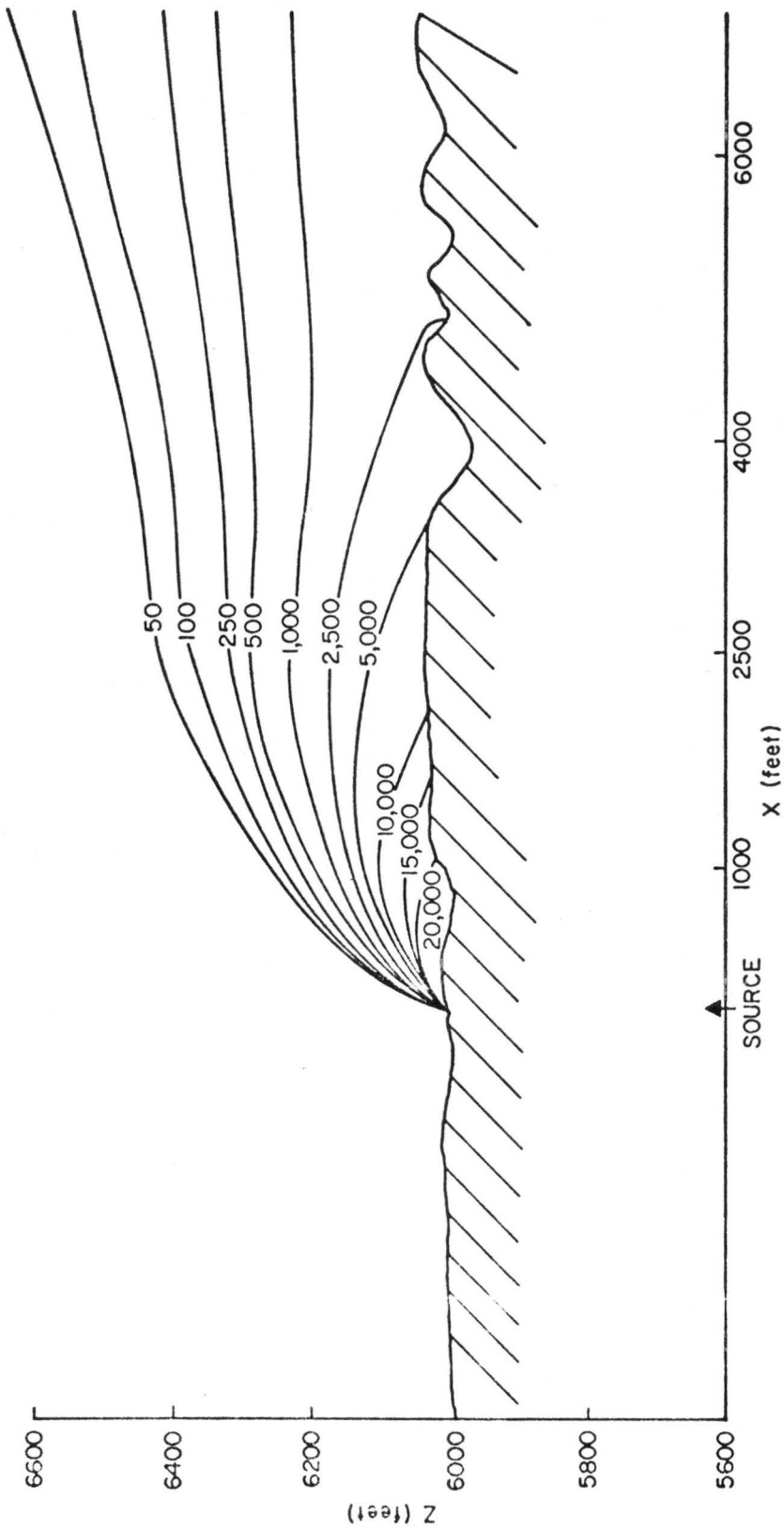

Fig. 23. Vertical concentration isopleth - source 6, wind orientation SE

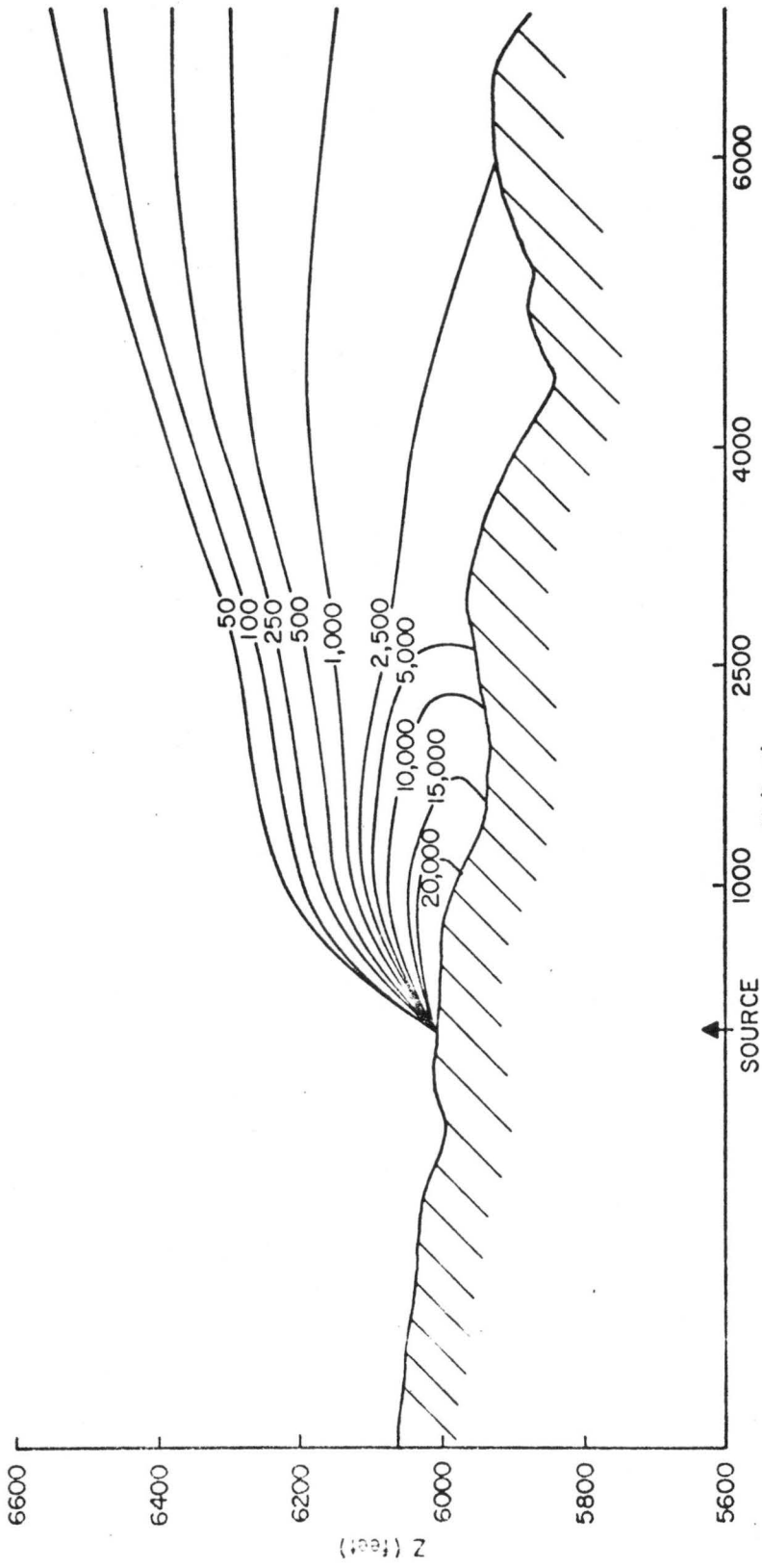

Fig. 24. Vertical concentration isopleth - source 6, wind orientation SW

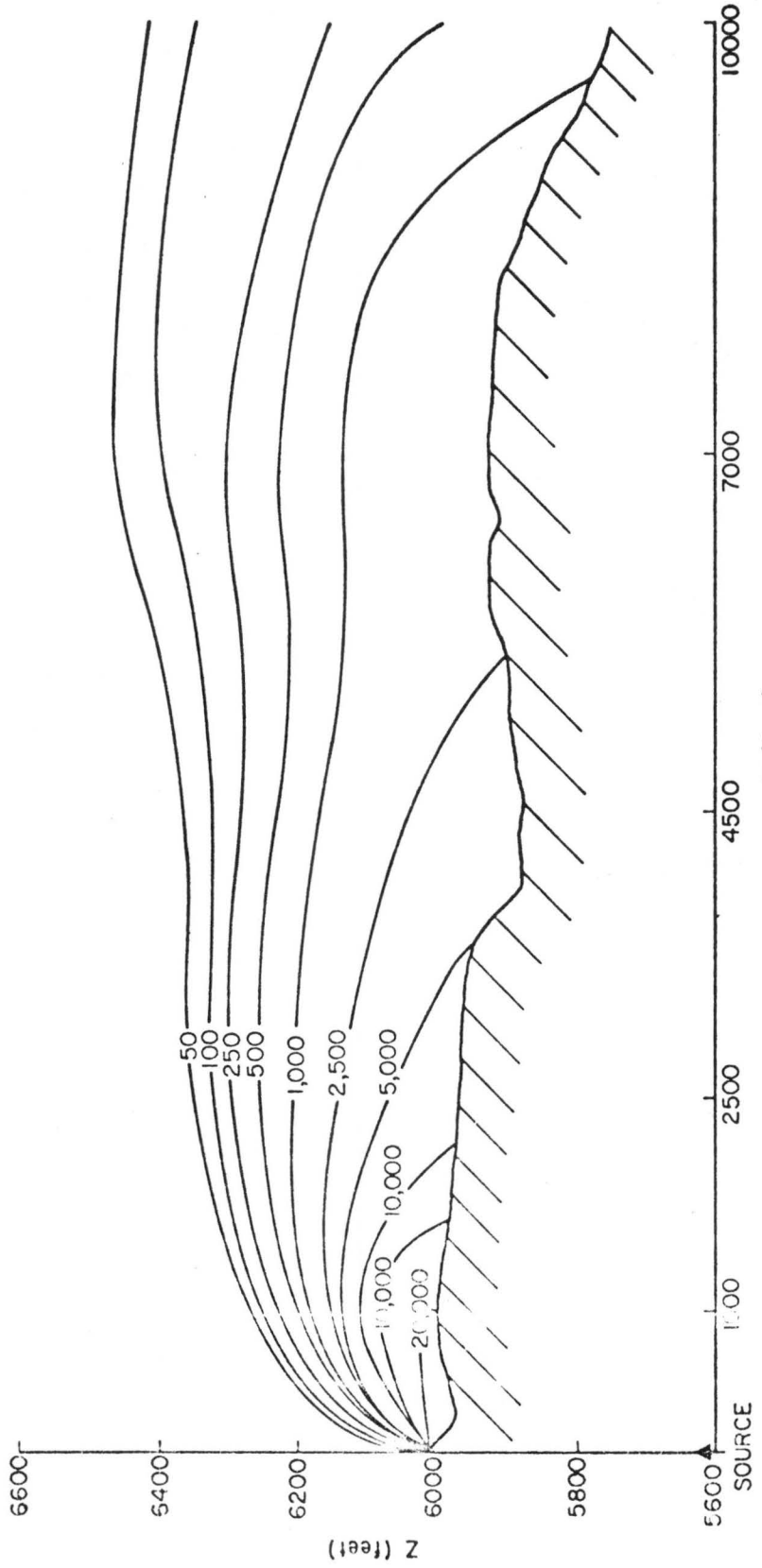

Fig. 25. Vertical concentration isopleth - source 7, wind orientation W

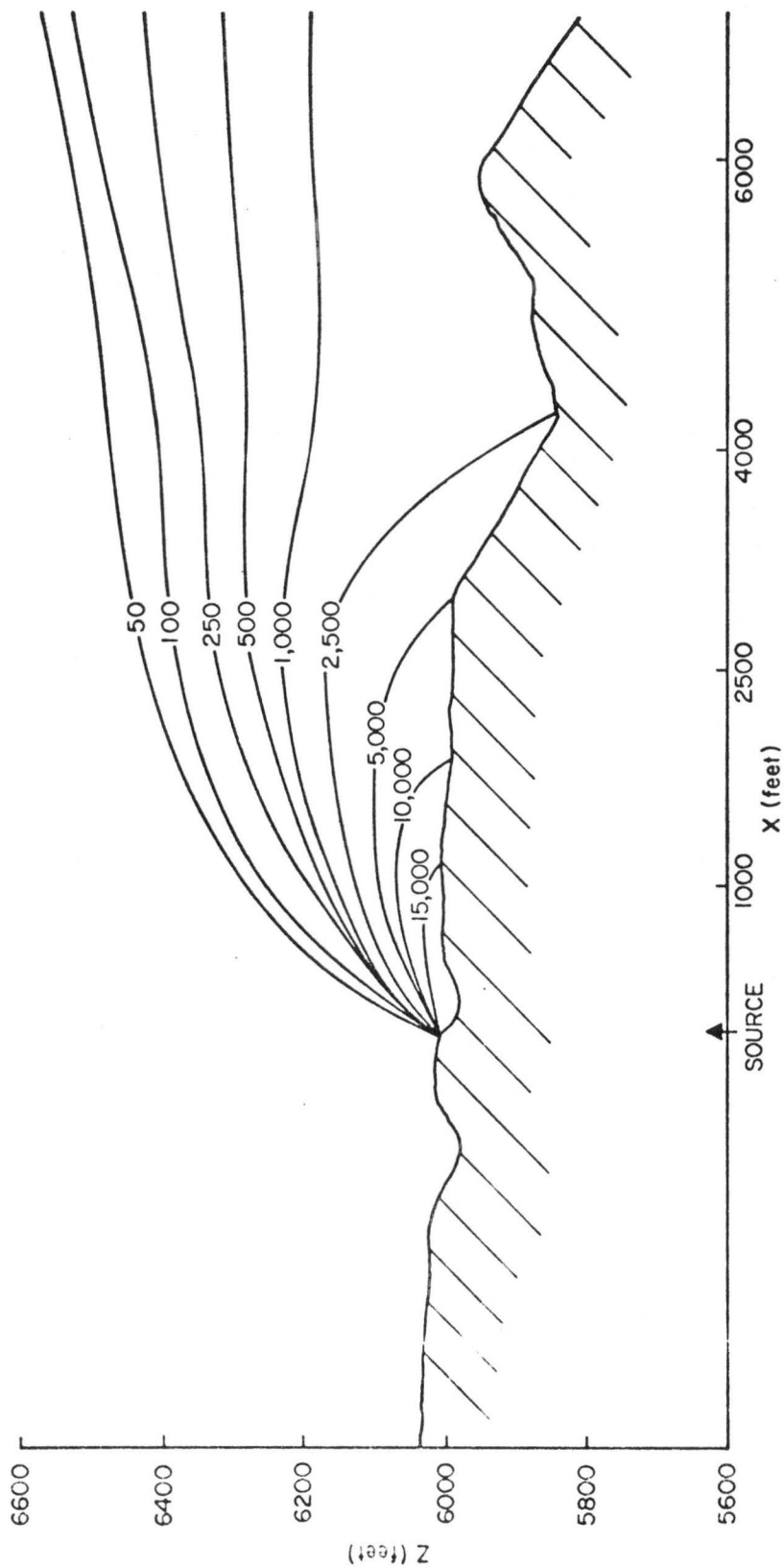

Fig. 26. Vertical concentration isopleth - source 7, wind orientation NW

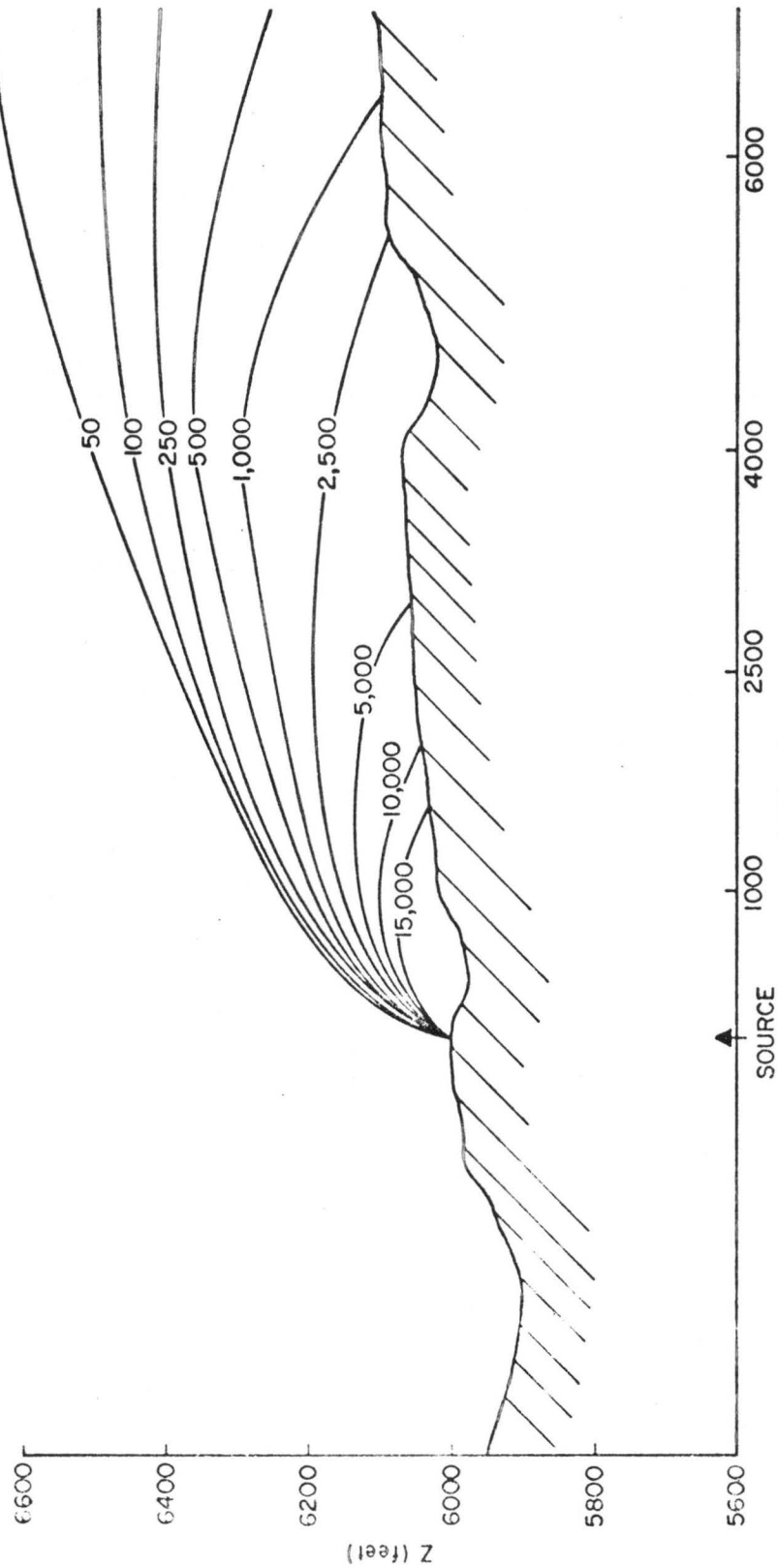

Fig. 27. Vertical concentration isopleth - source 7, wind orientation NE

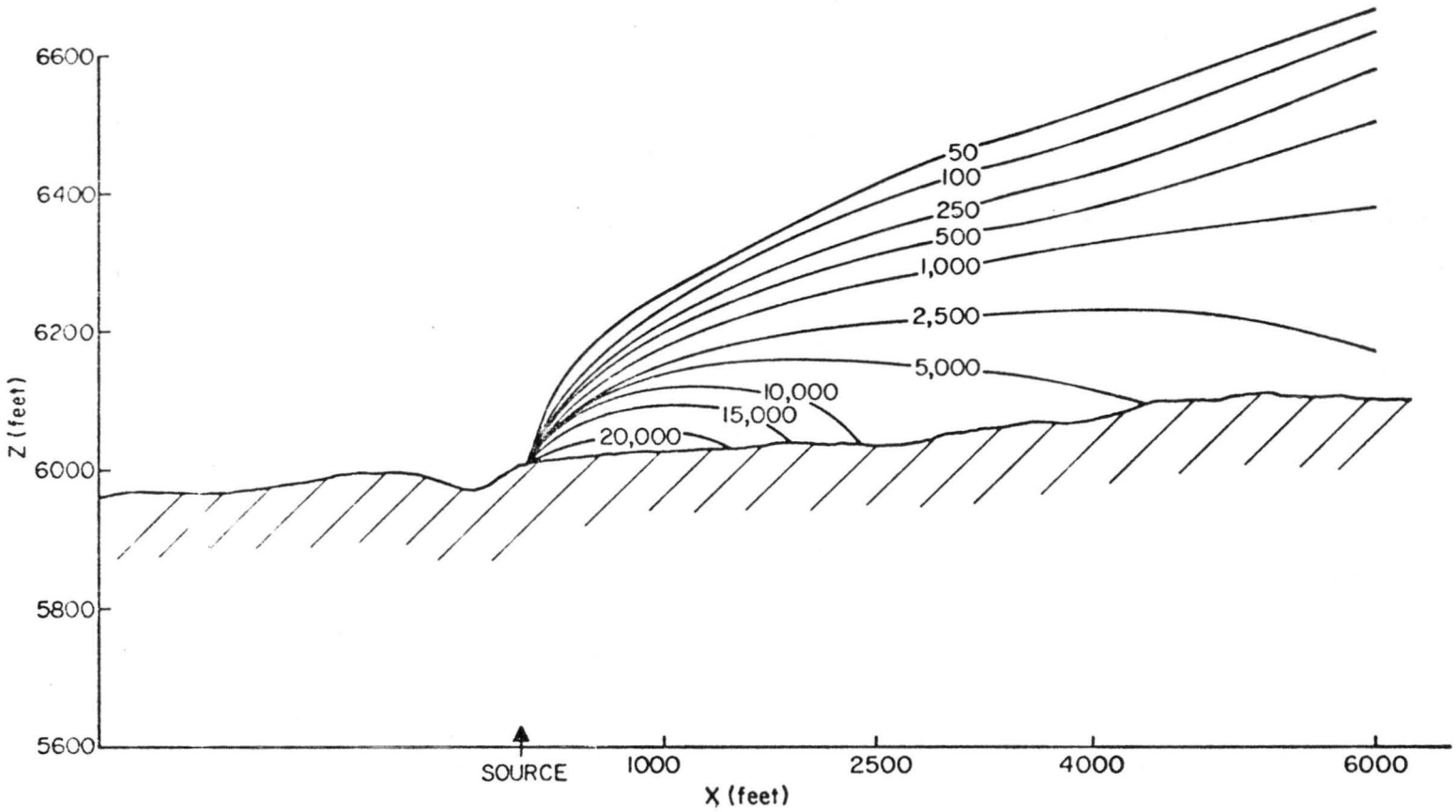

Fig. 28. Vertical concentration isopleth - source 7, wind orientation E

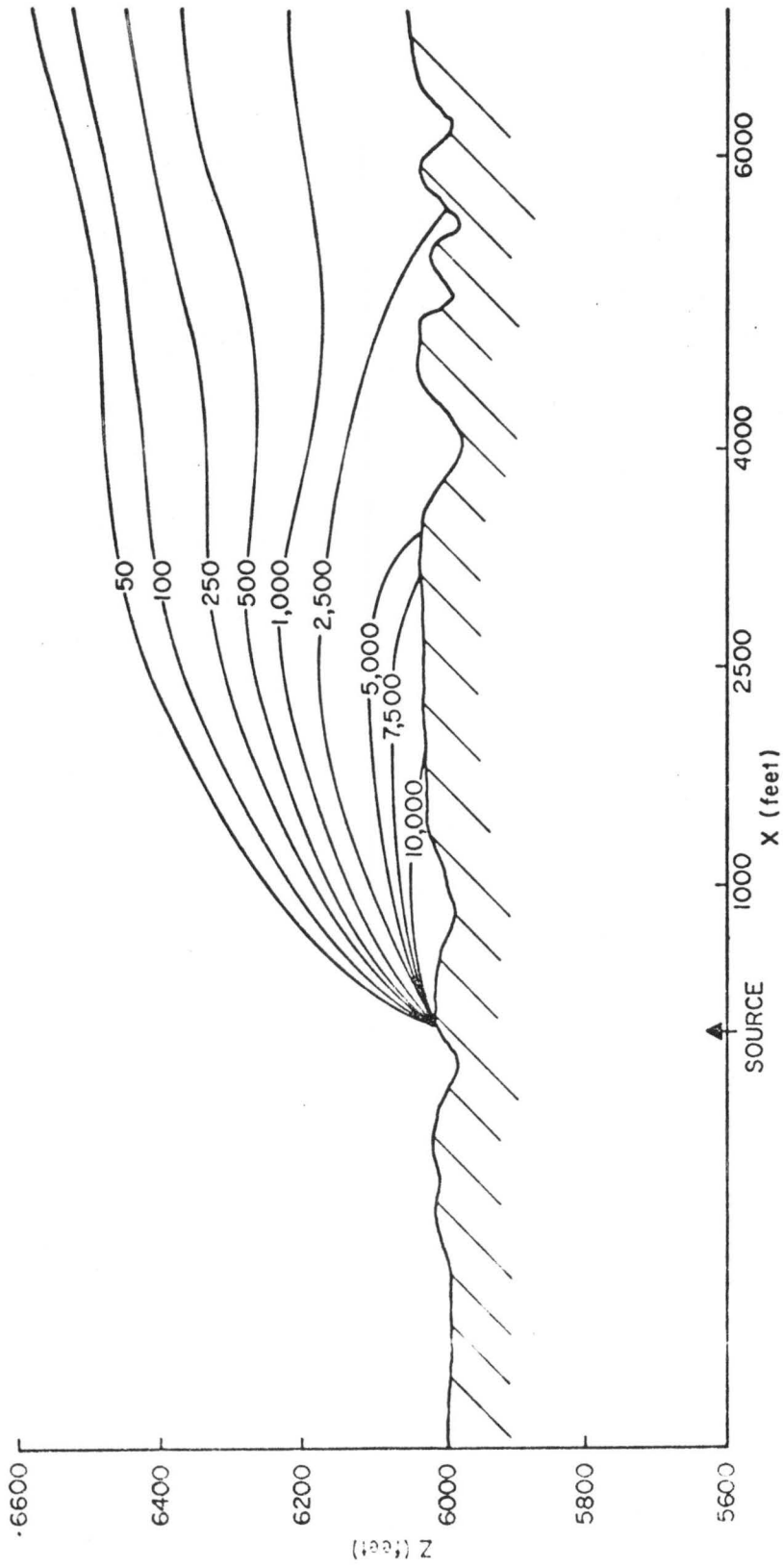

Fig. 29. Vertical concentration isopleth - source 7, wind orientation SE

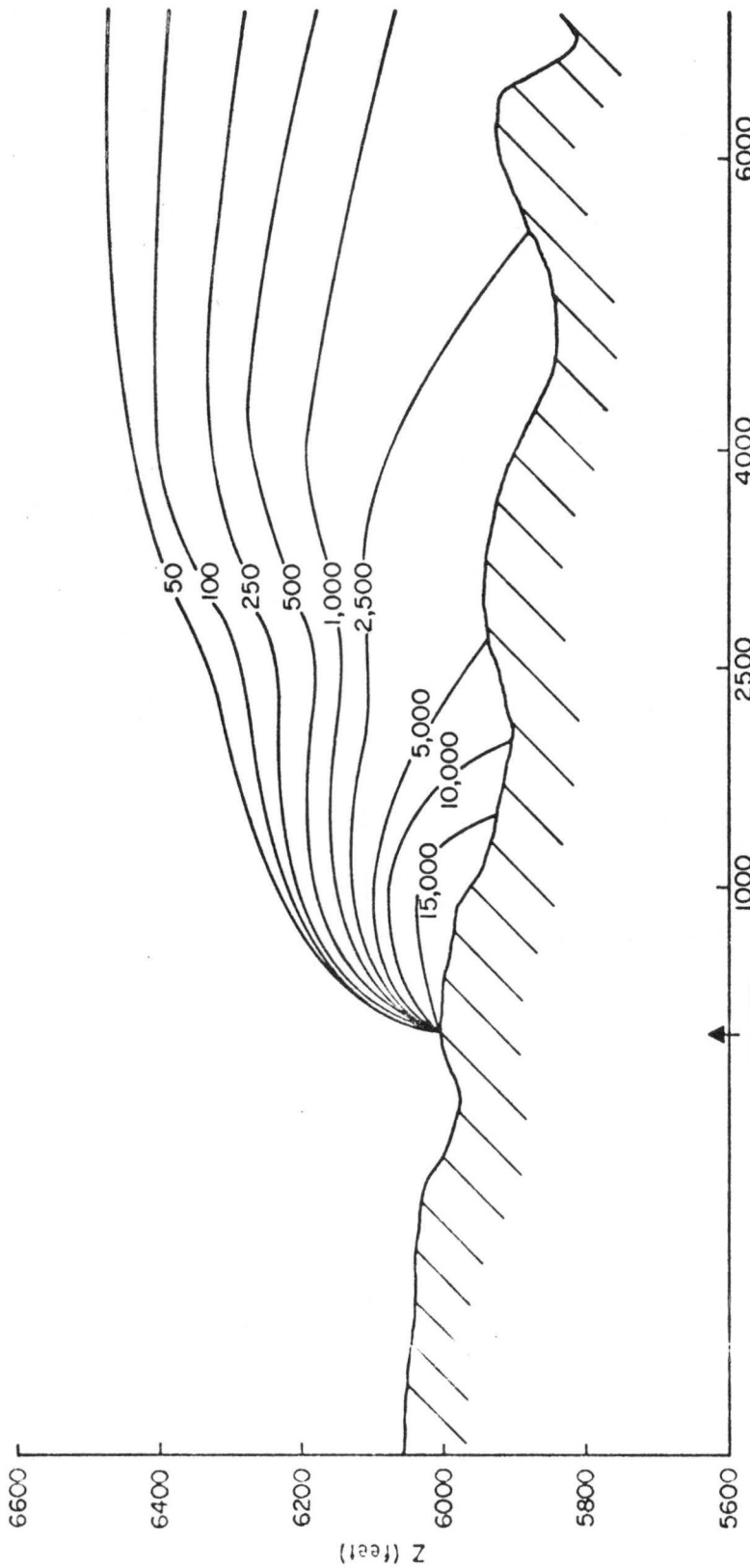

Fig. 30. Vertical concentration isopleth - source 7, wind orientation SW

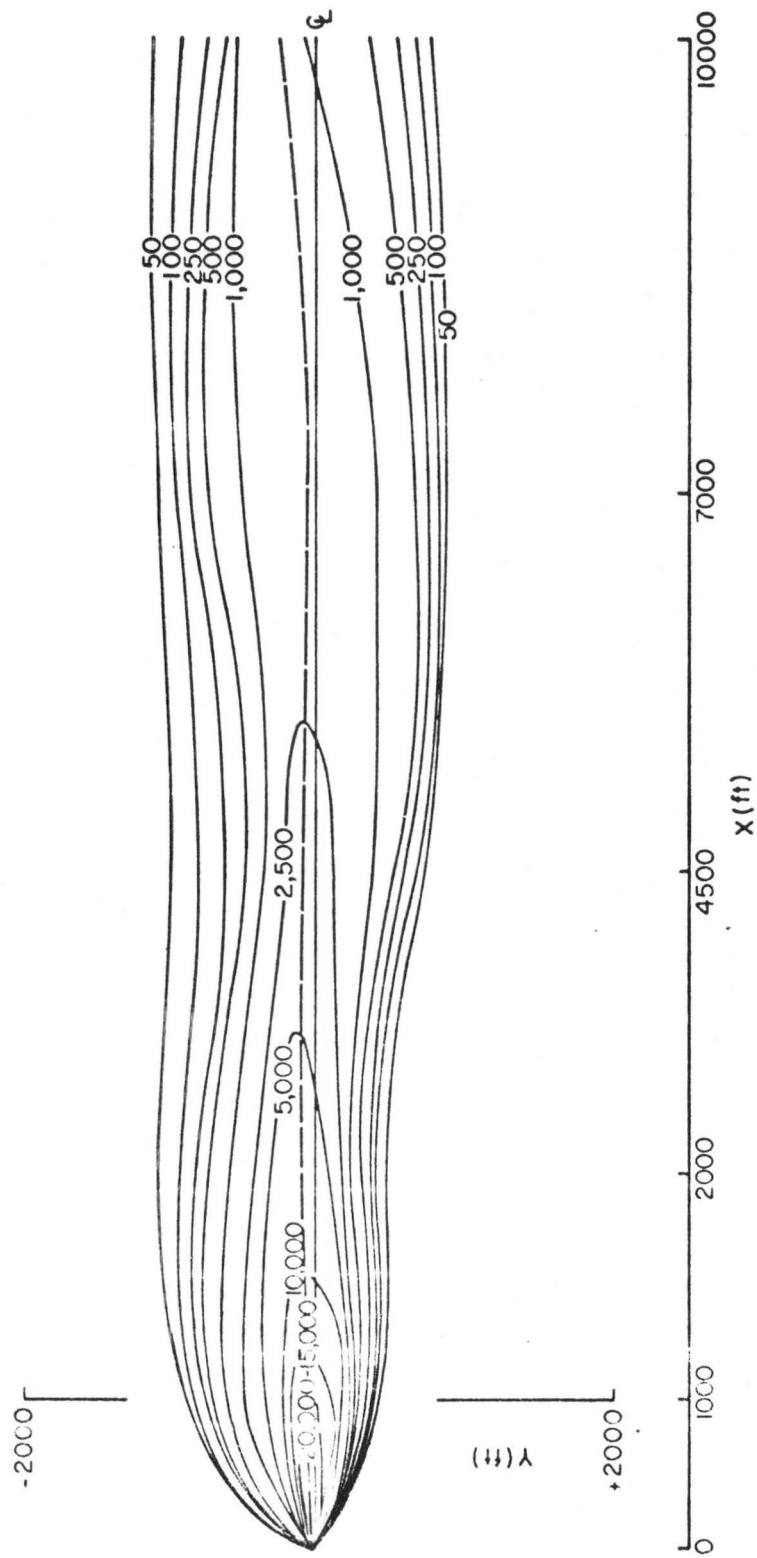

Fig. 31. Ground level concentration isopleths - source 7, wind orientation W

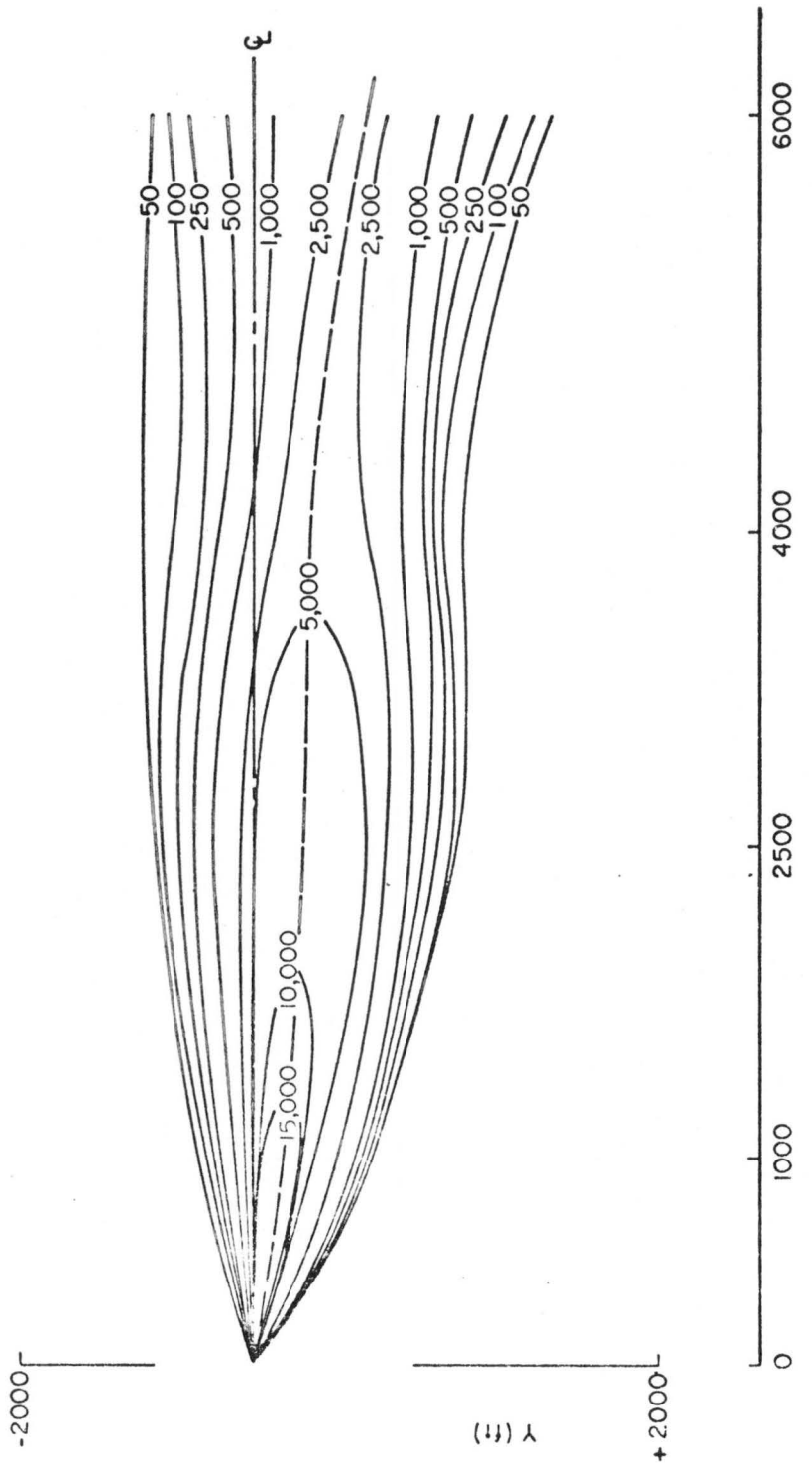

Fig. 32. Ground level concentration isopleths - source 6, wind orientation SW

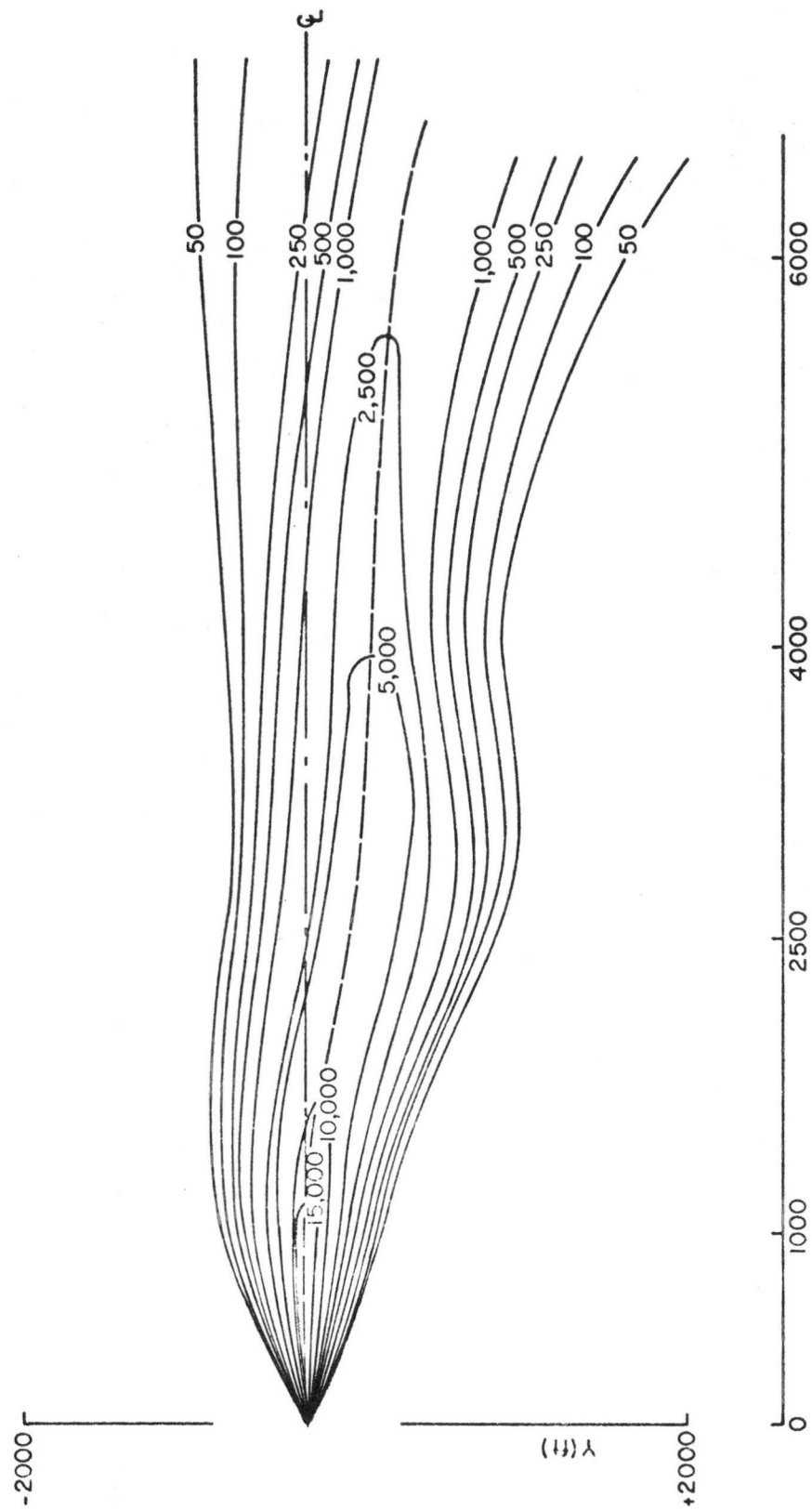

Fig. 33. Ground level isopleths - source 7, wind orientation SW

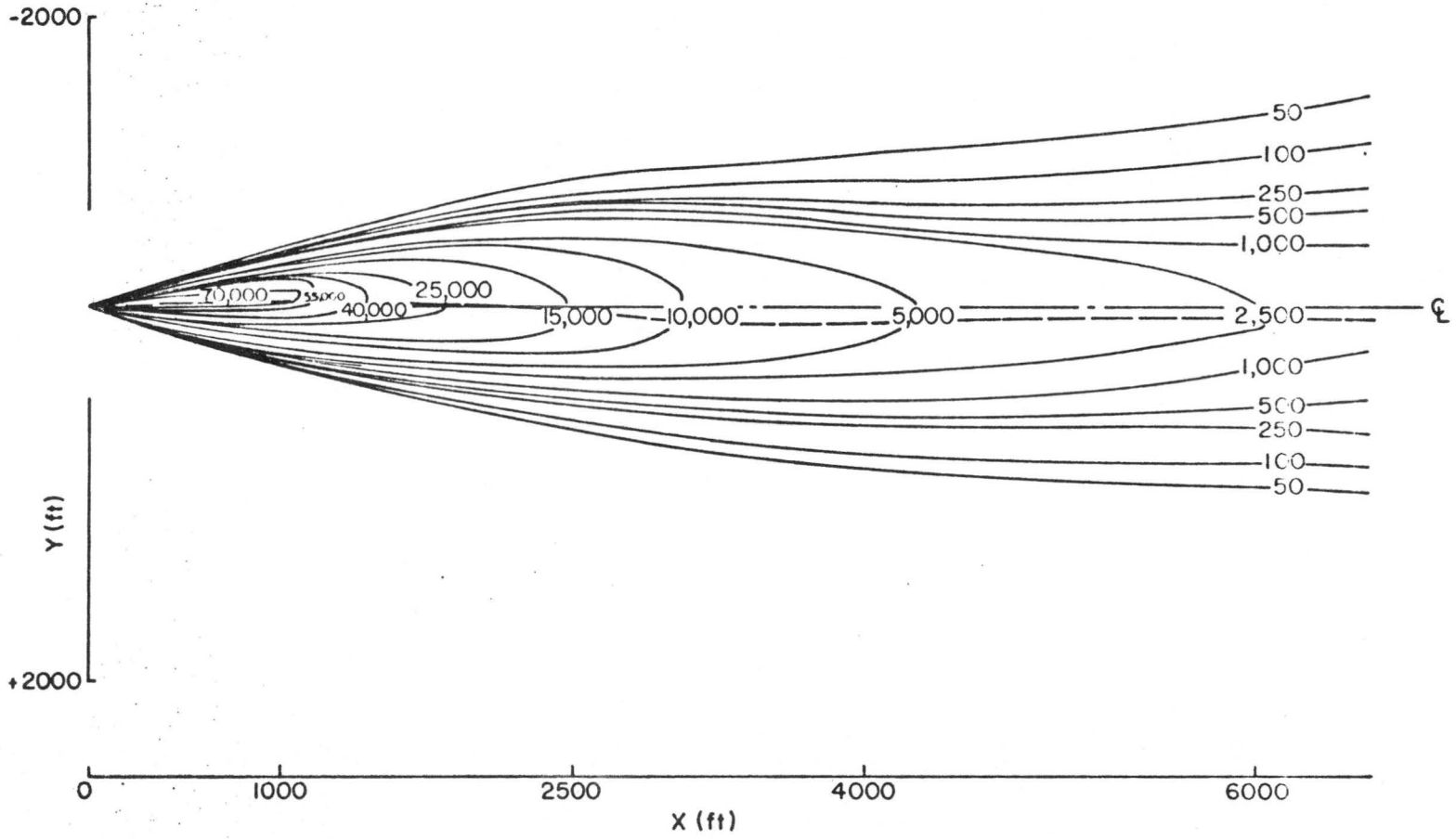

Fig. 34. Ground level concentration isopleths - source 4, wind orientation SW

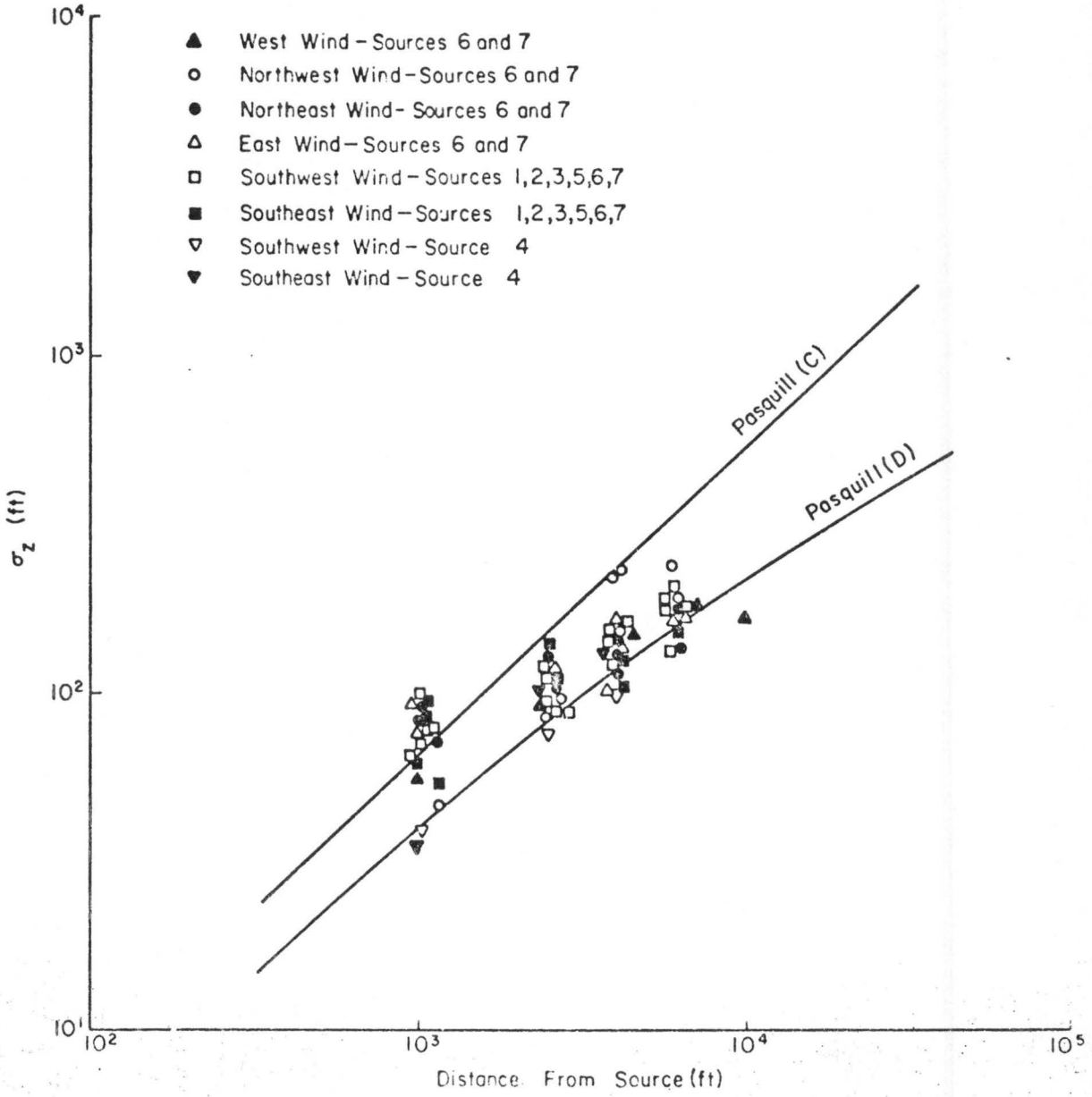

Fig. 35. Standard deviations of lateral concentration distribution

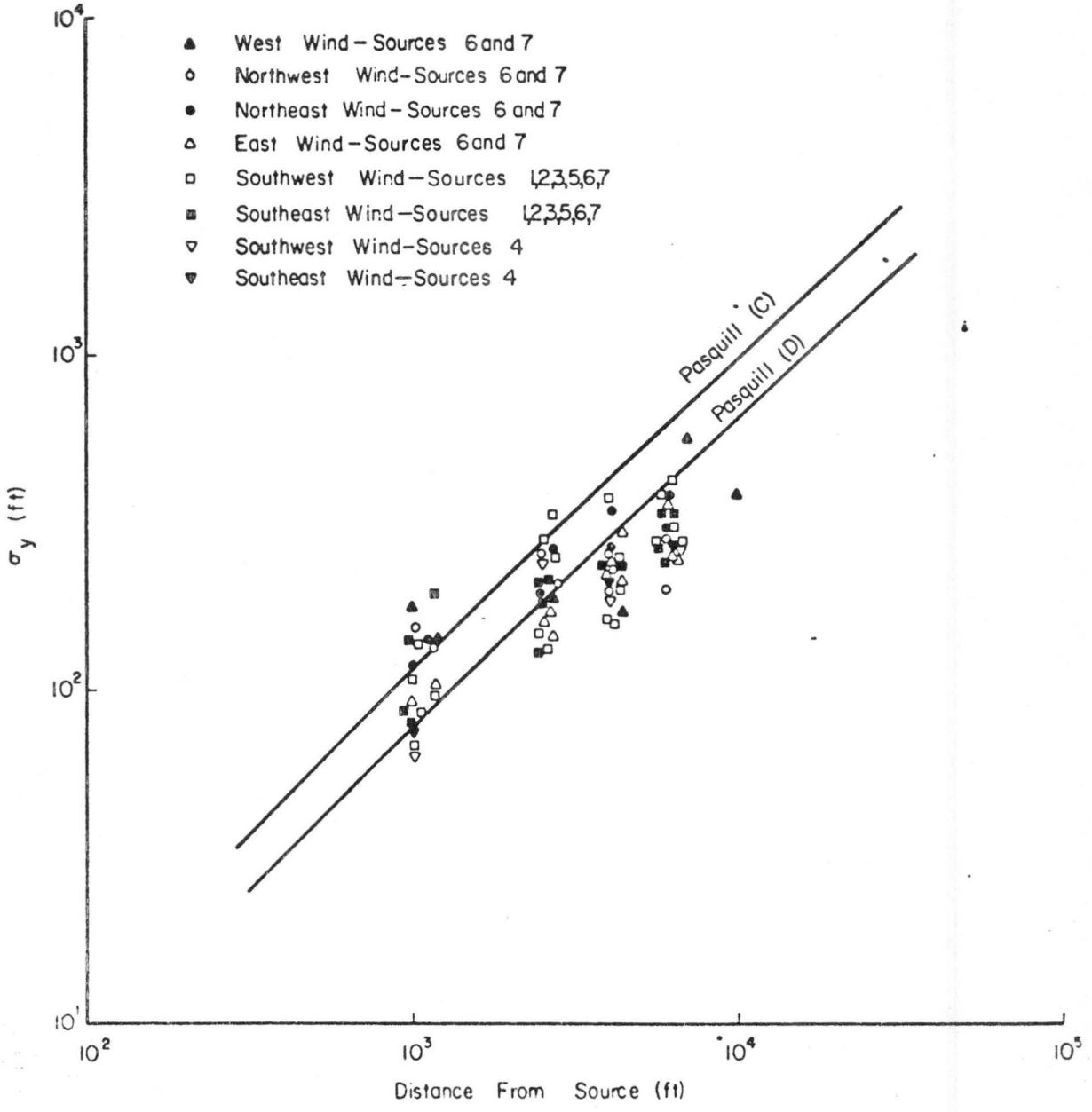

Fig. 36. Standard deviations of vertical concentration

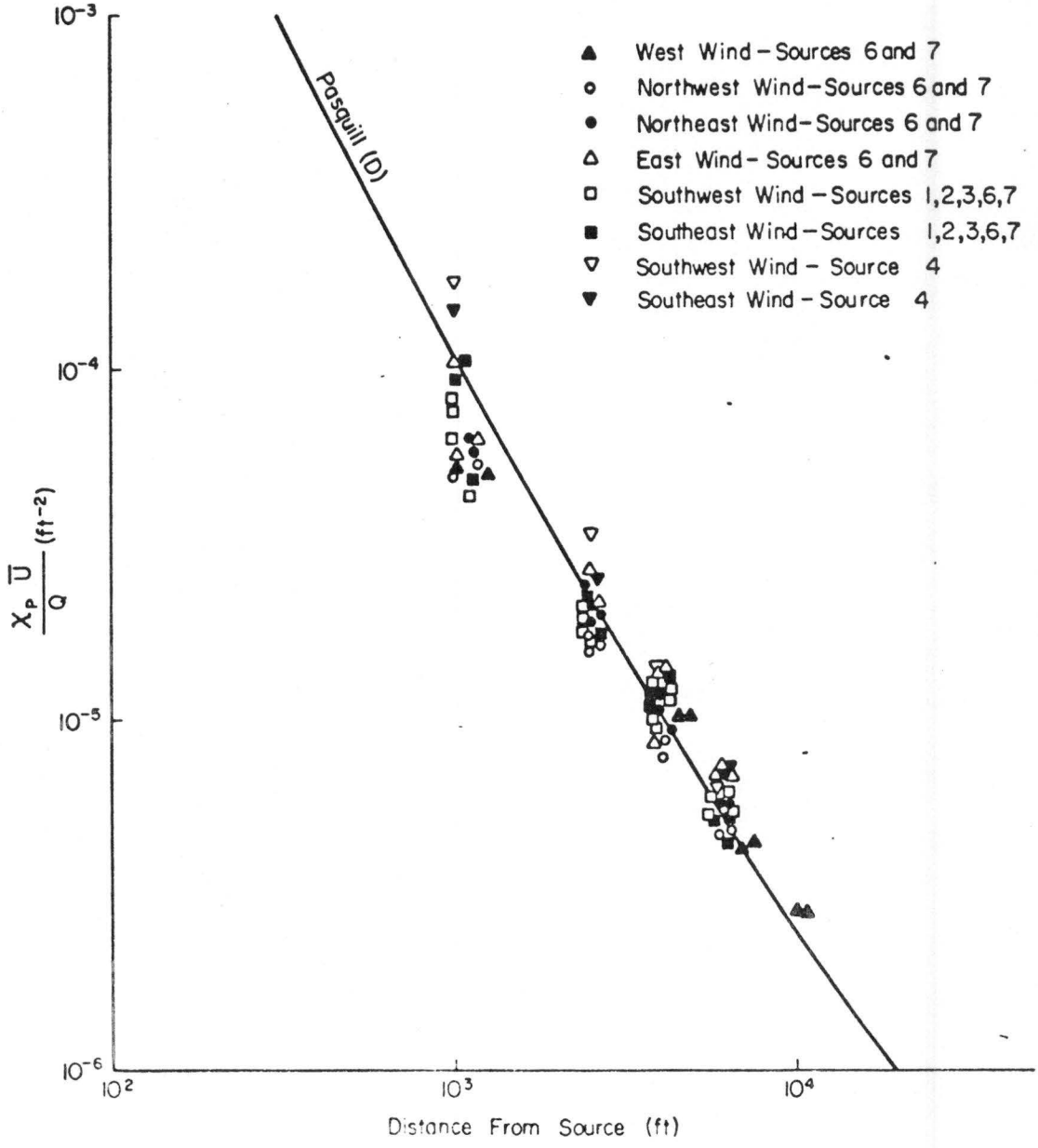

Fig. 37. Normalized ground level maximum average ground concentrations

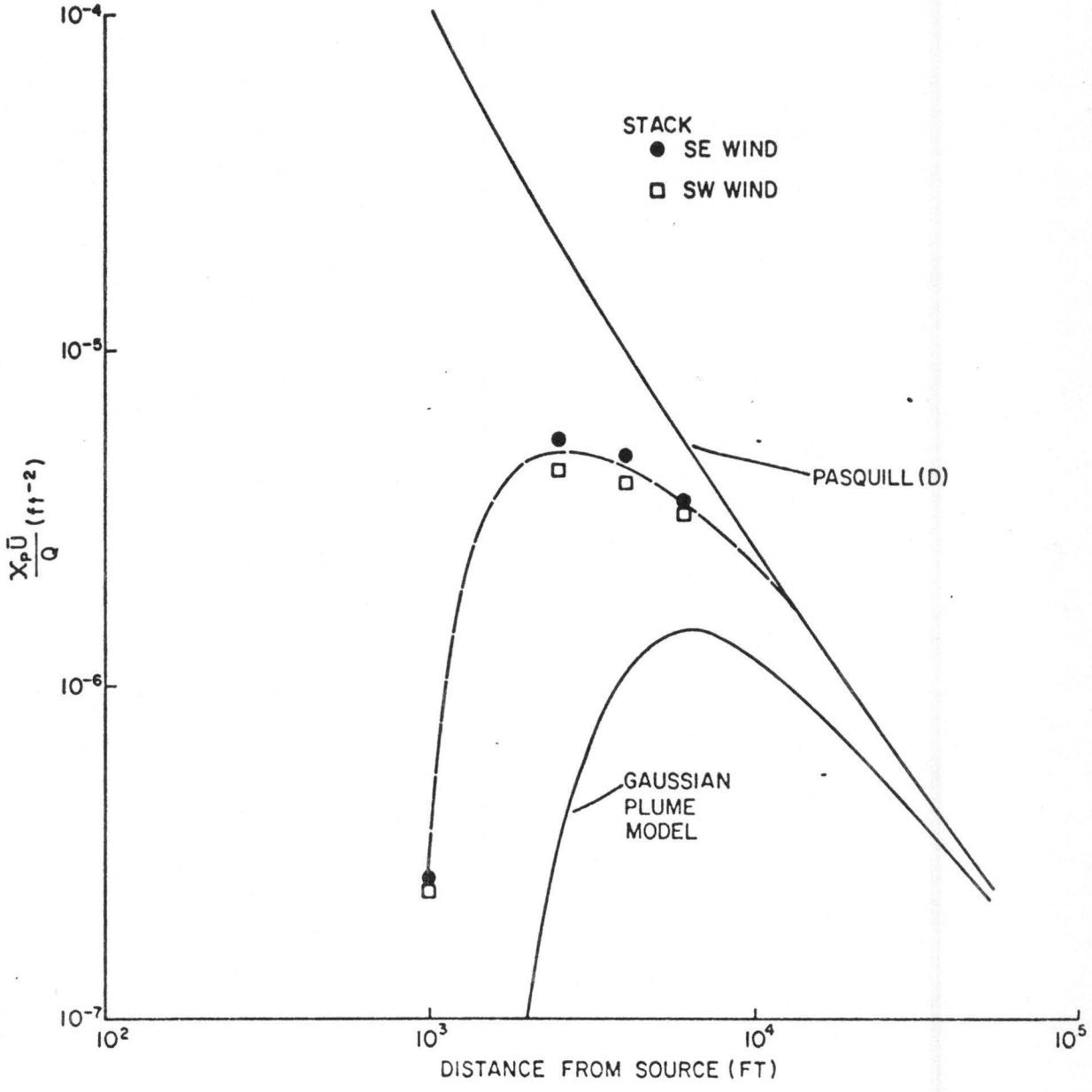

Fig. 38. Normalized ground level maximum average stack release

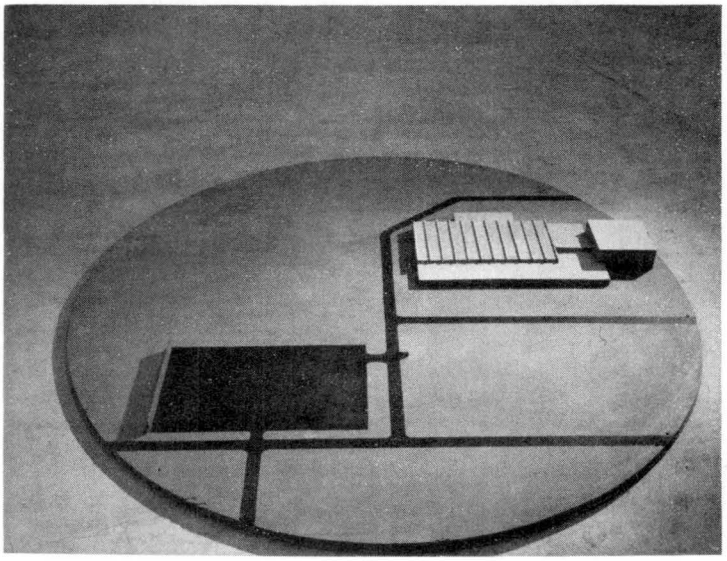

Fig. 39. Shelterbelt study model - parking lot and Bldg. No. 371

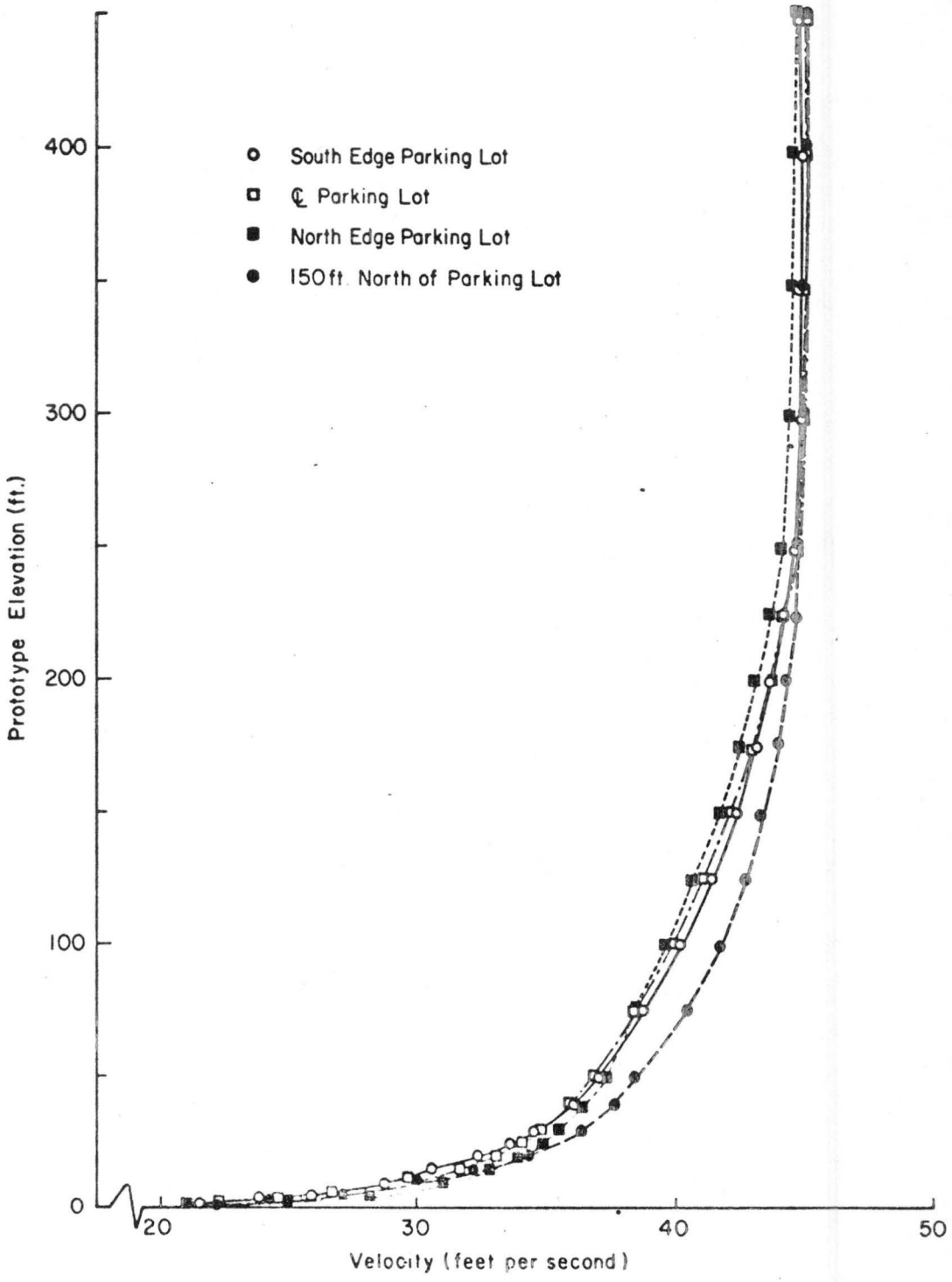

Fig. 40. Vertical wind profiles - west wind, U_∞^2 45 ft per sec.

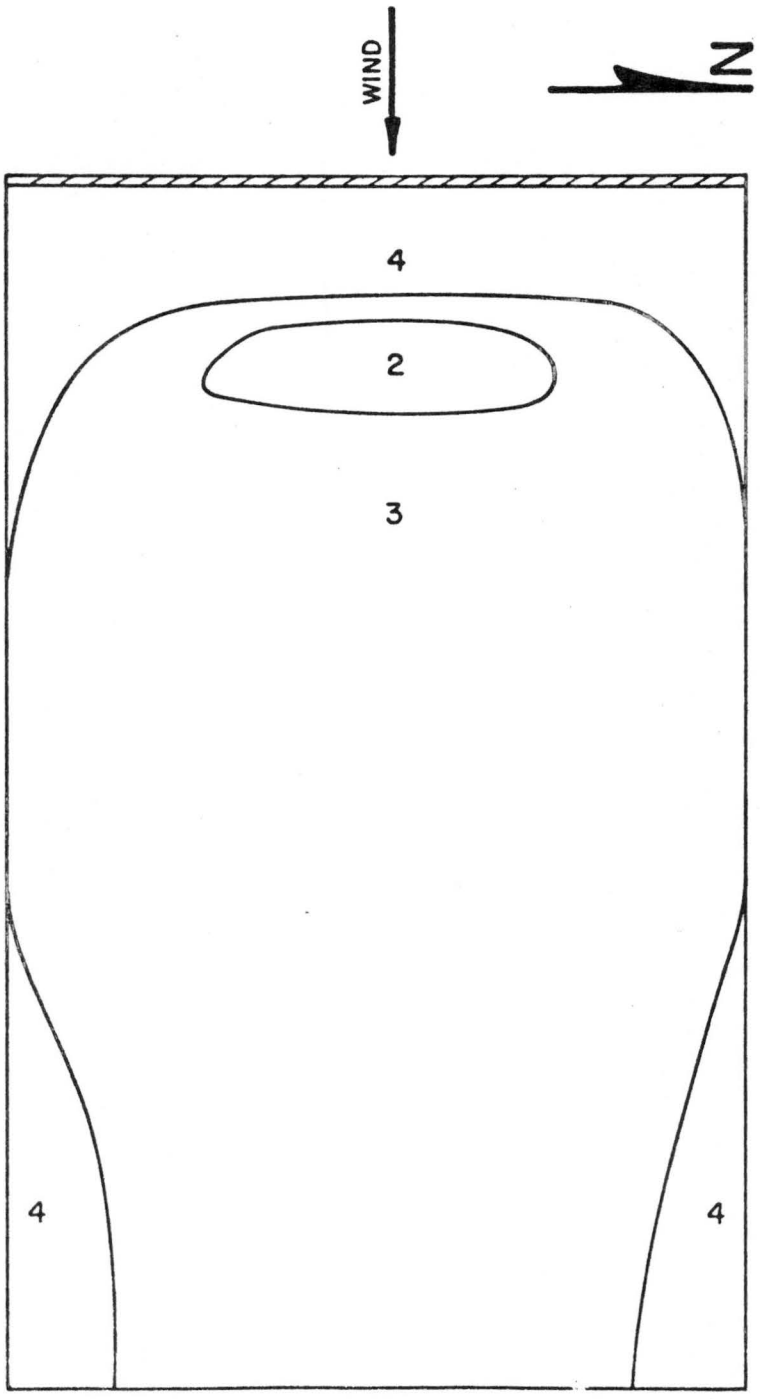

Fig. 41. Parking lot wind protection - H = 15', "Straight Across", W wind, loose porosity

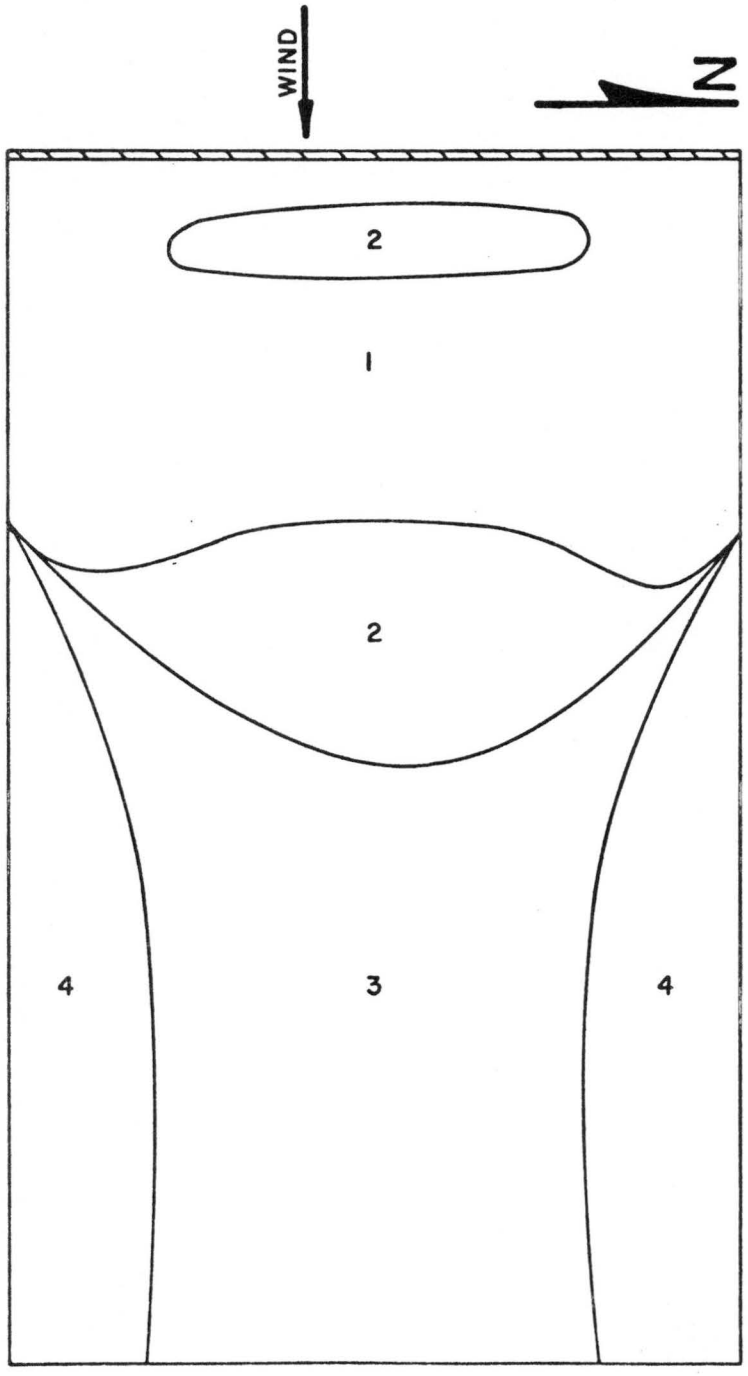

Fig. 42. Parking lot wind protection - H = 15', "Straight Across", W wind, medium porosity

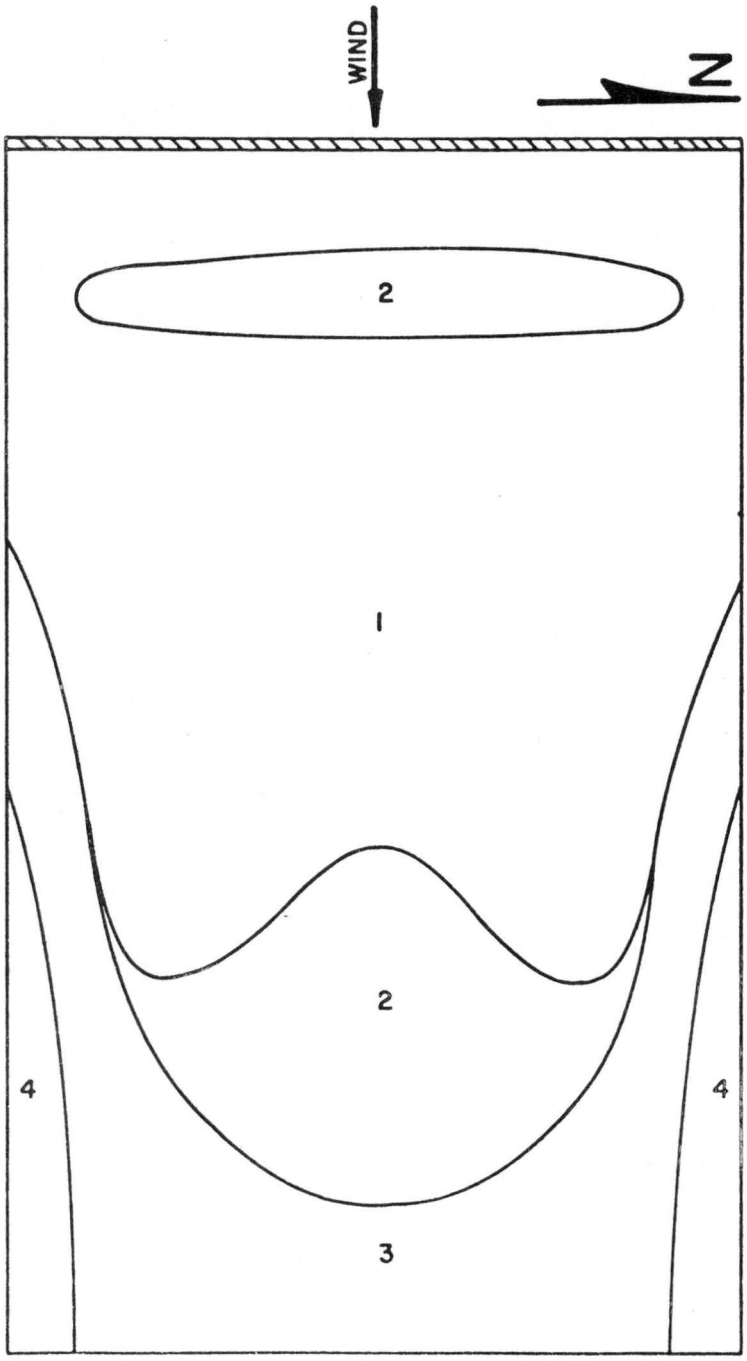

Fig. 43. Parking lot wind protection - H = 30', "Straight Across", W wind, medium porosity

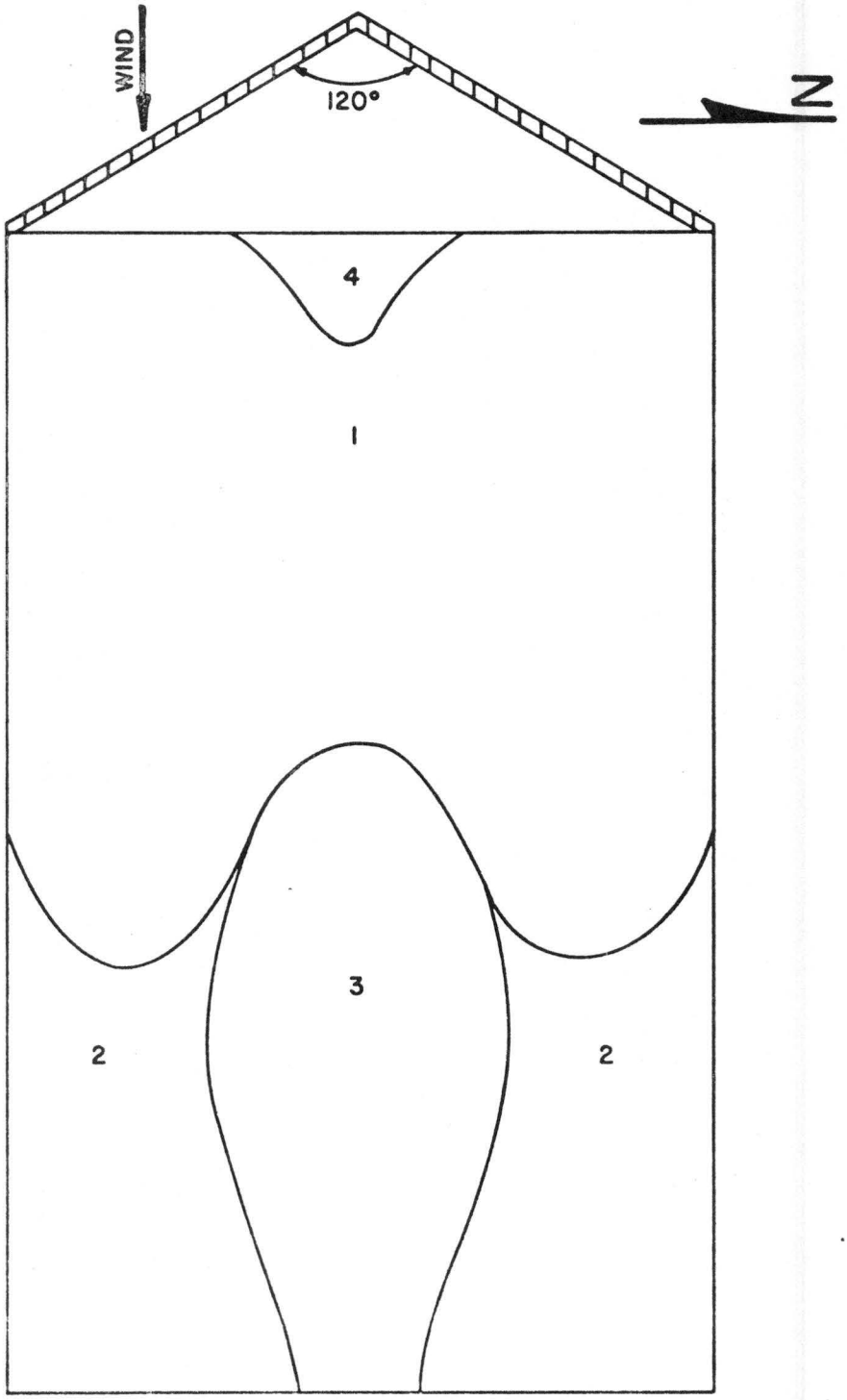

Fig. 44. Parking lot wind protection - H = 30', 120° wedge, W wind, medium porosity

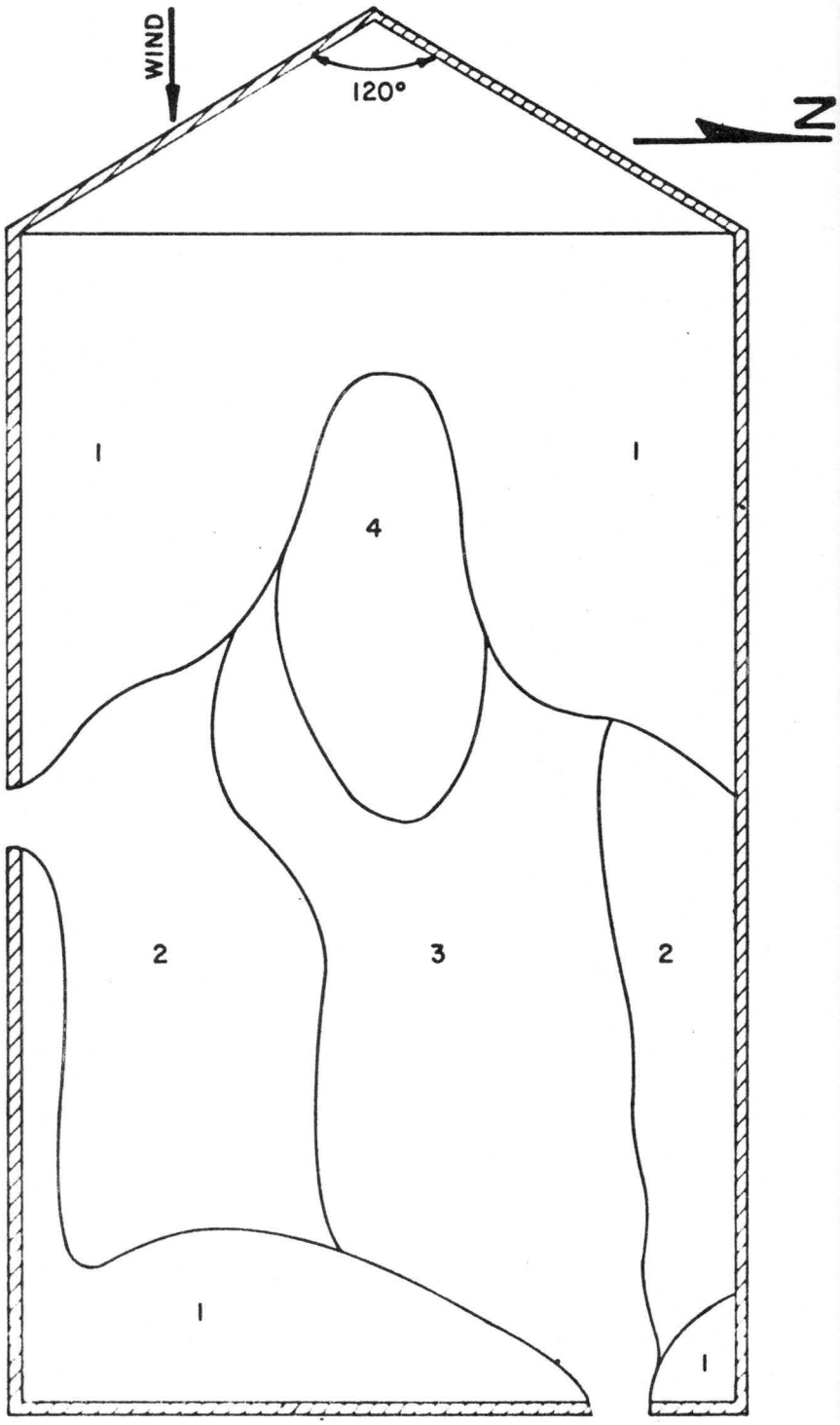

Fig. 45. Parking lot wind protection - H = 15', 120° wedge with "All Around", W wind, medium porosity

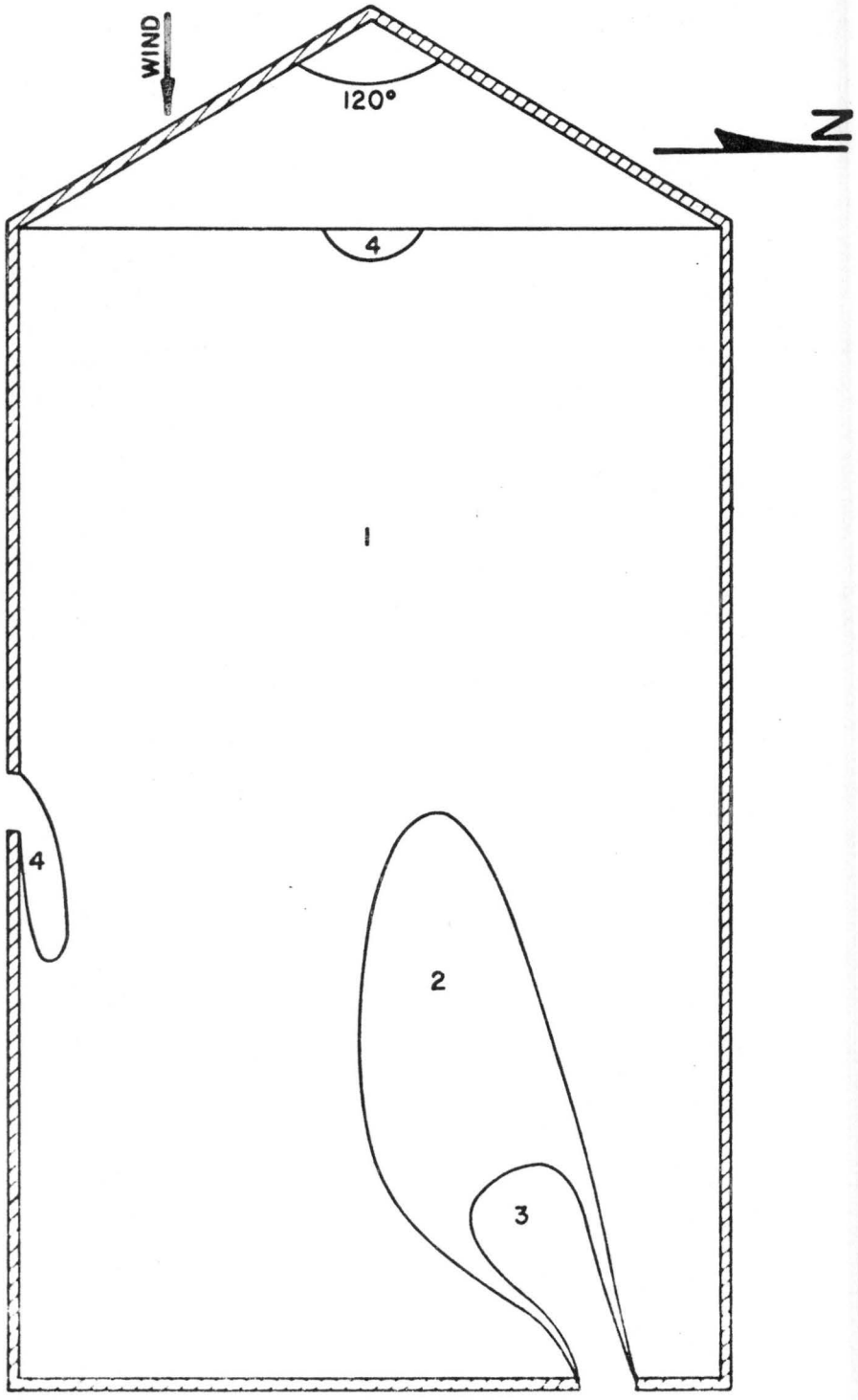

Fig. 46. Parking lot wind protection - H = 30', 120° wedge with "All Around", W wind, medium porosity

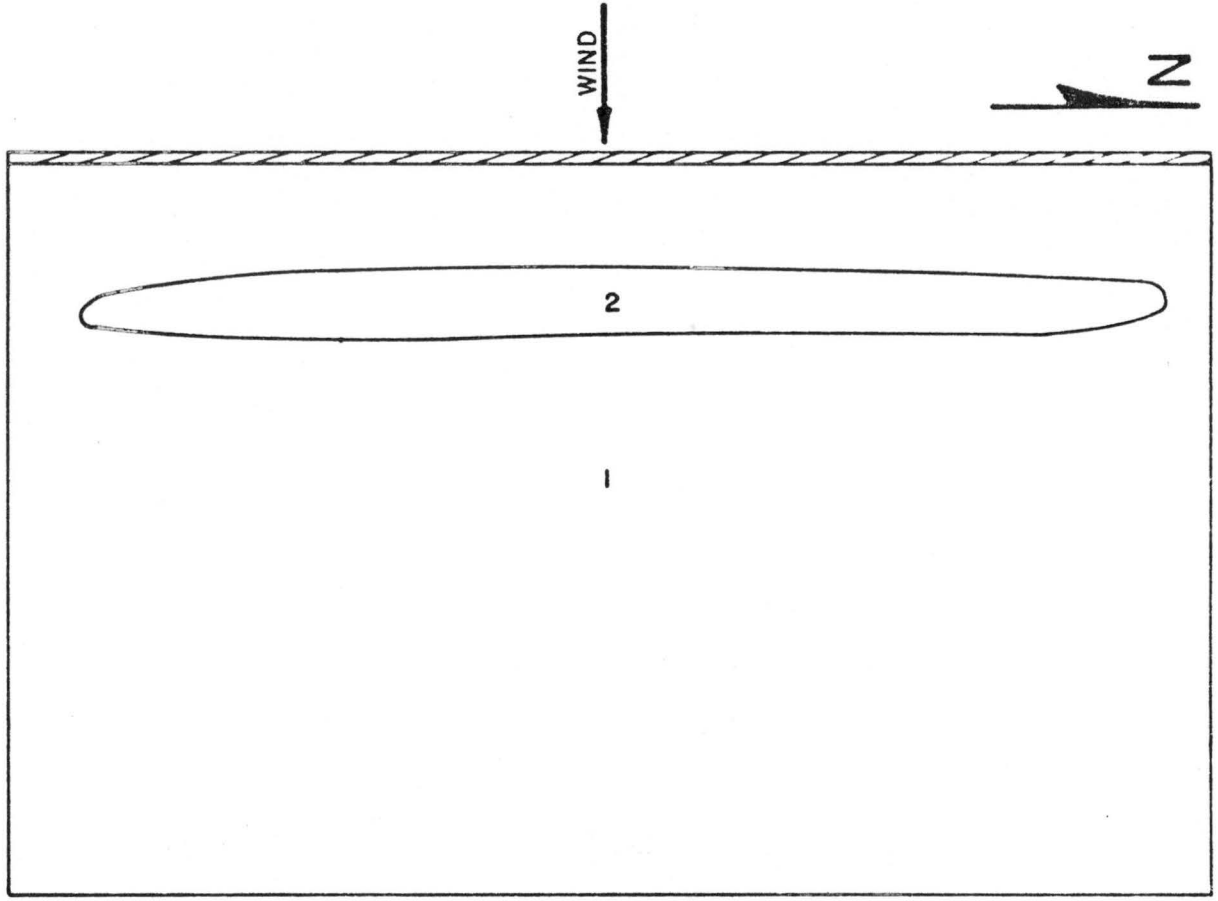

Fig. 47. Parking lot wind protection - H = 30', "Straight Across", lot orientation north-south, W wind, medium porosity

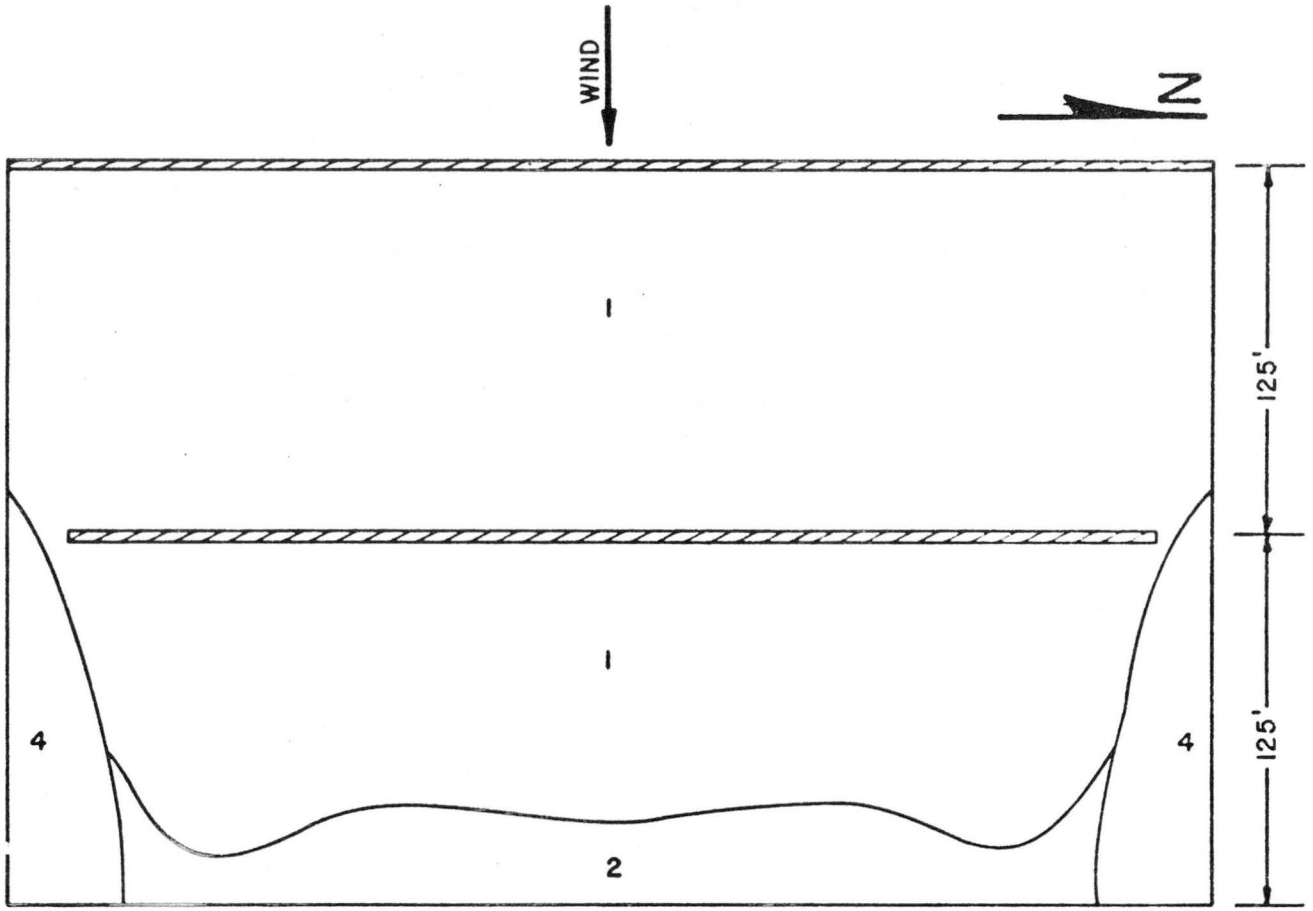

Fig. 48. Parking lot wind protection - H = 15', "Straight Across", two equally spaced, lot orientation north-south, W wind, medium porosity

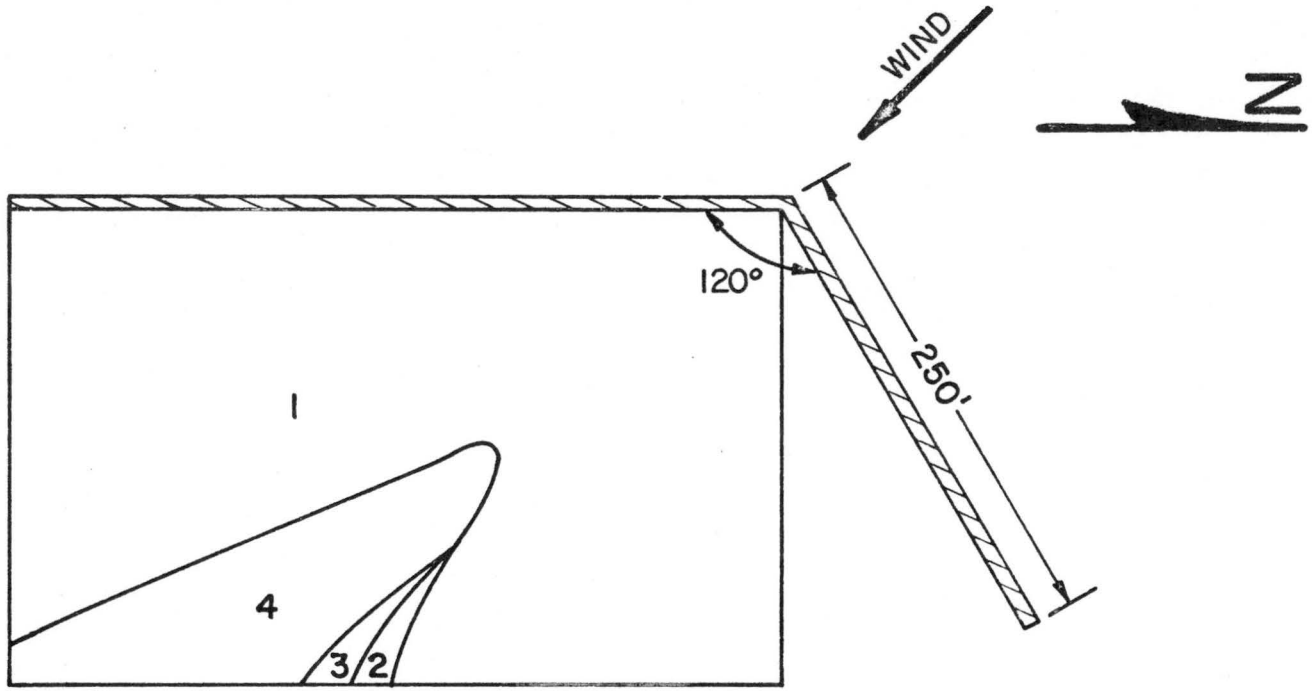

Fig. 49. Parking lot wind protection - H = 30', "Straight Across", with 120° extension, NW wind, medium porosity